Impact of soil moisture variability on convective rainfall activity over the Indian sub-continent

by

Mansi Bhowmick

Submitted in accordance with the requirements for the degree of

Doctor of Philosophy

The University of Leeds
School of Earth and Environment
December 2016

Declaration of Authorship

The candidate confirms that the work submitted is her own, except where work which has formed part of jointly authored publications has been included. The contribution of the candidate and the other authors to this work has been explicitly indicated below. The candidate confirms that appropriate credit has been given within the thesis where reference has been made to the work of others.

Chapter 3 was initially produced in the form of paper co-authored by Douglas J. Parker (University of Leeds), Stuart Webster (UK Met Office, Exeter), Cathryn E. Birch (University of Leeds), Luis Garcia-Carreras (University of Leeds), John H. Marsham (University of Leeds). The EMBRACE simulation was conducted by Stuart Webster and basic data extraction scripts were provided by him. The candidate produced all of the plots, analysis and first draft text of the paper. Then after discussion with co-authors and the candidate, keeping in mind the main aims of the study, all co-authors gave advice on further plots and analysis. Douglas Parker and Cathryn Birch have helped to refine the structure of the paper and wording of results and conclusions. The Chapter included here is the revised form of the paper submitted, based on the reviews received from reviewers of Journal of Hydro Meteorology.

The analytical solution to the quantitative model which forms the theoretical basis of Chapter 4 was computed and written jointly by Douglas Parker and the candidate. Parker identified the importance of the gradient of saturated equivalent potential temperature at the level of free convection, in enabling a solution to be found. The candidate identified from the literature the key equations which had to be solved and worked through the analytical details. The candidate is solely responsible for the data analysis for the evaluation of the new model, with some guidance from Parker.

Acknowledgements

Undertaking this PhD has been a truly life-changing experience for me and it would not have been possible to do without the support and guidance that I received from many people.

First and foremost, my sincere thanks to supervisor, Professor Douglas J. Parker, for accepting me as a Ph.D. student into his group, and then his constant encouragement, guidance, critical comments and detailed write-up corrections during the Ph.D. that has enriched my research experience. The joy and enthusiasm he has for the research was contagious and motivational for me, even during tough times in the Ph.D. I would like to extend my thanks to co-supervisors John Marsham and Stuart Webster for all their support and guidance throughout the Ph.D. Many Thanks to Chris Taylor for insightful comments and discussions.

I would like to acknowledge all members of the dynamics group for fruitful discussions, particularly Cathryn Birch, Luis Garcia-Carreras, and Sophie Cowie for providing much needed assistantship at various time. I greatly appreciate the IT support received from Richard Rigby at the school. I would like to extend my thanks to Stuart Webster for all the support with data extracting scripts and AJ Watling for MONSooN technical support. I very much appreciated the patient and prompt correspondence from Michelle Lesnianski during the long admission process.

Thank you to UK Met Office to give me access to MONSooN (the Met Office and NERC Supercomputing Node) without which analyzing EMBRACE simulations data would have been very difficult. Thanks to BADC for providing MIDAS Data. I am very grateful to Commonwealth Commission for funding this research (scholarship id. INCS-2012-161).

I am very thankful to Dr. Minz, Cathy Ellis and Jeanette Hannah for all their support. A special thanks to my family. Words cannot express how grateful I am to my Father and

lovely sisters Meenakshi and Vidisha for all their love, support and encouragement. I would also like to thank all of my friends Antje, Donna, Jess, Kamalika, Nabillah, Vittoria, Jen, Safa, Charlotte, Darpan and others who have provided much needed social support and distractions during tough times. Thank you.

Abstract

Soil moisture is an important geophysical parameter affecting land atmosphere processes, and hence free convection, by controlling the partitioning of the surface heat flux into latent and sensible heat flux. Interaction between these fluxes and the atmosphere gives rise to different types of soil moisture-precipitation feedback, namely "wet advantage" where rain is favoured over a wet (high latent heat flux) surface and "dry advantage" where rain is favoured over a dry (high sensible heat flux) surface. Previous studies over different parts of the world have shown that these feedback processes can take different pathways, according to one-dimensional and three-dimensional models. According to the one-dimensional model there is probability of rain initiation when the boundary layer top meets the level of free convection either by heating (increase in sensible heat flux over a dry surface) or by moistening (increase of latent heat flux over wet soil) of the boundary layer. On the other hand three-dimensional models explain convective triggering due to wind convergence near gradients in soil moisture.

This is a first study to compare and evaluate the existing soil moisture-precipitation feedback theories presented in the literature, over the Indian sub-continent under a single environment, by using high resolution convection-permitting (non-parameterized, or "explicit" convection) EMBRACE model simulation. Initially, a brief synoptic observational study shows evidence of surface-atmosphere coupling. More detailed case studies from the model output show further evidence for the land-atmosphere interaction in this region. The model indicates that all the processes defined by different theoretical models do exist under different surface, and atmospheric conditions.

The relative contribution of different processes under different soil moisture conditions prevailing over different climatic zones of the Indian sub-continent during the 20-day wet monsoon period from mid-July to early August is statistically studied. Dry-to-wet downwind soil moisture gradient is found to be the statistically significant pattern for initiation of the majority of afternoon convective initiation in the East, Centre and South study domains of India. It is also found that the so-called "CTP-HI_{low}" predictive

framework is not sufficient to address the observed behaviour of convective initiation under the full three-dimensional modelling environment. The use of the parameter HI_{low}, which is defined as the sum of humidity within and just above the inversion, as a predictive parameter is not physically understandable. This framework also lacks generality and solutions are empirically derived based on one-dimensional modelling and observations, which vary from place to place.

To offer a solution to these theoretical difficulties, this study provides a new quantitative model, using the basic idea behind the CTP-HI_{low} framework to find new predictive parameters depending on sound physical relationships instead of empirical solutions. The system is governed by two non-dimensional parameters, namely inversion Bowen ratio and a "stiffness ratio", and a third, dimensional parameter ΔR. Analysis of the EMBRACE simulations shows occurrence of both the dry and wet advantage, but the majority of the morning profiles favour prediction of dry advantage. Thus, the equations derived from the new quantitative model offer a quantitative prediction of wet and dry advantage occurring systematically, which is a question of great importance to weather and climate prediction, especially over moisture-limited areas.

Table of Contents

List of Figures

List of Tables

Abbreviations

1-D	**One D**imensional
3-D	**Three D**imensional
C	**C**entral study domain (blue box)
CAPE	**C**onvective **A**vailable **P**otential **E**nergy
CASCADE	Cascade Cloud-resolving simulations of the tropical atmosphere
CBL	**C**onvective **B**oundary **L**ayer
CIN	**C**onvective **IN**hibition
COSMO	**CO**nsortium for **S**mallscale **MO**delling
CTP	**C**onvective **T**riggering **P**otential
DW	**D**ry to **W**et in downwind direction
E	**E**ast study domain (white box)
EF	**E**vaporative **F**raction
EL	**E**quilibrium **L**evel
EMBRACE	**E**arth system **M**odel **B**ias **R**eduction and assessing **A**brupt **C**limate chang**E**
EZ	**E**ntrainment **Z**one
FA	**F**ree **A**tmosphere
FE03a	**F**indell and **E**ltahir (20**03a**)
GCM	**G**eneral **C**irculation **M**odels
HI_{low}	**H**umidity **I**ndex (**low**)
ISM	**I**ndian **S**ummer **M**onsoon
JJAS	**J**une, **J**uly, **A**ugust, **S**eptember
LCL	**L**ifting **C**ondensation **L**evel
LFC	**L**evel of **F**ree **C**onvection
LT	**L**ocal **T**ime
MCC	**M**esoscale **C**onvective **C**omplex
MCS	**M**esoscale **C**onvective **S**ystems
Met UM	**Met** Office **U**nified **M**odel
MFC	**M**oisture **F**lux **C**onvergence
N	**N**orth study domain (red box)

NCMC	**N**on-**C**lassical **M**eso-scale **C**irculations
NE	**N**orth-**E**ast
PBL	**P**lanetary **B**oundary **L**ayer
Pdf	**P**robability **d**ensity **f**unction
RAMS	**R**egional **A**tmospheric **M**odelling **S**ystem
RH	**R**elative **H**umidity
S	**S**outh study domain (black box)
SW	**S**outh-**W**est
T11	**T**aylor *et al.* 20**11**
TRMM	**T**ropical **R**ainfall **M**easuring **M**ission
USA	**U**nited **S**tates of **A**merica
UTC	**C**oordinated **U**niversal **T**ime
WD	**W**et to **D**ry in downwind direction

Parameters

α	Albedo
a_r	Aerodynamic Roughness Length
Ar	Entrainment constant
β	Surface Bowen ratio
β_i	Inversion Bowen ratio
β_v	Slope of the dry virtual adiabat
Cp	Specific heat at constant-pressure
Δp	Pressure difference between the inversion and the level of free convection
$F_{s\theta}$	Surface heat flux
$F_{i\theta}$	Entrained downward heat flux
g	Acceleration due to gravity
G	Ground heat flux
Γ	Static stability of the troposphere
Γ_+	Stability of the profile just above the boundary layer capping inversion
Γ_{es}	Stability of LFC (vertical gradient in saturated equivalent potential temperature)
H	Sensible Heat Flux
k_s	Thermal conductivity
L	Latent heat of vaporization of water
LE	Latent heat flux
p	Pressure
P_i	Pressure-depth of the mixed layer or Pressure at inversion
P_{LCL}	Pressure at Lifting Condensation Level
P_{LFC}	Pressure at Level of Free Convection
p_s	Surface pressure
q	Water-vapour mixing ratio
R	Rate of change of Δp with time
R_N	Net downward radiative flux
S_d	Down welling solar radiation
SM_E	Mean surface Soil Moisture in the immediate vicinity of the Event area

SM_s	Mean surface Soil Moisture over the Surrounding area
SM_X	Surface Soil Moisture of any piXel within the surrounding area
S_n	Net solar irradiance
θ	Potential temperature
θe	Equivalent potential temperature
θes	Saturated equivalent potential temperature
T	Temperature
T_d	Dew point temperature
u	Wind directions in x-direction
v	Wind directions in y-direction
w	Wind directions in z-direction
γ_{es}	Stiffness ratio
z	Height above surface
z_i	Inversion height
z_s	Thickness of soil layer

1 Introduction

1.1 Motivation

The majority of India's population live in villages and the occupation of villagers is agriculture. In agricultural planning, weather and climate is a resource and considered as a basic input. All agricultural practices such as ploughing, harrowing, land preparation, irrigation and transport of farm produce etc. are affected by weather. So the forecast of weather events helps for suitable planning of farming. Since the majority of tropical rainfall is convective in nature it will be very useful to understand the underlying processes which give rise to convective rain. The basic spatial scale of convective rainfall can vary from isolated showers, through Mesoscale Convective Complexes to tropical cyclones. Convective rainfall basically arises from convective cells, which are the basic elements of thunderstorms. Their origins are mainly due to instabilities in the atmosphere. Instability is a condition in which air will accelerate in the vertical freely on its own due to positive buoyancy. This is the reason air rises so quickly to form thunderstorms.

Convective cells often undergo three stages:

1) development stage consist of updraft persisting throughout the cell;
2) mature stage which consists of updraft and downdraft, the updraft often reaching deep into the troposphere, attaining the height of 12-14km or higher; and
3) dissipating stage characterized by downdrafts.

Well-developed convective systems are often referred to as hot towers because of the large release of latent heat of condensation.

Apart from knowledge about synoptic scale processes, forecasting convective weather events also requires understanding of earth system processes including interaction between land and atmosphere, because this plays an important role in the evolution of

land-atmosphere processes and associated convective precipitation (Guo *et al.*, 2006; Taylor and Ellis, 2006; Findell and Eltahir, 2003a).

Changes in vegetation cover and soil moisture impact surface energy partitioning, water and carbon fluxes and ultimately affect precipitation patterns. Findings reported by Douglas *et al.* (2006, 2009), Lee *et al.* (2008), Niyogi *et al.* (2010), Kishtawal *et al.* (2010) provide evidence that the land surface feedback due to agricultural intensification/irrigation or urbanization over northern India has become sufficiently coherent or organized to impact the regional rainfall processes. Douglas *et al*. (2009) used the Regional Atmospheric Modelling System (RAMS) over the Indian monsoon region to simulate an event between 16-20 July 2002 under various land conditions: (i) a control with Global Land Cover land use and observed Normalized Difference Vegetation Index, (ii) an irrigated crop scenario, (iii) a non-irrigated crop scenario, and (iv) a scenario for potential (natural) vegetation. Results showed agricultural changes that occurred due to increase in irrigation led to an increase in regional moisture flux which in turn modified the Convective Available Potential Energy (CAPE). This caused reduction in surface temperature, modified regional circulation pattern and hence changes in mesoscale precipitation.

In view of the above ideas, the objective of this study is to get a deeper quantitative understanding of the regional, seasonal and diurnal variation of convective initiation and precipitation in relation to varying soil moisture conditions.

1.2 Physics of land-atmosphere coupling

Before going into details of land atmosphere coupling processes let us first define some commonly used meteorological parameters that have been used repeatedly to describe the undertaken study.

1.2.1 Boundary Layer processes

Stull (1988) defines the Planetary Boundary Layer (PBL) as the part of the troposphere that is directly influenced by the presence of the earth's surface, and responds to surface

forcing with a timescale of one hour or less. In other words it is the interface between atmosphere and earth surface with greatest thermal response due to greatest energy absorption by day and depletion by night (Oke (1987, pp 37)). The PBL is a very important part of the atmosphere because this is where people spend most of their lives. Daily weather forecasts of fog, dew, frost, and temperatures are essentially boundary layer forecasts. The height of PBL typically affects the evolution of clouds.

The PBL thickness is quite variable in time and space, ranging from hundreds of metres to a few kilometres. On a sunny day with light thermal winds, dry convection may pushed up to 1000 to 2000 m above the surface. With weak winds and little clouds or at night the depth can be depleted to 100 to 200 m. To find the top of the boundary layer is not always simple. It is considered to be the depth of the turbulent activity (Oke 1987, pp 41). Turbulance is random eddy motion of air which mixes the air and tends to result in a well-mixed profile. Thus, mostly, PBL height is measured to the height of the lowest inversion from the surface.

The top of the PBL is capped by a layer of stable thermal stratification, which is commonly known as the capping inversion. The interface between the capping inversion and the PBL is called the Entrainment Zone (EZ) which separates the PBL from the Free Atmosphere (FA). The daytime overland PBL is often capped by a well-defined inversion, which rises each morning in response to the growing convective activity below and fades or recedes as the surface heating tapers off near sunset (Figure 1.1). At night or over the ocean when the PBL has stable stratification, the top of the PBL may not be well defined.

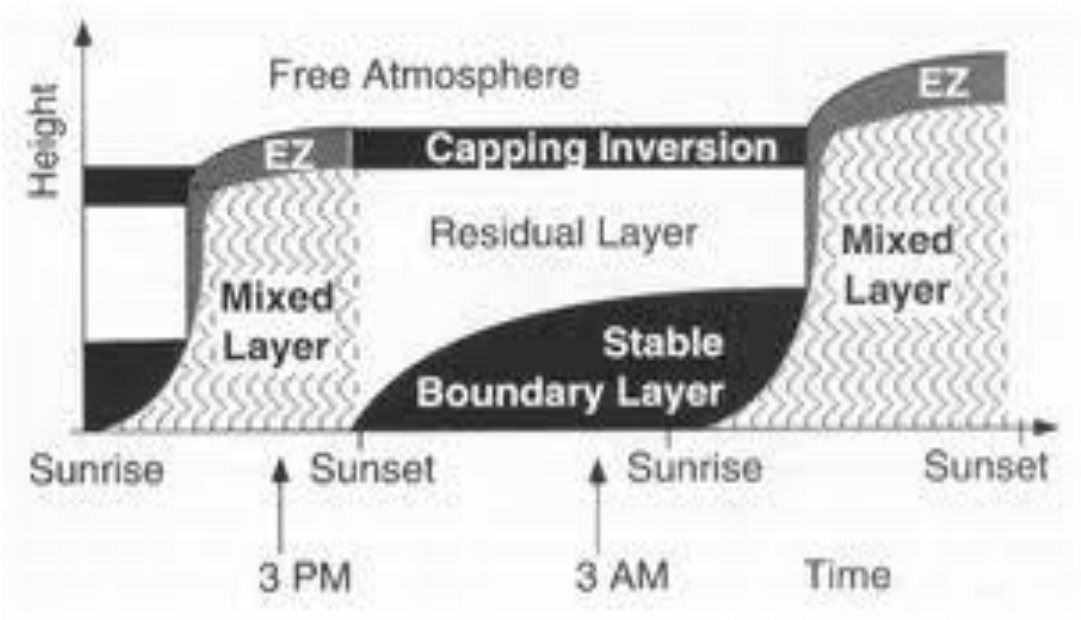

Figure 1.1: A typical diurnal evolution of Planetary Boundary Layer over a 24 hour period (Stull 2000).

(i) Convective Boundary Layer

During daytime, the lowest part of the PBL is characterized by a shallow super-adiabatic surface layer (about 30-50m deep) of the PBL called the turbulent surface layer. The behaviour of this layer, and its exchange of heat or momentum with the underlying surface, controls the process of land-atmosphere, or air-sea, interaction.

In the afternoon the turbulent region above the turbulent surface layer up to the top of the PBL (90% of the depth (about 1 to 2 km)) is called the Convective Boundary Layer (CBL). Due to day time heating there is formation of convective thermals that causes a well-mixed boundary layer. This mixed layer is often capped by a stable layer (inversion where temperature rises with height) into which the layer of shallow cumulus or congestus clouds develops.

While the surface layer is typically super-adibatic under conditions of daytime solar heating, in the mixed layer, profiles of climatic properties, such as the daytime potential temperature profile, show very little variation with height (a property which is exploited in the 1-D boundary layer model as proposed by Betts, Carson, Tennekes all published in (1973) and presented in Section 1.2.1 (iii)). The sensible heat flux profile usually

decreases with height, becomes zero near the inversion base and then actually reverses direction in the topmost 10% of the mixed layer. Sometimes this well mixed boundary layer overshoots to the overlying warmer air and when they are repelled they transport heat downwards, referred to as convective entrainment, and causing the negative heat flux at the top of the mixed layer.

(ii) Nocturnal Boundary Layer

The surface heat flux, H, falls to zero in late afternoon – often this happens before sunset due to the strong longwave cooling and downward ground heat flux, at a time when the solar heating is falling fast. Due to this cooling, the unstable surface layer rapidly stabilises, and turbulence is largely restricted to a shallow layer. A true mixed layer is not present but turbulent transfer in residual layer removes heat from the lowest layer to form a stable boundary layer, on the order of 100 m deep (Figure 1.1).

(iii) Betts, Carson and Tennekes model for simple CBL

In the absence of cumulonimbus clouds, horizontal warming and cooling by advection is relatively low. Under these conditions to the daytime heating of the land generates convective turbulence that causes the well mixed boundary layer. For this reason, during the day, a one-dimensional model of vertical boundary layer growth (mixed layer model) can be used: this was developed by Betts, Carson and Tennekes (Betts 1973; Carson 1973; Tennekes 1973) on the basis of a budget of energy from the surface, with a simple estimate of entrainment from the upper lid (The Forecasters‘ handbook for West Africa, Parker *et al*., January 2017).

In the mixed layer model CBL is characterized by mean depth z, height-independent mean potential temperature θ, and height-independent water-vapour mixing ratio q. It considers constant ambient static stability of the troposphere, Γ, into which the PBL grows in the morning. At the inversion there is jumps in potential temperature and mixing ratio, defined as $\Delta\theta$ and Δq (Figure 1.2).

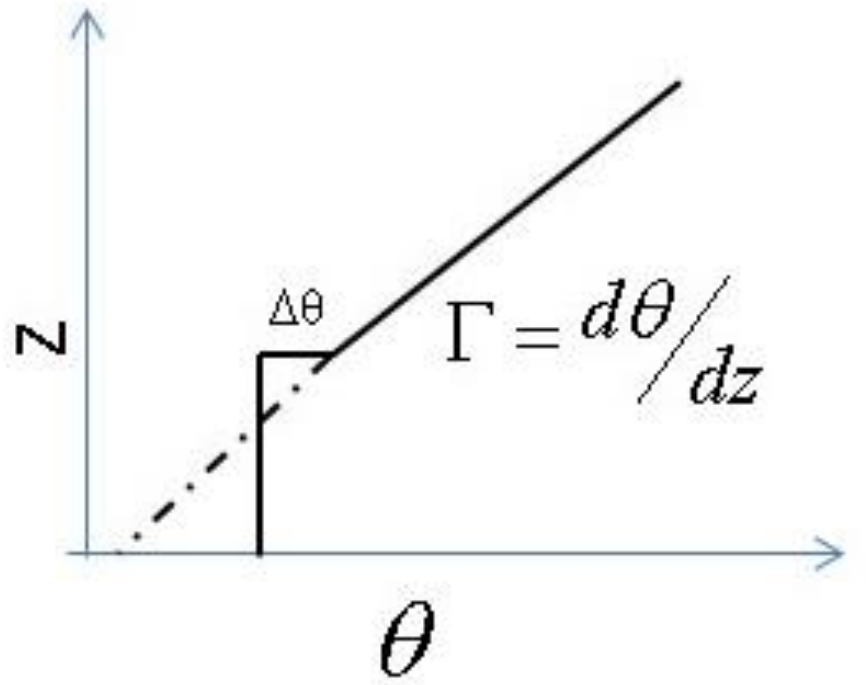

Figure 1.2: Schematic of the bulk mixed/boundary layer model whose solution yields (equation 1.2 and 1.3). The well-mixed CBL has constant potential temperature, θ, and is capped by a jump in θ, at a height $z=z_i$, above which there is constant stratification. The one-dimensional solution to this model gives increase of θ and q in time.

Turbulence in the PBL results in entrainment of warm air from the free troposphere into the PBL causing an increase in mixed layer depth, and leads to downward heat flux. This entrained downward heat flux ($F_{i\theta}$) is assumed to be a constant fraction A_r, of surface heat flux ($F_{s\theta}$).

$$F_{i\theta} = -A_r F_{s\theta} \qquad (1.1)$$

Betts (1992) represented the simplified bulk mixed layer budgets of θ and q (given by equation 1.2 and 1.3 and ignoring horizontal advection) whose one-dimensional solution gives solutions describing the rise in θ and q in the boundary layer in terms of inversion height (z_i), surface Bowen ratio (β), inversion Bowen ratio (β_i) and entrainment constant A_r; given by

$$C_p \frac{d\theta}{dt} = \left(\frac{F_{s\theta}}{\rho z_i}\right)\left[1 + A_R \frac{\beta_i}{\beta} \frac{(\beta - \beta_v)}{(\beta_i - \beta_v)}\right] \qquad (1.2)$$

$$L\frac{dq}{dt} = \left(\frac{F_{sq}}{\rho\, Z_i}\right)\left[1 + A_R\,\frac{(\beta - \beta_v)}{(\beta_i - \beta_v)}\right] \quad . \qquad (1.3)$$

The first term in equation 1.2 and 1.3 is the tendency of the surface fluxes to warm and moisten the boundary layer and the second term is the contribution from entrainment. In practice, the value of the entrainment constant, A_r, can vary from 0.2 to 0.4, but from quantitative study its value is often found to be large and 0.4 is used in most of the models. These equations are further exploited by Betts and Ball (1995) to calculate the equivalent potential temperature budget (equation 5d, Betts and Ball (1995)) and a simple solution for boundary layer growth (equation 15, Betts and Ball (1995)). In Chapter 4 of this thesis we have used these equations from Betts and Ball to develop a new predictive model for convective initiation.

1.2.2 Land surface processes

Boundary layer processes commonly known as land atmosphere interaction processes are the key processes by which land conditions affect the lower troposphere. They explain the flow and transformation of energy and momentum between land and PBL. Our aims in this study are to understand these processes through theoretical, modelling and observational studies.

(i) Surface Energy Balance

During the day, the surface is heated by the Sun so there is an upward transfer of heat into the cooler atmosphere. In contrast, during the night when the earth surface cools more rapidly than the atmosphere, there is a downward transfer of heat. This temperature-dependent transfer of heat can be quantified as the term Sensible heat flux (H). Similarly, transfer of heat due to phase changes of water at the surface is quantified by the Latent heat flux (LE). The magnitude of energy fluxes in the PBL typically depends on the partitioning of fluxes at surface. The surface energy budget represents the balance in energy fluxes in the form of incoming and outgoing radiation to the surface underlying the boundary layer. According to Pielke (2001) the surface energy budget is given by

$$R_N = G + H + LE \qquad (1.4)$$

where R_N is the net downward radiative flux, G is the downward ground heat flux, H is the upward sensible heat flux and LE is the upward latent heat flux. Here sign conventions (directions) are for daytime heat flux behaviours. The surface energy balance give rise to a temperature gradient and soil heat flux in the sub-surface layer which is directed downward in day and upwards in night.

The partitioning of surface flux into latent and sensible heat flux is dependent on the characteristics of the underlying surface i.e. the degree of surface wetness. Thus, soil moisture plays an important role in the surface energy balance and hence the depth of the boundary layer.

(ii) Surface Bowen ratio or Evaporative fraction

Land- surface processes are strongly affected by partitioning of the surface heat flux, and the partitioning of surface fluxes depends on the soil moisture conditions. An important term that measures the partitioning of the fluxes (which may vary for instance, according to wetness of the surface) is the Surface Bowen ratio (β), defined as the ratio of sensible heat flux to latent heat flux,

$$\beta = H / LE, \qquad (1.5)$$

or the "evaporative fraction",

$$EF = LE / (LE + H). \qquad (1.6)$$

A wet surface tends to have low sensible heat flux, low β (less than 1) and hence high evaporation of moisture to the boundary layer. Similarly, dry soil will have high sensible heat flux (greater heating) and low evaporation. Negative β indicates that the two fluxes have opposite signs. This is common in night when the sensible heat flux is downward (negative) but evaporation continues so that LE is away from the surface (positive). Thus β or EF have a significant impact on the characterization of boundary layer and these quantities will be used in subsequent chapters to analyze the model representation of atmospheric response to soil moisture.

(iii) Albedo

Albedo is a measure of surface reflectance. It is mainly controlled by the surface properties like colour of the surface. It is defined as constant fraction, α, of downwelling solar radiation (S_d), and is mathematically given by

$$S_n = (1-\alpha)\, S_d \qquad (1.7)$$

Where S_n is net solar irradiance

It is high over bare ground and low over vegetated surfaces. Increasing the soil moisture tends to darken the bare soil, reduces its albedo (α), and leads to a higher amount of solar energy input to the soil. The albedo can be important for transient effects under hot conditions: for instance, a high albedo decreases the likelihood of a rapid increase in β, thus slowing the increase in surface temperature. Also if the surface is wet (low β), heat capacity will be high which prevent the surface temperature from rising rapidly.

(iv) Heat capacity

Heat capacity relates to the ability of a substance to store heat and express the temperature change produce as a result of gaining or losing heat (Oke 1987, pp43,45). The value of soil heat capacity is strongly depend in a linear fashion to soil moisture content. It increases approximately linearly with soil moisture. This implies that high heat capacity is often associated with low β

(v) Ground Heat Flux (G)

It is related to thermal conduction of heat energy within the ground. Heat flux is exchanged within soil layers. It depends upon a simple physical principle that heat flows from a hot to cold matter. Its bulk estimate is given by equation

$$G = K_s \frac{\partial T}{\partial z_s} \qquad (1.8)$$

Where k_s is thermal conductivity, z_s is thickness of soil layer and T is soil temperature.

Thus, the heat from the surface layer flows downward towards deeper layers during the afternoon and upward during the night when the upper surfaces are cooler than deeper

layers. Since ground heat flux is directly proportional to thermal conductivity and thermal conductivity increases with increase in moisture (Oke,1987, pp43) so G increases with increase in soil moisture.

(vi) Surface Roughness

On a smaller scale, roughness is the spacing density of individual obstacle or roughness element. For example, the leaves of many trees, plants and crops can form a canopy elevated above the ground surface. If we imagine that a large box could be placed over one whole plant or tree that would just touch the top and sides of the plant, then the volume of this box is called *space* taken by the plant. The *total surface area* of the plant, including the area of both side of each leaf can be theoretically estimated. The *area density of roughness element* $\boldsymbol{S_r}$ is defined as plant surface area divide by space volume (Stull 1988).

Another measure of the surface roughness is the *aerodynamic roughness length* $\mathbf{a_r}$. This roughness measure is based on the observed wind shear in the surface layer. It is defined as the height where the wind speed is zero. There is a one-to-one correspondence between roughness element and a_r but once determined for a particular surface, a_r does not change with wind speed, stability or stress. Higher roughness elements, are associated with larger aerodynamic roughness lengths. In all cases, however, the a_r is smaller than physical height of roughness element.

(vii) Summarizing effects of soil moisture and vegetation fraction on various parameters of surface energy balance.

Notes summarizing the effect of increase in soil wetness or vegetation fraction on the above mentioned parameters affecting land surface process are given in Table 1.1. Bowen ratio and Evaporative fraction both more or less define the partitioning of surface fluxes but have the opposite tendency in response to increases in soil moisture and vegetation fraction. Albedo on the other hand decreases with moistening or increase in vegetation fraction, which tends to darken the surface colour. Heat capacity tends to increase with increases in soil moisture as well as for increase in vegetation fraction. This is because increase in vegetation fraction increases water content hence heat capacity. Reducing the areal coverage of vegetation increases ground heat flux whereas increasing Leaf Area

Index decreases Ground heat flux (Yang *et al.*, 1999). Finally, surface roughness increases with increase in vegetation fraction and has no effect from changes in soil moisture.

Parameter	Effect of increasing Soil moisture	Effect of increasing vegetation fraction
Surface Bowen ratio	Decrease	Decrease
Evaporative fraction	Increase	Increase
Albedo	Decrease	Decrease
Heat capacity	Increase	Increase
Ground heat flux	Increase	Decrease
Surface roughness	No effect	Increase

Table 1.1: Effects of soil moisture and vegetation fraction on various parameters of surface energy balance.

1.2.3 Rainfall

Rainfall is one of the most variable parameters in tropical climate. Three types of rainfall occur in the tropics: convective, stratiform and orographic. The summer (June, July, August, September (JJAS)) monsoon rainfall over India is the manifestation of moist convective processes.

Convectional rainfall generally occurs over a limited spatial scale of between 10-20 km^2 and 200-300 km^2 (McGregor and Nieuwolt,1998,pp 187). Thus, the spatial scale of convective rainfall has considerable spatial variability and is dependent on whether convection cells forms individually and remain in the place of origin or become organized into weather systems such as squall lines. *Convective rainfall* is a short period and intense type of rain with large rain drops; sometimes in solid form as hail. An important

atmospheric condition for convective storm/cloud formation is the release of instability. The stability of an air mass is dependent on its moisture status.

Stratiform rainfall is mostly a characteristic of mid latitude rainfall. But, in tropics when convection decays, clouds become stratiform and co-exist with the embedded convective columns of rapid updraft. Stratus clouds in tropics are limited to areas of wide spread convergence (like anvil tops of towering cumulonimbus), easterly waves or low level fog. It leads to a persistence kind of rainfall with lower intensity and smaller rain drops compared to convective rainfall.

Orographic rainfall is the result of condensation and cloud formation in moist air that has been physically forced over topographic barriers. Orographic precipitation, unlike conventional and stratiform precipitation, is not mobile and is limited to the mountain barrier to which it owes its origin.

(i) Climatology of Indian rainfall

In global studies the tropics are perceived as an invariably wet region. However, the tropics have intra-seasonal, seasonal and inter-annual variability of rainfall according to variability in land-atmosphere-ocean systems. Indian climate can be broadly distributed in four seasonal conditions 1) Pre-monsoon which is very dry and hot, 2) Monsoon is hot and humid, 3) Post-monsoon is transition phase from humid to dry, 4) Winter is dry and cold. About 80% of the total rainfall over the Indian region is received during the Indian Summer Monsoon (ISM) season, i.e. JJAS (Sahai *et al.*, 2003; Das *et al.*, 2014).

Inter-annual variability and trends: Since the majority of annual rainfall over the Indian sub-continent is delivered during the South-West monsoon, it is critical for the availability of fresh drinking water, irrigation, and water resource management. This variability in the last decade is found to be not very large, the standard deviation is only about 10% of mean over ISM region (Gadgil, 2003). Mechanisms leading to interannualar variation depend on various other phenomena including teleconnection with El Nino (Gadgil, 2003).

***Seasonal variability*:** In contrast to large oceanic basins, tropical continent and adjacent sea areas have important seasonal temperature and pressure changes. The seasonal reversal in land-atmosphere temperature difference produces changes in atmospheric pressure gradient force, the basic driving force of the wind. These large scale wind reversals are often termed as the "monsoon". The Indian sub-continent has two monsoon seasons; the South-West (SW) and the North-East (NE) monsoon. The SW monsoon is often referred to as the Indian summer monsoon. The dominant period of the SW monsoon is June to September and it spatially covers almost all of the Indian sub-continent except the extreme North-East India and extreme South-East coast (Tamilnadu state) of India. June is the time of the onset of the summer wet monsoon which is associated with northward movement of Inter Tropical Convergence Zone from the equator, while September is the retreat phase of the SW monsoon in which the monsoon starts withdrawing from north-west India.

Apart from the monsoon, pre-monsoon and post-monsoon seasons, India also receives some amount of rainfall due to tropical cyclones and pre-monsoon convective activities. The winter season is mostly dry throughout the country, except that a small part of the country receives rain due to NE monsoon. The NE monsoon has temporal spread between October-November (Gadgil, 2003), and spatial spread in extreme NE India and the east coast of Tamilnadu (south-east tip of the Indian sub-continent).

Intra-seasonal variability: In addition to inter-annual and seasonal variation, the monsoon system experiences intra-seasonal variation in rainfall in the form of active and break phases, which are described (Blenford, 1886, as cited by Gadgil, 2003) as the fluctuation between spells "during height of rains" and "intervals of droughts". Active spells are characterized by a sequence of time-clustering, partly overlapping development of monsoon disturbances (Murakami, 1976) and cyclonic vorticity above the boundary layer (Sikka and Gadgil, 1978). It is the period of above normal rainfall on country or regional level. The break phase is characterized by a marked change in the lower tropospheric circulation over the monsoon zone, with the vorticity above the boundary layer becoming anticyclonic. It is also the situation in which the surface trough is located close to the foothills of the Himalayas (Gadgil, 2003). It refers to below normal rainfall at country or regional level.

***Climate change**:* A proper temporal trend (inter-annual) analysis of ISM rainfall is required for social and economic planning towards climate change. Several studies have been conducted to investigate the trend of ISM rainfall at country, regional or station level. A few studies have shown there is no significant trend of average annual rainfall at country level (Mooley and Parthsarthy, 1984; Lal, 2001; Sinha Ray and De, 2003), but significant trends were observed at regional level during monsoon month and season (Das *et al.*, 2014). It is worth mentioning here that trends in rainfall found in studies are highly dependent on period and type of data analysed (station data, zonal average or gridded data).

(ii) Monsoon rainfall and monsoon depressions

Over the Indian peninsula the monsoon brings over 80% of the total rainfall (Das *et al.*, 2014; McGregor and Nieuwolt, 1998, pp 224). The Indian monsoon is the manifestation of moist convective processes over the Indian peninsula. A distinct structural feature of the monsoon is the development of cyclonic vortices called monsoon depressions. Monsoon depressions are elliptical isobars around a core of low pressure system as visible on synoptic charts. Development of these vortices plays a key role in the rapid changes that occur in cloudiness and rainfall patterns at the time of monsoon onset (Krishnamurti,, 1985). The most important area of origin of monsoon depressions is the Bay of Bengal, but occasionally they also develop over the Arabian Sea. Once formed, these monsoon depressions are seen to consist of potential vorticity maxima that have peak amplitude in the middle troposphere and propagate westward by nonlinear, horizontal adiabatic advection (i.e. beta drift) (Boos, 2015). They also appear to be steered by interaction with the Himalayas (Hunt and Parker, 2016). Strong wind shear in the monsoon flow prevents the depression from developing into a tropical cyclone (McGregor and Nieuwolt , 1998, pp 160).

(iii) Organisation of convective rainfall

The process of upward movement of air is called convection. Convection contributes to the majority of vertical heat and momentum fluxes in tropical region. The convective cell is the basic spatial entity that gives rise to a range of tropical disturbances. It originates mainly due to instabilities in the atmosphere. These instabilities can be caused by either free convection (surface heating) or forced convection (orographic forcing) (McGregor

and Nieuwolt,, 1998)**.** In the context of land-atmosphere interaction we think that variations in surface Bowen ratio can lead to circulations which trigger convection (Garcia-Carreras *et al*., 2011; Taylor *et al.*, 2011).

Isolated showers / thunderstorms

The basic condition for development of thunderstorms over land are warm and humid air masses, which will become unstable over considerable vertical layers. Thunderstorms have a short life span (1-2 hour) and are small in size (less than 10Km)**.** The thunderstorm process can be divided into three stages defined in Section 1.1. These thunderstorms are often called hot towers or deep convective cells (height ~ 18000m) in South Asia. Their geographical distribution changes markedly from the pre-monsoon, when they cluster along the Indian Subcontinent east coast, to the monsoon season, when they occur preferentially in the western Himalayan indentation region. These cores have strong diurnal cycle with maximum occurrence in the evening (Romatschke *et al*. ,2010).

Organised convective systems

Convective cold pools within individual convective systems act to trigger convection, leading to organisation of the systems (into Mesoscale Convective Systems (MCCs'), squall lines etc). These systems are probably less sensitive to surface-based triggers, because the cold pool delivers triggering regardless of the surface state. MCCs' are large cloud clusters with dimensions 100-1000 km in diameter, whereas, squall lines are linear structures aligned in bands of hundreds of kilometres while their width is of the order of 10-30 km. The dissipating stage of these organised convective systems gives rise to stratiform rainfall.

(iv) Convective physics, Parameters and the Tephigrams

During the course of time, over many years convection has been studied in detail and some parameters have been defined that help to explain convection processes. Some of these parameters are defined and discussed here: they are collectively referred to as convective parameters.

The tephigram is a thermodynamic diagram used to represent the vertical structure of the atmosphere: basically it is a plot of temperature, humidity (in terms of dew point temperature) and wind profiles (direction from geographical north and speed). It is a very

useful tool to interpret various thermodynamic properties of the atmosphere, particularly in the troposphere, such as stability, Convective Available Potential Energy (CAPE) and Convective Inhibition (CIN). The tephigram also helps to define and separate various meteorologically important levels such as the Lifting Condensation Level (LCL), Level of Free Convection (LFC) and Equilibrium Level (EL). The tephigram is commonly read and interpreted by comparing temperature and humidity profile of the environment with a parcel ascent profile. Here, the environment profiles are usually obtained from a radiosonde ascent, whereas the parcel is a hypothetical mass of air having adiabatic properties, so that it ascends at the rate of dry adiabatic lapse rate (i.e. 9.8 ^{0}C km^{-1}) till it is saturated, then after saturation the parcel ascends at the rate of the moist adiabatic lapse rate. Figure 1.3 is a simple schematic to represent these characteristics of a parcel ascent in a tropospheric profile supporting deep convection (conditionally unstable profile).

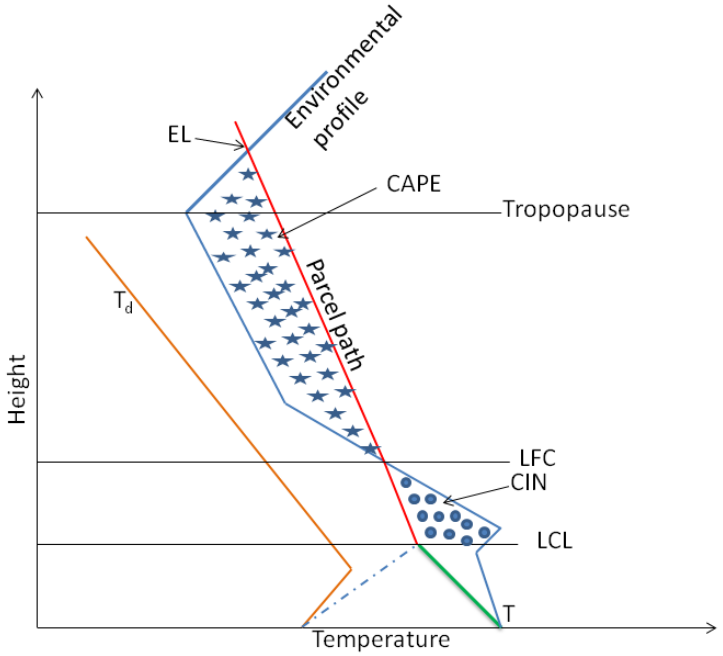

Figure 1.3: Schematic of tephigram.

With reference to Figure 1.3, initially the parcel is considered to have temperature equal to the surface temperature, then starts to rise by following the dry adiabatic lapse rate (green line) until it starts condensing at the lifting condensation level (LCL). At the LCL, the temperature of the parcel becomes equal to the dew-point temperature (dash-dot line).

Mostly some form of forced ascent is required for this to happen, because at the point, the parcel is still cooler than its environment and negatively buoyant. Once the parcel starts condensing it rises further by following the moist adiabatic lapse rate (red line). The level at which the parcel becomes warmer than its environment is the level of free convection (LFC). Once the parcel reaches the LFC it becomes buoyant and continues to rise until its temperature is again equal to the environmental temperature (the equilibrium level, EL). The heights of the LFC and the equilibrium level are measures of the cloud base and top heights respectively. The sensitivity of the LFC to the parcel curve will be used conceptually in Chapter 4, as the basis for explaining how convective triggering responds to surface state.

CAPE is the positive buoyancy (maximum energy a parcel could have if lifted vertically through atmosphere) and is the area bounded by the moist adiabat and environmental profile between the LFC and EL (area shaded by stars). The negative buoyancy (energy barrier to convection) is called the Convective Inhibition (CIN) and is the area bounded by moist adiabat and environmental profile between LCL and LFC (area shaded by dots). In order for CAPE to be released, energy needs to be added to the system to overcome CIN, and therefore this instability is described as "conditional instability".

1.3 Observations and models of land-atmosphere coupling in literature.

In the wet climates where soil has plentiful water, evaporation is controlled by the net radiative energy and not by the amount of soil moisture. Thus we can say that in moist climates, boundary layer moisture and hence profile and rainfall is not dependent on soil moisture. In a dry climate, evaporation rates are controlled by soil moisture but generally the evaporation is too small to affect precipitation. Thus, it is expected to be near transition zones (Koster *et al.*, 2004), that soil moisture-controlled evaporative fraction is sufficient to trigger moist convection through changes in the boundary layer thermodynamics. Thus feedbacks between soil moisture and precipitation are seen to be important for weather prediction in many regions of world where there are spatial contrasts in surface moisture availability (Koster *et al.*, 2004), including the Great Plains of the USA, the Sahel, and Northern India as shown in Figure 1.4 yellow-red regions.

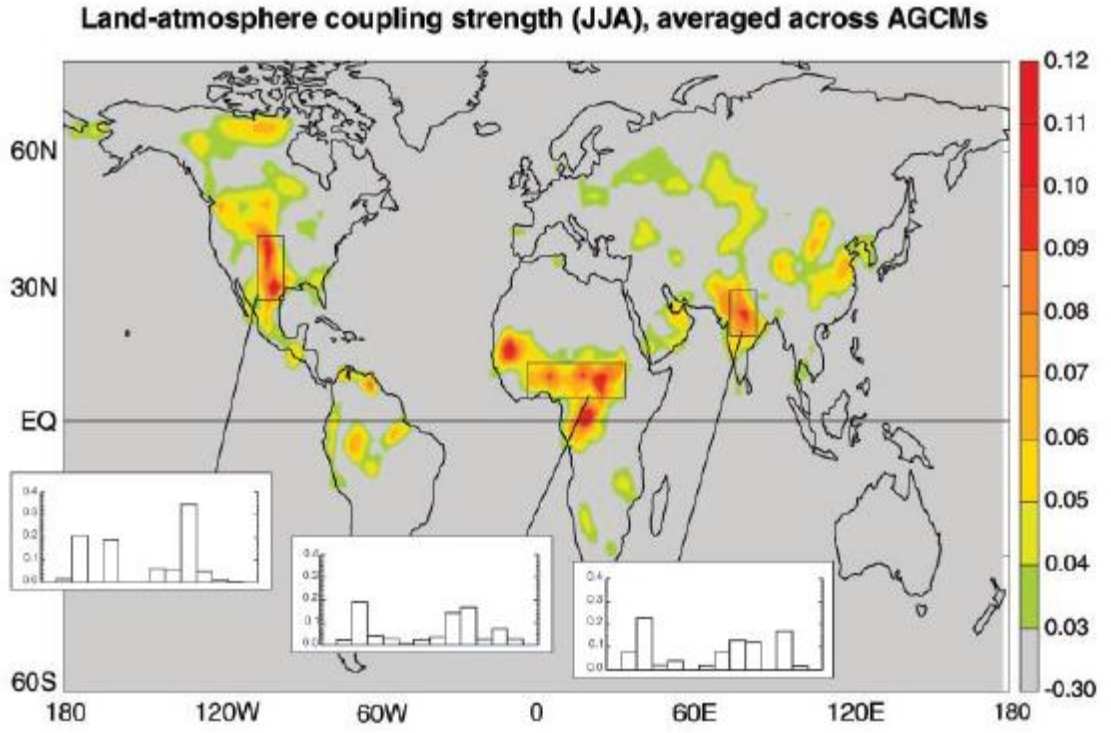

Figure 1.4: The land atmosphere coupling strength diagnostic for boreal summer (June, July, August) averaged across 12 models participating in GLACE (Koster *et al*., 2004).

A study conducted by Segal and Arritt (1992); based on various observational and modelling studies, defined perturbed areas as the area in which the values of sensible heat flux are suppressed (or in some cases enhanced) compared with surrounding areas by, for example, patchiness due to soil wetness, vegetation, cloudiness or snow etc. The conclusion of the study is that Non Classical Mesoscale Circulations (NCMCs) do generate flow of the strength of a lake breeze or sea breeze which may persist for timescales of hours to days to even seasons, according to the characteristics (such as strength of gradient or length of patchiness) of perturbed areas.

Further, Peilke (2001) demonstrated the link between surface moisture, heat fluxes and cumulus convective rainfall on the basis of published work. He reviewed the then available literature to examine how alteration in the surface energy budget directly affects the heat, moisture and momentum flux within the boundary layer and concluded that boundary layer depth is directly influenced by the surface heat and moisture fluxes. His study further pointed out that both mesoscale and regional landscape patterning and average landscape conditions exert a major control on weather and climate. The overall

conclusion of this study is that vegetation and soil moisture changes directly affect the energy and moisture fluxes which ultimately alter the environment for thunderstorms.

1.3.1 Modelling studies

Operational weather models are important tools for decision makers. These models use a combination of all available up to date data, from satellite, airborne and surface-based measurements, for prediction of meteorological variables at different time scales. Several numerical studies have been performed with global and limited-area atmospheric models to study land–atmosphere interactions in more detail. The first numerical model and scaling of NCMC (like a Lake Breeze, vegetation breeze or snow breeze etc.) forced by horizontal variation of the soil surface moisture availability was reported by Ookouchi *et al.* (1984). Their results suggest that in an extreme case of contrast between saturated soil and very dry soil the intensity of the thermally induced surface flow is similar to that of a sea breeze with maximum surface wind speed ~ 5m s^{-1}, while the surface temperature contrast is ~18 K. In general, modelling studies indicate that anomalies in soil moisture and soil temperature can result in significant changes in atmospheric circulation patterns and precipitation (e.g., Charney *et al.*, 1977; Walker and Rowntree, 1977; Shukla and Mintz, 1982; Pielke and Avissar 1990; Shukla *et al.*, 1990; Meehl 1994; Liu and Avissar, 1996, Koster *et al.*, 2004,2006; Guo *et al.*, 2006).

At the global scale Koster *et al.* (2004, 2006) inter-compared General Circulation Models (GCM) to determine the sensitivity of temperature and precipitation to land surface conditions. They identified global hotspots for the coupling of soil moisture to precipitation during boreal summer (June-July-August) as West Africa, mid-west USA and India. These are the regions of soil moisture transition zones between wet and dry. According to this map the Central India, Sahel and mid USA are hotspot regions for land atmosphere coupling (Figure 1.4, highlighted by red and yellow colour in the map). Guo *et al.* (2006) further analyzed the model runs of Koster *et al.* (2006) and concluded that hotspots of coupling were located on transition zones between dry and wet climate.

The impact of soil moisture on precipitation has been also established in numerous Atmospheric GCM studies (Koster *et al.*, 2004; Liu and Avissar, 1999; Dirmeyer, 2000).

Gantner and Kalthoff (2010) performed a set of sensitivity studies using the COSMO model over West Africa to investigate the response of mesoscale convective systems to soil moisture properties. As evident in other studies, the convection was initiated along soil moisture heterogeneity in the vicinity of orography. Another interesting result was regarding the change in sign of feedback from initiation (negative feedback) to mature stage (positive feedback).

Kang and Bryan (2011) used large eddy simulations to investigate the processes of moist convection initiation over heterogeneous surface fluxes. They also found that clouds initially tend to form over relatively warmer surfaces with higher amplitude of surface flux heterogeneity, similar to the observations recorded by Taylor *et al.* (2007) and Gantner and Kalthof (2010). Further investigation by Kang and Bryan (2011) showed that over strongly heterogeneous surfaces (higher amplitude of surface sensible heat flux variation), convective initiation and its development into deep convection is less dependent on surface moisture: in contrast, over relatively weak heterogeneous and homogeneous surfaces, surface latent heat flux plays a significant role for the development of deep moist convection. Also they found that shallow clouds initiate when CBL depth first exceeds the LCL and deep (precipitating) clouds initiate at later times when the LFC over a warm patch has decreased to roughly the same value as the LCL. This observed condition for initiation of precipitating cloud was initially used by Findell and Eltahair (2003a) in the conceptual establishment of their theoretical model, and is also further used in Chapter 2 and 4 to develop a new predictive model.

A modelling study by Garcia-Carreras *et al.* (2011) showed that equivalent potential temperature, θe (closely related to CAPE) are both maximised on convergence lines, at the boundaries of surface moisture contrasts. Triggering of storms, and rainfall maximised on these boundaries.

According to a study conducted by Findell *et al.* (2011) using North American reanalysis data, they showed that high evaporation enhances the probability of afternoon rainfall in the eastern United States and Mexico during summer, leading to a positive evaporation precipitation feedback. In contrast, the intensity of rainfall is largely insensitive to surface fluxes.

In contrast to these various previous results, in the Indian context there is a relatively limited number of studies: particularly regarding this topic related to convective initiation, past work is more focused on the strength and onset of monsoonal rainfall. Lohar and Pal (1995) in a regional study over west Bengal found that an increase in soil moisture due to irrigation significantly hinders the formation of pre-monsoonal thunderstorm activity in that area. In contrast Raman *et al.* (1998) performed sensitivity simulations for variable soil moisture over the Indian subcontinent and found that wet soil conditions intensify the large scale circulations, which further enhance the convective activity and precipitation. A recent study conducted by Asharaf *et al.* (2012) concluded that pre-monsoonal soil moisture (which has recently been artificially modified by irrigation) has a significant impact on monsoonal rainfall.

1.3.2 Observational studies

Geostationary satellite data such as cloud imagery allow us to study processes over larger areas with higher temporal resolution. Taylor and Ellis (2006) for the first time used satellite data to identify mesoscale soil moisture rainfall feedback processes. They found that during afternoon and early evening hours' when storms tend to initiate in response to strong daytime heating, there is a strong suppression of convection over wet soil i.e. negative feedback. However they are not able to give an explanation for this with the limited information from satellite data. Later, Taylor *et al.* (2007), used flight data over the Sahel that provides the first observational evidence that spatial variability in soil moisture and heat flux significantly affect the low level wind field. They found that convergence of warm air occurred over the warmer surface (drier surface), close to the boundary with adjacent wet soil. Dixon *et al.* (2013) showed that these convergence features were reasonably robust in observations, in winds of order 5 m s^{-1}.

In another study, Taylor *et al.* (2010) found that the residual soil moisture patterns produced by an MCS can act as a precursor for a new storm in Sahel. In the study they found that clouds tend to appear over gradients of soil moisture and rapidly deepened and expanded over the drier surface surrounded by wetter surface. In this study they have also

pointed out the possible impact of gravity wave generated from a remote MCS that interfered with convective system under investigation.

In 2011, Taylor *et al.* conducted a scale analysis study using satellite observations of cloud and land surface temperatures over West Africa (a semi-arid region) to demonstrate that the surface exerts a strong control on storm initiation through patches of soil moisture on length scales of approximately 10-40 km. According to the study, convective initiations are twice as likely above strong positive soil moisture gradients compared to uniform soils. They found that 37% of all initiations analyzed occurred over the steepest 25% of gradients. Further extension of these observational studies at global scale, Taylor *et al.* (2012) showed across six continents, afternoon rainfall preferentially occur over soils that are relatively dry compared to surrounding area which contrast with results found in the study of GCMs.

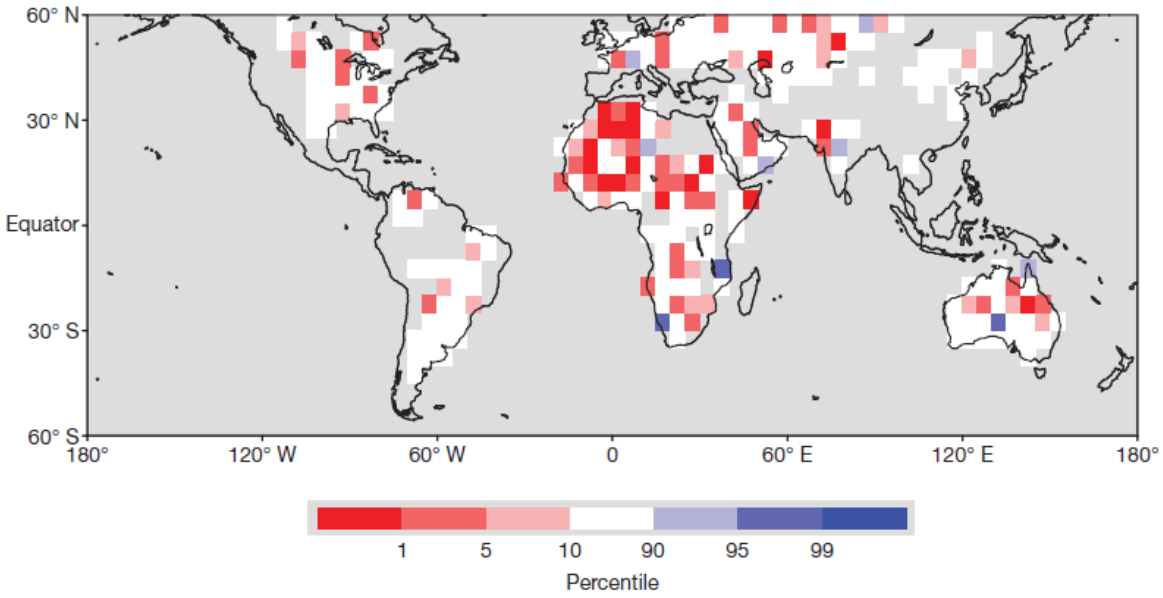

Figure 1.5: Low (high) percentile indicate where rainfall maxima occure over locally dry (wet) soil more frequently than expected. Cited from Taylor *et al.* (2012).

In Figure 1.5 red regions are regions which preferred dry advantage at 95th or 99th percentile whereas blue regions are preferred wet advantage regions but with almost negligible confidence limit. According to this map, Central India is unusual in that it appears to have wet advantage. However, this feature is not statistically significant, because the 10% significance level was used in the study. Guillod *et al.* (2015) also found,

globally, that spatial analysis of rainfall indicates greater prevalence of triggering over locally dry surfaces.

1.4 Theoretical Models

The main driving force behind convective initiation is heat. This heat can either be in the form of latent heat flux from state change of water in the atmosphere, or sensible heat flux. Soil moisture is an important input variable which along with other environmental variables influences the partitioning of these moisture and heat fluxes across the land-atmosphere interface. So far, from the literature review we have found that land surface and atmosphere interaction processes can have multiple pathways and lead to different kinds of feedback processes. During land-atmosphere interaction, different kinds of feedback (positive or negative) can occur between the soil moisture and precipitation (Brubaker and Entekhabi, 1996; Eltahir, 1998). Positive feedback occurs when wet surface leads to precipitation and dry surface inhibits the formation of rain. Similarly in negative feedback, a dry surface favours precipitation whereas wet surface cannot.

1.4.1 1-D models

There is a significant role of the height of the boundary layer in the formation of clouds (Haiden, 1997) and occurrence of rain (Findell and Eltahir, 2003a). Haiden (1997) uses the fact that cloud starts forming in the atmosphere when the PBL height becomes equal to the Lifting Condensation Level (LCL). As noted above, this condition of the PBL approaching the LCL may be applicable to the development of shallow cumulus, but is less relevant to deep convection, for which the LFC is critical. On the other hand Findell and Eltahir (2003a) make use of the idea that there is convective rain when the PBL height reaches the LFC.

The significant study done by Findell and Eltahir (2003a) (here onwards FE03a) has used morning profiles as observed from a radiosonde to force a 1-D slab model. They studied the sensitivity of atmospheric convection to soil moisture conditions over Illinois in the USA and worked out dominant atmospheric conditions when these feedbacks occur.

In this study they looked at characteristics of the morning profile and developed a forecasting framework by defining two parameters, Convective Triggering Potential (CTP as described in Figure and Equation 3.1 in Chapter 3) and Humidity Index (Low), (HI_{low}) (Equation 3.2 in Chapter 3), whose values can predict whether atmosphere is conductive of convection influenced by soil conditions or atmospherically driven. Therefore, this framework could separate behaviour of occurrence of rainfall over wet or dry soil based on threshold values of CTP-HI_{low}. By an empirical study over Illinois, FE03a worked out the threshold values of CTP and HI_{low} required for a convective profile to have wet or dry advantage (Figure 1.6). As observed in Figure 1.6, wet advantage is favoured for CTP between 0 and 200 J kg^{-1} and HI_{low} in the range 5 and 10K, whereas dry advantage occurred for CTP greater than 200J kg^{-1} and HI_{low} in the range 10 and 15K.

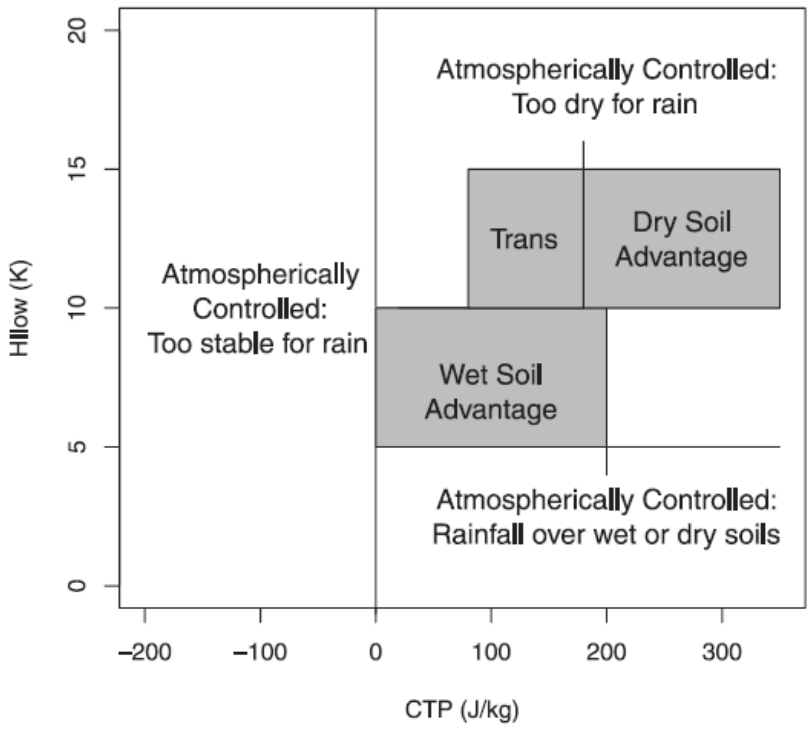

Figure 1.6: CTP-HI_{low} framework, regions in which wet soils and dry soils promote precipitation, as well as transition region, as cited by Tuinenburg *et al.* (2011) from FE03a.

The explanation given by FE03a, for positive feedback (Figure 1.7) over wet surface, is that the convection is triggered by bringing the LFC down to the PBL top through a strong increase in equivalent potential temperature i.e. moistening.

In conditions supporting negative feedback (Figure 1.8 where x-axis denotes time of day) over a dry soil there is smaller latent heat flux, larger sensible heat flux and thus higher surface Bowen ratio and a deeper planetary boundary layer. So, instead of bringing the LFC down to PBL, convection is triggered by bringing the PBL top up to the LFC through strong warming. In contrast during negative feedback, the wet surface cannot produce rain because it exhibits a shallower, moister and cooler boundary layer. So, understanding these feedbacks is important for weather forecasting and there are several modelling and observational studies that have addressed these processes. Some of these studies have been reviewed in this section.

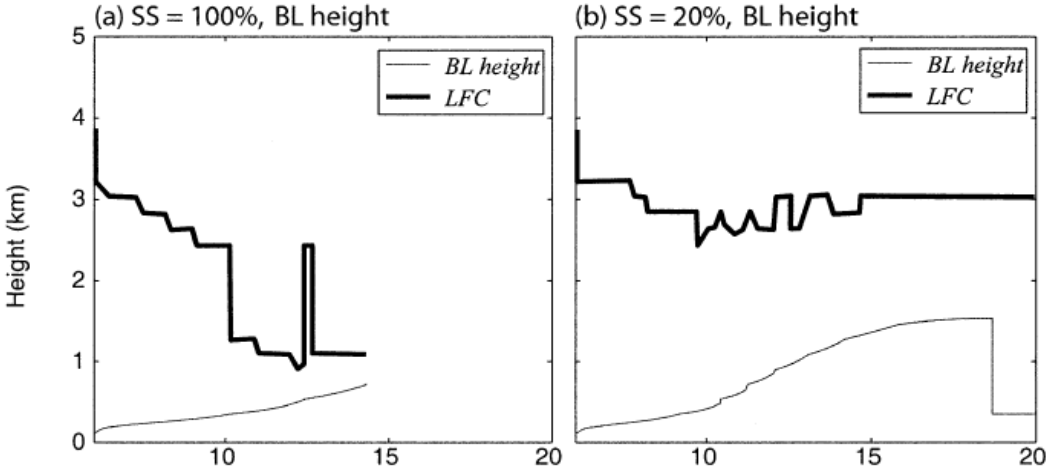

Figure 1.7: Positive feedback mechanism (as cited from FE03a)

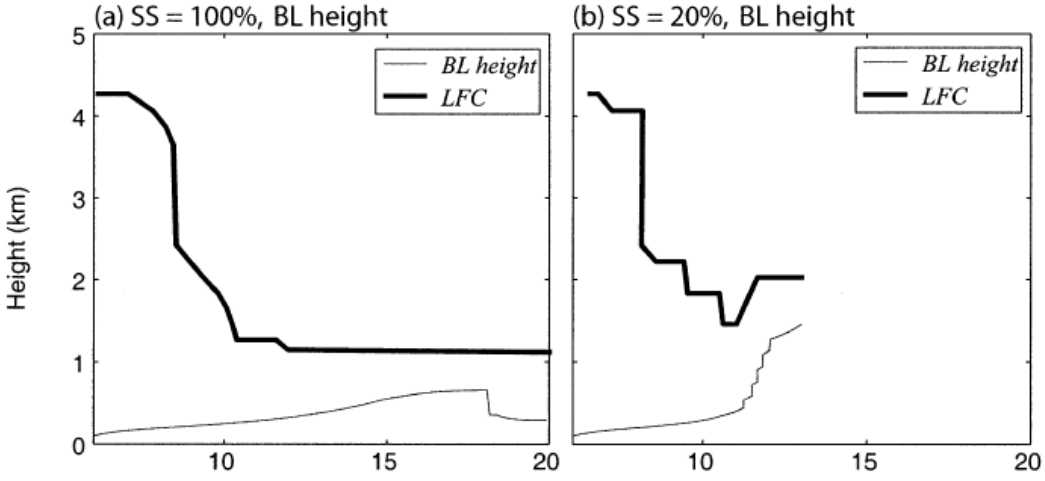

Figure 1.8: Negative feedback mechanism (as cited from FE03a)

1.4.2 3-D models

According to the 3-D model, a surface with heterogeneous soil moisture give rise to focused regions of mesoscale circulation (Segal and Arrit, 1992). In two separate studies (Taylor *et al.*, 2011 and Garcia- Carreras *et al.*, 2011) found convective initiation to be favoured on the downwind side of dry surfaces (crop land), close to wetter surfaces (forested regions).

The mechanism includes idealized soil moisture induced flow (blue arrow Figure 1.9) under light synoptic wind creating an ascent region where the shallow strong current opposes the mean wind. The preferred location of convective initiation coincides with the ascent region induced by the heating gradient at the downwind edge of the dry patch (Taylor *et al.*, 2011, here onwards T11).

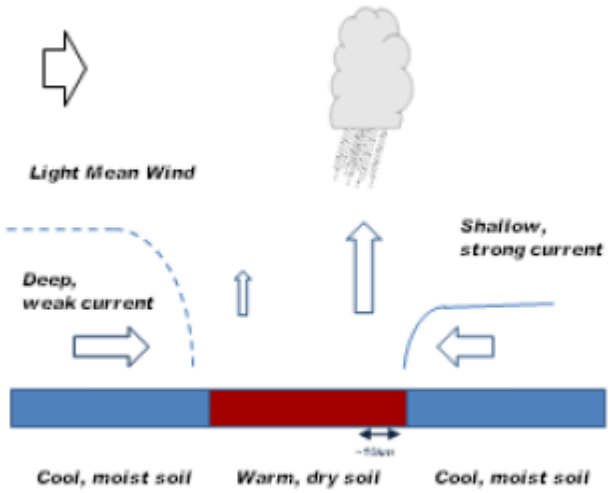

Figure 1.9: Mechanism depicting convective cloud initiation over heterogeneous soil moisture surfaces as cited from Taylor *et al.* (2011).

Note that these mechanisms (1-D and 3-D) only refer to the first initiation of convection. Organised convection, such as MCSs, has its own internal triggering mechanisms and is less sensitive to surface-forced triggering. Hartley *et al.* (2016) indicate that large organised squall lines over West Africa have a different response to the surface state than isolated convection events.

1.4.3 Other Land-atmosphere feedback mechanisms

Schar *et al.* (1999) investigate the land-atmosphere feedback processes as direct and indirect mechanisms over continental Europe. In the direct (or recycling) mechanism, the surplus of precipitation over wet soils derives directly from evaporation within the same region (Figure 1.10a). In contrast, in the indirect (or amplification) mechanism the surplus of precipitation derives from a remote location and is transported over long distances by the atmospheric circulation, but the efficiency of the precipitation processes is determined by the state of the soil (Figure 1.10b). In this case there is surplus of precipitation over wet surface instead of dry, which is provided by atmospheric advection of moisture.

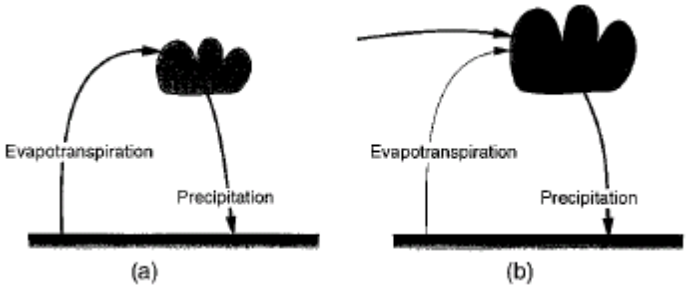

Figure 1.10: a) recycling mechanism; b) amplification mechanism (Schar *et al*., 1999)

Schär *et al.* (1999) has given three reasons for above process to occur. First, high values of CAPE due to buildup of moist entropy into a shallow layer over wet (low Bowen ratio) surface. Secondly, high values of relative humidity over a low Bowen ratio surface leads to lowering of LFC. These two factors agree well with the Betts *et al.* (1996) discussion that entrainment of free tropospheric air into growing boundary layer will ultimately control the potential for convective instability. Third, the surface energy balance shows the presence of positive feedback mechanisms of radiative origin. It is based on the fact that net radiative flux (which ultimately can be converted into low level moist entropy and convective instability) is large over moist soil, in spite of increased cloud cover.

1.4.4 Evidence supporting different theoretical models

By the use of the same slab model used by FE03a, applied to 25 years of sounding data, Tuinenburg *et al.* (2011) worked out the threshold values for the FE03a model (CTP-HI_{low}) for the Indian region and found the values to be slightly higher in India to trigger convective activity, compared to the USA. They further observed that during onset and retreat of the monsoon, the east and south of India show more potential for feedbacks than the north, which was, they suggested, because of large scale irrigation over these areas. On testing this hypothesis they found a positive trend in the precipitation just before the monsoon onset over irrigated stations whereas there was no such forward trend over non irrigated stations.

Ferguson and Wood (2011) investigated 7 years of satellite remote sensing data to produce global maps of coupling signals of CTP-HI_{low} and validated them using radiosonde observations. They have also produced a modified CTP-HI_{low} framework. According to modified framework they found that India is mostly having wet advantage.

Taylor *et al.* (2013) compared regional simulations using a single model, run at different spatial resolutions, and with convective parameterizations switched on or off against Sahelian observations. The results from convection permitting simulations shows formation of the soil moisture heterogeneity driven circulations that in turn generate convergence and reduce convective inhibition in the hours preceding initiation. At the daily time scale, the explicit (parameterized) simulations show suppressed (enhanced) rainfall probabilities over wet soil, indicative of negative (positive) feedback at scales of 12–156 km, and making agriculturally important dry spells less (more) likely (Taylor *et al.*, 2013).

1.4.5 Final remarks

Although now it is well established that soil moisture and precipitation/moist convection feedbacks do exist, in the literature there are two branches of explanation for these processes

i) 1-D model relating wet and dry advantage to the ambient profile conditions (FE03b), and

ii) A 3-D mesoscale circulation model (Liu and Avissar, 1996; Pielke, 2001; Garcia-Carreras *et al.* 2011; Taylor *et al.* 2011), in which convergence on boundaries of surface forcing controls the spatial pattern of triggering.

However, it is still not clear under which circumstances, which theoretical model is best and also are they sufficient for all soil moisture conditions from heterogeneous to homogeneous at the length scale of convection? The 1-D model considers only point values of soil moisture to describe wet and dry soil. It is not clear whether we can extend the applicability of 1-D model to 2-D or 3-D soil moisture conditions i.e. can soil moisture heterogeneity be accommodated in 1-D model?

1.5 Summary, and Research Questions

This chapter summarizes the main motivation behind this study which is the importance of land-atmosphere interactions in Indian monsoon rainfall. Understanding and predicting these interactions is needed for accurate rainfall forecasts, for a rain-fed economy. The chapter has summarized the physics of land atmosphere coupling by studying boundary layer processes, surface energy balance, coupling parameters like surface Bowen ratio and evaporative fraction, simple 1-D mixed layer model, convective parameters such as CAPE and CIN etc. This chapter has further revisited the existing literature on soil moisture-precipitation coupling in terms of modelling and observational study. There are two main branches of literature explaining soil moisture-precipitation feedback as 1-D model (FE03a) and 3-D mesoscale circulation (Segal and Arrit, 1992, Taylor *et al.*, 2011 and Garcia- Carreras *et al.*, 2011).

The objective of this research is to examine the impacts of variability in soil moisture distribution on convective rainfall initiation over the Indian sub-continent using theoretical, observational, and mesoscale atmospheric models. The majority of the study will be tested under a convection-permitting mesoscale modelling environment. Thus, in this context the focus of the research is:

1) An observational and modelling case study to find signals of land-atmosphere coupling as described in Chapter 2.
2) Categorization of soil moisture state (Dry, wet, gradient, null (explained later in Chapter 3)) at regional scale.
3) Quantitative study of key questions in land-atmosphere interaction for India; what is the impact of soil moisture variability on convective rainfall initiation? Is there any kind of advantage (or not) either over soil moisture gradients, null conditions, wet or dry soil?
4) Test the existing theories of land-surface forcing on convection over the Indian sub-continent, under a mesoscale modelling environment as summarized in Chapter 3.
5) To explain the findings of the quantitative analysis by exploring the physical relationship between the boundary layer parameters like surface Bowen ratio, convergence, stability etc. using a new theoretical framework, as described in Chapter 4.

2 Evidence for Land Atmosphere Interaction in this region using observations and modelling data.

This chapter aims to show evidence of land-atmosphere interaction over the Indian sub-continent, from observations and modelling data. It attempts to relate theoretical models described in Chapter 1 to the observed atmospheric phenomenon.

Over the Indian sub-continent**,** the in situ observations are very limited and irregular, so to investigate the effect of the surface condition on the boundary layer, synoptic observations are used in the first part of this chapter. Our initial approach was to see the response of the boundary layer to the indirect change in the soil moisture conditions. We know the boundary layer responds to surface fluxes, which directly affect the surface temperature and humidity and ultimately all the boundary layer properties. So, we took the antecedent rain event as a factor to account for changes in soil moisture conditions and observed the response of surface temperature and relative humidity (RH) for several days after and one day before the rain event day. We have also studied the daily lowest Lifting Condensation Level (LCL) height which is a function of surface parameters.

The second part of the chapter is attributed to case studies from the EMBRACE output. Cases are chosen based on their significant surface, dynamic, synoptic and one-dimensional profile properties. Later in summary, depending on the observed properties, an attempt is made to relate the cases to the theoretical thermodynamic and dynamical models described in Chapter 1. Thus these case studies provide a firm base to carry out further investigation of the afternoon initiations based on one-dimensional and three-dimensional perspectives, which is done in Chapter 3 and Chapter 4.

2.1 Analysis of Synoptic Observations:-

The Indian subcontinent can be broadly divided into 3 categories of agro climatic conditions: i) Humid ii) Semi-arid and iii) Arid as shown in Figure 2.1a. Thus for the analysis of the synoptic surface data, we have chosen four stations (Figure 2.1b) in different agro-climatic conditions during the monsoon period, which includes the June, July, August and September months. Here Jodhpur has the arid conditions, Delhi and Ahmdabad have semi-arid conditions, whereas Bhubaneswar has humid conditions.

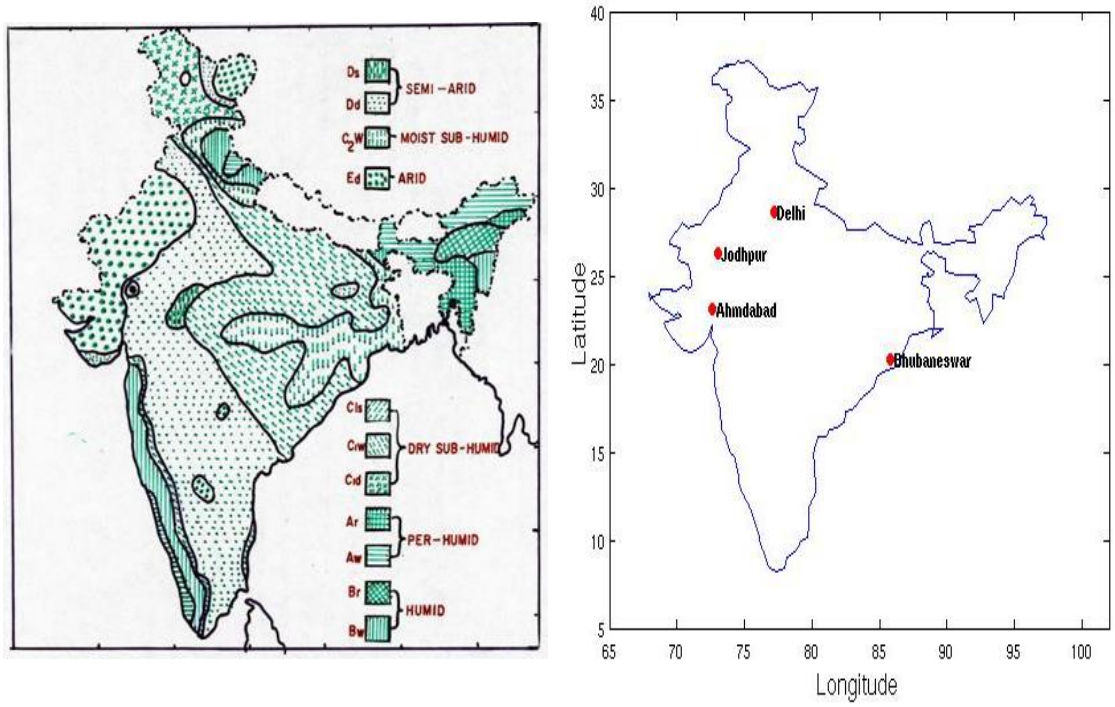

a) b)

Figure 2.1: a) Agro climatic classification of the Indian sub-continent. (imdagrimet.gov.in) b) Location of various synoptic stations considered for analysis.

Using 10 years (2002 to 2011) of the surface data from synoptic stations for the monsoon period (JJAS), the average trend (green line in Figure 2.2) of the daily maximum temperature, minimum RH and the lowest LCL with respect to the rain event is plotted. In the plots the rainfall day is denoted by zero on the x-axis, while the positive numbers on the x-axis represent the day number after a rain event and negative numbers represent the day number before a rain event day. The y-axis denotes the value of the parameter

considered, such as ℃ for temperature. Blue circles are the scatter-plot of 10 years of the maximum temperature data over a station. The green line is the mean trend of the temperature and red bars are error bars.

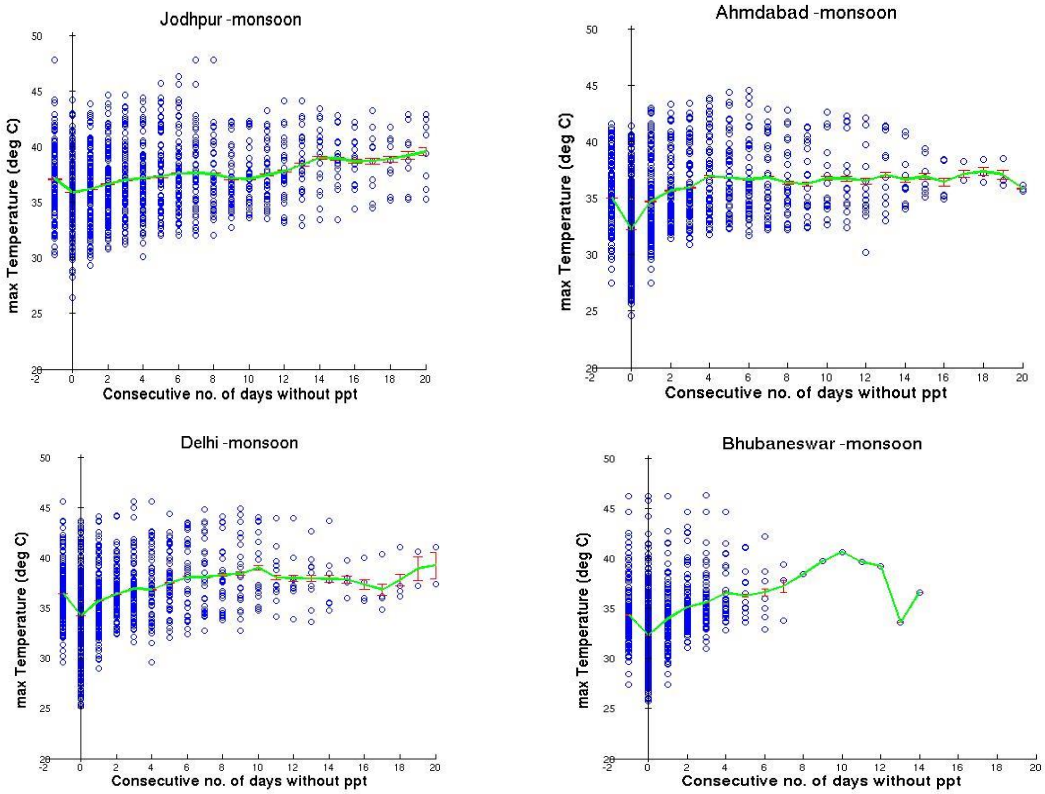

Figure 2.2: Surface temperature (y-axis) response to the rainfall for the four different synoptic stations. Here time-axis denotes day number before (negative number) and after (positive numbers) the rainfall day (x=0). The green line shows the 3-day running mean trend of the surface temperature. The vertical red line denotes the error bars based on standard errors.

From Figure 2.2 it can be seen that there is a significant drop of around 3 ℃ of maximum temperature in semi-arid stations Delhi and Ahmdabad due to rainfall. The atmosphere takes around two days to get back to the seasonal mean daily max temperature. Over humid and arid stations Bhubaneswar and Jodhpur this drop of temperature is comparatively low. Also, over the station Jodhpur the recovery time is least, which is nearly 1 day. The reason for this quick recovery of the maximum temperature over the Jodhpur is because there is a very small drop in maximum temperature due to rainfall, which may be due to small amounts of rainfall that evaporate rapidly.

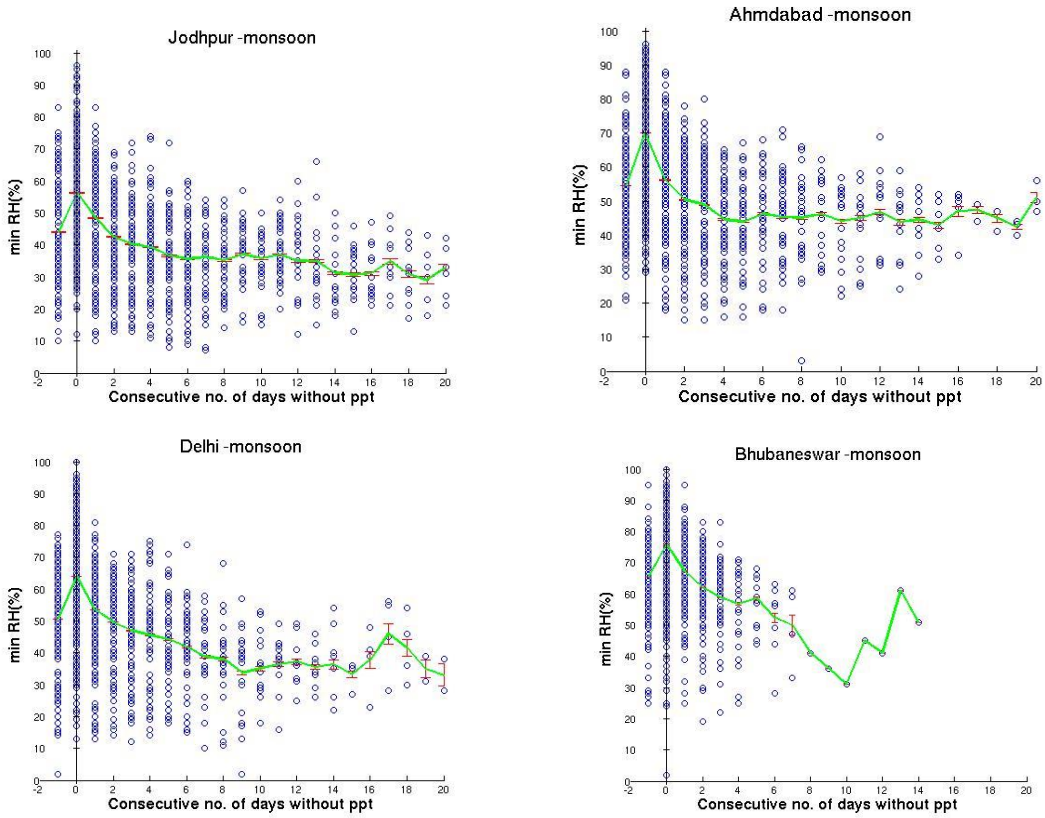

Figure 2.3: Same as 2.2 but parameter plotted is daily minimum relative humidity (%) on y-axis.

Similar to the maximum temperature, from Figure 2.3, the minimum RH rises more for the semi-arid regions Delhi and Ahmdabad during the rainfall day and takes around 2-3 days to fall back to the seasonal mean. In Figure 2.4 pressure at LCL (P_{LCL}) of the arid station Jodhpur falls 40 hPa from the previous day to the event day which is more comparable to semi-arid stations. However, over Bhubaneswar the P_{LCL} drop is minimum. P_{LCL} takes two days to recover for the arid and semi-arid stations whereas one day for humid station like Bhubaneswar.

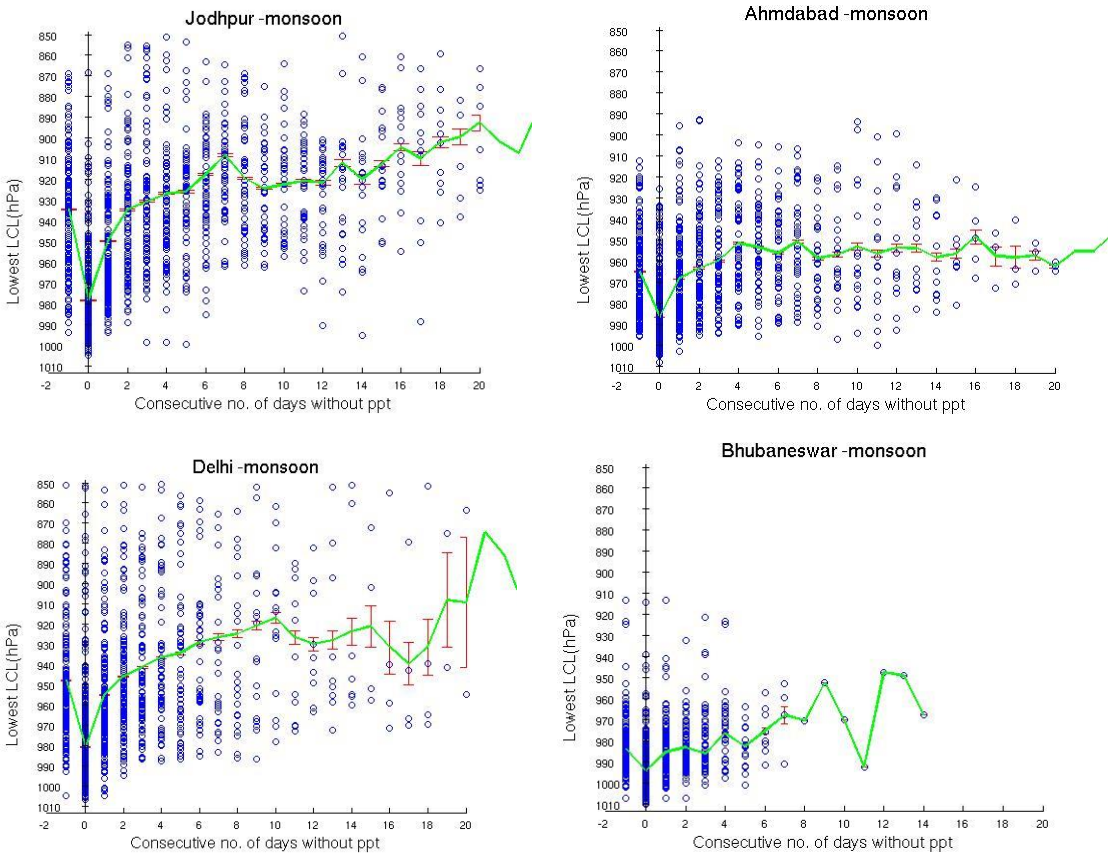

Figure 2.4: Same as 2.2 but parameter plotted is daily lowest LCL level (hPa) on y-axis.

In summary, we can say that the sensitivity of surface parameters to rainfall or changing soil moisture is about one to two days in general but could be sometimes three days, depending on agro-climatic conditions. Over the humid region the rise and drop of the maximum temperature and humidity are recovered within one day. Similarly, over the semi-arid region there is a drop and recovery of 3℃ of the daily maximum temperature, 10-12% rise and drop of minimum RH, and nearly 30 hPa drop and recovery of P_{LCL} within 2 days approximately. Thus in general, for the semi-arid regions, the recovery period from an anomaly of surface parameters is greater compared to arid and humid regions for most of the parameters. The reason for this longer response time to changes in the soil moisture in semi-arid region could be attributed to limited water availability which affects the release of energy due to heating in the form of latent heat of condensation. Taylor *et al.* (2013), on studying CASCADE simulations similar to EMBRACE but for the Sahel also found preference for initiations to occur near the downwind end of mesoscale regions of lower latent heat flux produced by rainfall patterns in the previous 1-2 days. Therefore, we have evidence that changes in soil moisture

condition affect surface parameters and hence the boundary layer to the time scale of several hours up to a few days.

In Figure 2.2 to 2.4 the relative role of advection on local land-surface feedbacks are not taken into account due to data limitation from synoptic stations. For instance in cases of strong synoptic advection, warming and cooling will be dominated by the large-scale winds rather than local processes. These effects can be studied if we consider for example only light wind cases and omit advection cases by taking into account large scale model data like ERA Interim . We can also filter out the cases if corresponding radiosonde wind observations are provided.

2.2 Case studies from model output

This section exploits non-parameterized mesoscale simulations to illustrate the important boundary layer processes that cause afternoon deep convective initiations. In the form of case studies, temporal evolution of the various boundary layer parameters and their connection to each other is studied. The model data are then explored more deeply in Chapters 3 and 4.

2.2.1 The numerical model

Diagnostics from a limited area model simulation of the Met Office Unified Model (Met UM), run as part of the Earth system Model Bias Reduction and assessing Abrupt Climate change (EMBRACE) project, are used for this study. The UK Met Office Unified Model (MetUM) version 8.2 has been run at various resolutions like 24, 12, 8, 4, 2.2 km. Some of the runs include parameterized convection and some are non-parameterized convection summarized in Table 2.1. Out of all the above mentioned resolutions, the 8, 4, 2.2 km model runs are available for the non-parameterized convection simulation and used a 3D Smagorinsky scheme for sub-grid mixing.

Resolution	Convection type
24 km	Parameterized
12 km	Parameterized
8 km	Parameterized
8 km	Non-parameterized
4 km	Non-parameterized
2.2 km	Non-parameterized

Table 2.1: Summary of resolution and corresponding convective scheme used in EMBRACE simulation.

Using a semi implicit, semi-Lagrangian scheme (Davies et al. 2005), the non-hydrostatic deep-atmosphere equations of motion are solved. For horizontal grid uses a staggered Arakawa C-grid and in vertical levels a terrain following hybrid-height Charney–Phillips vertical grid are used. For representing small and complex processes a comprehensive set of parametrisations are used, such as surface exchange (Essery et al. 2001), boundary layer mixing (Lock et al. 2000), mixed-phase cloud microphysics (Wilson and Ballard 1999), and an optional mass flux convective parametrisation scheme (Gregory and Rowntree 1990).

It considers four soil levels, with thickness (starting with the surface and working downwards) of 0.1, 0.25, 0.65 and 2 metres. The soil moisture was initialised by downscaling the soil moisture in the global model analysis. The soil moisture stress is kept the same as in the global model which means that the soil moisture is the hi-res models is different to that in the global because of the more detailed soil properties in the hi-res model. The soil hydraulics follows the "van Genchten" model (Genuchten, 1980). The model run with 4 km grid-spacing over a large domain containing the entire Indian subcontinent has been considered for further study throughout this thesis. The model is initialised at 18/8/2011 00z with the Met Office global operational analysis flow fields and run for 21 days. Lateral boundary conditions are updated every hour and derived from a series of 6 hour long global MetUM simulations run from each successive operational analysis which is available every 6 hours. EMBRACE simulation configuration is described in detail in Willetts et al. (2017 in press).

Previous studies with the same model have been able to validate its performance in representing convective rainfall. Marsham et al. 2013 using CASCADE simulations over Sahel showed that explicit moist convection significantly improves the diurnal cycle of cloudiness, and outgoing radiation, compared with observation. The timing of the diurnal maxima in precipitation is similar to that of observation, which is 6 hour later than parameterized simulation.

Pearson et al. (2013) found substantial improvement in diurnal cycle of rainfall in 4 and 12 km explicit compared to 12 km parameterized. Study of same CASCADE simulation by Taylor et al. (2013) in the Sahel region at different resolution and with the convective scheme on and off has shown that a convection-permitting simulation at 4 km can produce reasonable spatial relationships between soil moisture and convective triggering similar to those inferred from observational proxy data.

Willetts et al. (2017 in press) has evaluated the EMBRACE simulations and found that the later convection (similar to observation) in convection-permitting simulations over land improves the diurnal cycle of rainfall, thus improves the diurnal cycle of the land-sea pressure gradient, and hence enhances the onshore moisture advection. It further showed that the ability of the simulations to capture the diurnal cycle of convection is not only important for radiation and surface fluxes, but also for the dynamical couplings between convection and the larger scale flows like the monsoon flow. According, to a comparative study by Willetts et al. (2017 in press), mean total rainfall amounts in the monsoon trough in EMBRACE simulation with 2.2, 4 and 8 km explicit convection runs, compare relatively well with satellite products compared to and 24, 12, 8 km parameterized convection runs. Pearson Correlation Coefficients (PCC) with TRMM, 4 km explicit capture the day-to-day variability over the subcontinent (and the monsoon trough region) best with PCC value 0.57 (0.52).

On comparing the hourly mean rainfall of 8, 4, 2.2 km run subjectively as shown in Figure 2.5, it is apparent that the 4 km run is more close to reality, for instance over the wide scanty rainfall region of the Ganges and comparatively higher rainfall over Central India. However, the model has less rainfall for the Western Ghats.

Thus, in view of above studies and considering the available computing resources, 4 km convection permitting simulation is chosen to study impact of soil moisture on convective activity over the Indian sub-continent.

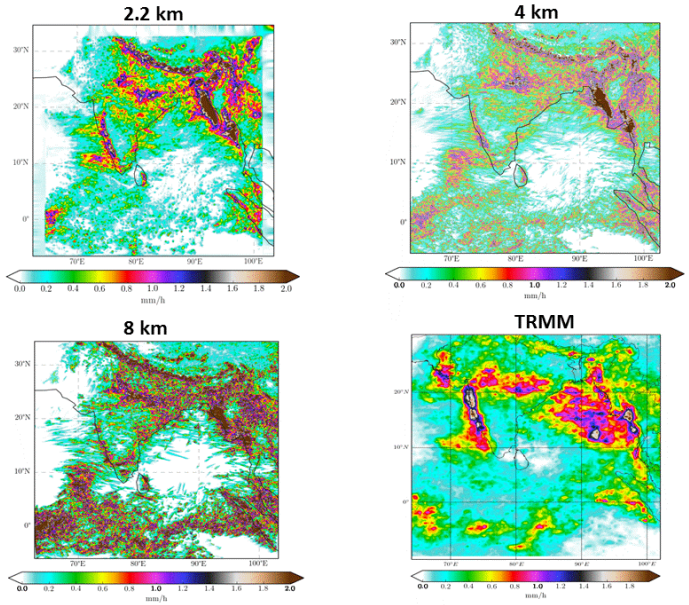

Figure 2.5: Hourly mean rainfall (mm hr^{-1}) state for different resolutions non-parameterized run and TRMM (cited from Peter Willetts EMBRACE research work).

The model run with 4 km grid-spacing over a large domain containing the entire Indian subcontinent has been considered for further study throughout this thesis. The simulation is convection-permitting, in which the circulation, triggering and life cycle of the convection is allowed to develop explicitly, unlike the standard climate models (with parameterized convection) presented in the Taylor *et al.* (2012) study. A rain event is diagnosed with a method similar to Taylor *et al.* (2013) using hourly accumulated precipitation between 1130 local time (LT) and 2030 LT (where LT is UTC plus 5.5 hours). To analyse the soil moisture conditions, three-hourly average soil moisture prior to the rain initiation is computed.

2.2.2 Data and methodology

All the analyses have been performed in the immediate vicinity of regions that have received afternoon rainfall. The very first step in the method is to identify a continuous

rain area (Ebert and William, 2009) using the flood fill algorithm and thresholding technique. According to this technique all the adjacent pixels exceeding a given threshold value of rainfall are collectively considered as one rain event. The minimum number of pixels to define a rain event as significant, in this study is considered as 3 pixels which is 48 sq. km. The minimum rain threshold for all the domains is taken as 3mm accumulated rain in one hour. Then, the location of initiations is traced back to a single grid point, using 10-minute accumulated rainfall. Finally, an afternoon rainfall event is defined where there is no rainfall in the chosen area in the 3 hours preceding 1130LT. The purpose of performing this filtering is to separate stratiform rainfall events (that continued from overnight) from the locally initiated convective events which can take place during the afternoon due to the local forcing. Based on the identification of these rain initiations (as shown in Figure 2.6), the rest of the study in Chapter 3 and Chapter 4 on soil moisture, orography, morning profile (e.g. CTP-HI_{low}) analysis and wind convergence analysis has been carried out.

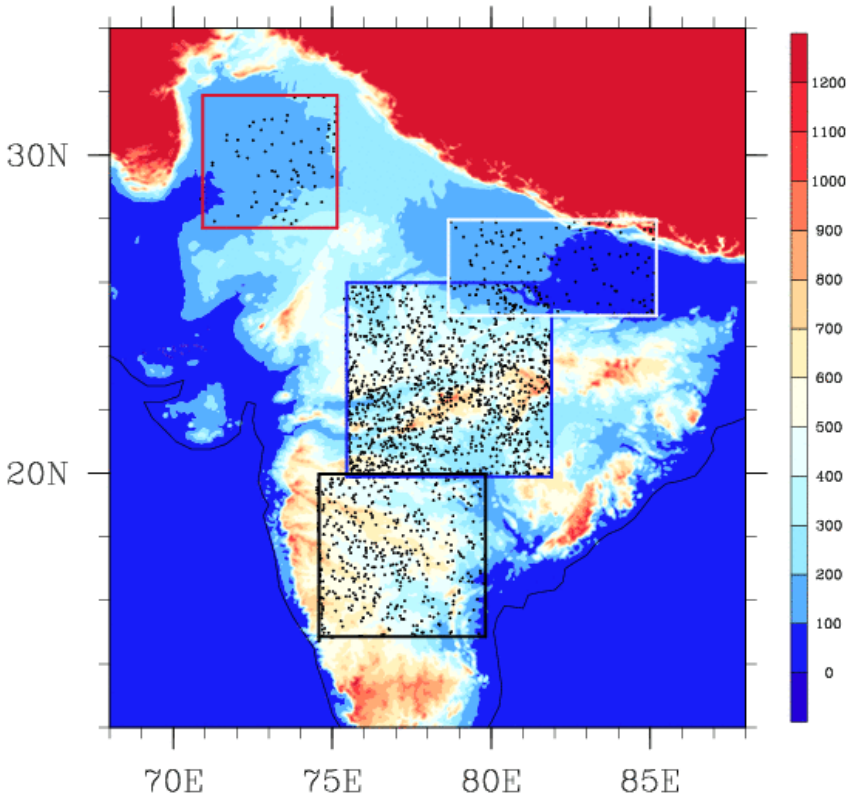

Figure 2.6: Black dots represents afternoon rain initiations during the 20 day simulation period across the four considered domains describe in detail in the Chapter 3.

2.2.3 Data analysis

In this section we have chosen certain extreme cases of the soil moisture conditions, like very wet, dry or gradient conditions, along with some dynamic and synoptic cases. Then these cases are studied in detail by looking at the various thermodynamic and dynamic parameters. To analyse the cases, moisture budget components and boundary layer parameters are plotted. All the cases considered here have flat orography to diminish the effect of orographically induced rainfall.

To compute moisture budget components such as horizontal, and vertical moisture convergence, a moisture budget method (Banacos and Schultz, 2005) is employed. The moisture budget for an air parcel is defined as

$$\underbrace{\frac{\partial q}{\partial t}}_{\substack{local\ rate\ of \\ change\ of\ q}} + \underbrace{\nabla.(qV_h)}_{-horizontal\ MFC} + \underbrace{\frac{\partial(qw)}{\partial p}}_{-vertical\ MFC} = \underbrace{E - P}_{sources\ and\ sinks}$$

Here MFC implies moisture flux convergence. Evaporation is referred as a source and precipitation is referred to as sinks of moisture in the atmosphere.

$$Horiz.MFC = -\nabla.(qV_h) = \underbrace{-V_h.\nabla q}_{advection} - \underbrace{q\nabla.V_h}_{convergence}$$

$$Horiz.Moisture\ Convergence = -q\left[\frac{\partial u}{\partial x} + \frac{\partial v}{\partial y}\right]$$

$$Horiz.Moisture\ advection = -u\frac{\partial q}{\partial x} - v\frac{\partial q}{\partial y}$$

Figure 2.7a represents horizontal moisture convergence whereas 2.7b represent horizontal advection. Figure 2.7c represents vertical moisture convergence along an east to west line defined as

$$Vert.Moisture\ Convergence = \frac{\partial(qw)}{\partial p}$$

Where q is specific humidity and u, v, w are wind directions in x, y and z direction. b)

Case 1: Gradient soil moisture case I

This is a case of 19 July 2011 of the EMBRACE simulation. In Figure 2.7a, 2.7b, 2.7d (and subsequent figures) the coordinate (0,0) denote the point of convective initiation. Figure 2.7a represents horizontal moisture convergence at 925 hPa whereas 2.7b represents horizontal moisture advection and 2.7c represents vertical moisture convergence all prior to two hour from initiation. Figure 2.7d shows a dry to wet soil moisture gradient in the downwind direction at 925 hPa similar to T11 (heterogeneous conditions). Prior to the convective initiation, a strong vertical moisture convergence (Figure 2.7c) in the upper levels is observed. At the same time, there is

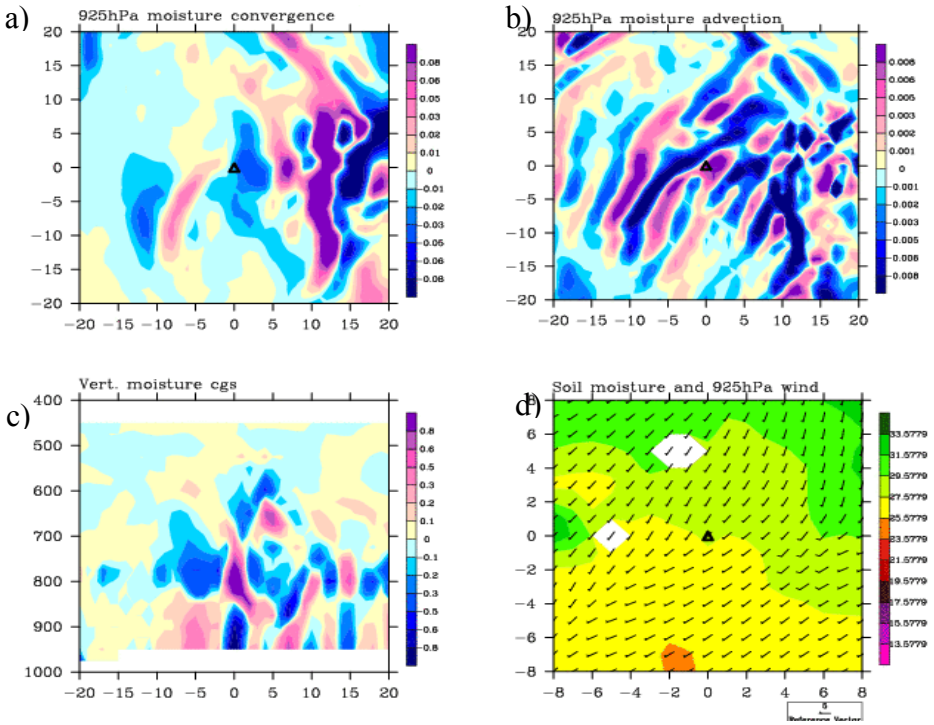

Figure 2.7: a) 925 hPa horizontal moisture convergence; b) 925 hPa moisture advection; c) vertical moisture convergence East-West crossection passing through initiation point. All are computed two hours prior to initiation and d) three hourly average soil moisture prior to initiation, overlaid by 925hPa wind barb, two hours before the rain initiation for Case 1.

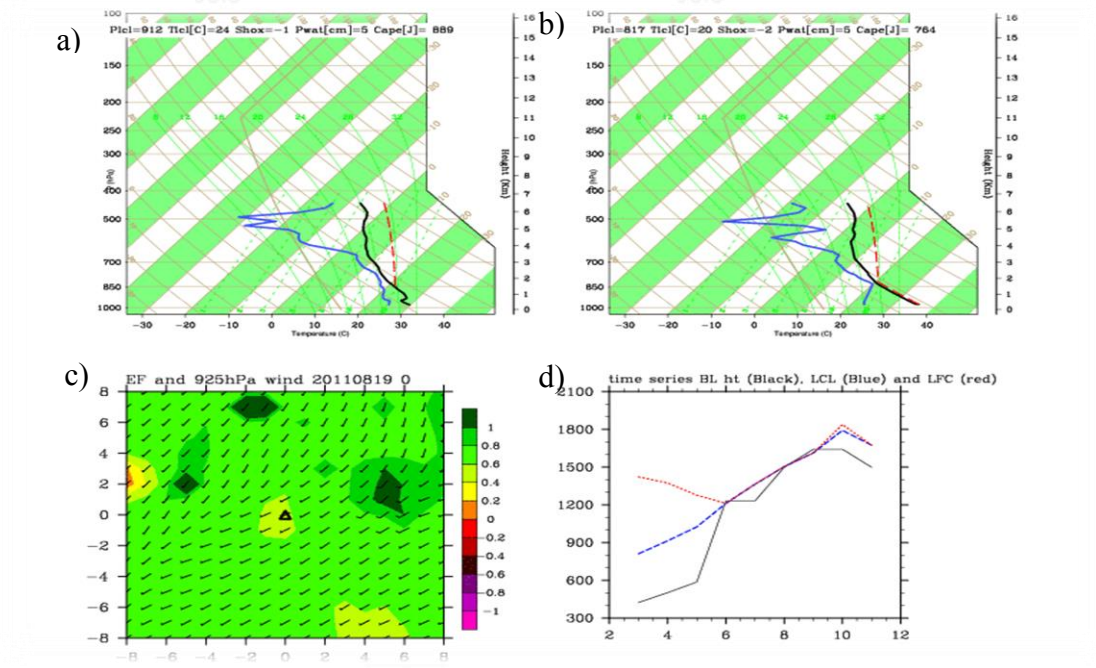

Figure 2.8: a) Tephigram of the morning 0830 LT profile for Case 1; b) Tephigram of the profile two hours prior to the initiation; c) Three hour average of evaporative fraction prior to the initiation overlaid by 925 hPa wind two hour before of the initiation; d) time series of the boundary layer height (black), LFC(red), LCL(blue) from 3UTC (0830LT) to the initiation time.

strong horizontal moisture advection is seen (Figure 2.7b): this could be related to synoptic forcing during the monsoon season.

The morning profile of 0830LT (0300UTC) indicates low-level temperature inversion (Figure 2.8a) which means slight stability at lower levels. By afternoon, that is 1430LT (0900UTC) due to mixing in the boundary layer by surface heating, the temperature inversion vanishes (Figure 2.8b). Apart from this there is a decrease of the LFC due to moisture convergence. However, observed increase of the LCL and boundary layer height (Figure 2.8d) results from strong surface heating of a relatively low evaporative fraction area as seen in Figure 2.8c. It is worth to note here that the LFC (red curve) and LCL (blue curve) tendencies are opposite initially, which implies that Haiden's (1997) approach of analysing the behaviour of LCL would not be useful here to study the deep convective initiation.

Case 2: Gradient soil moisture case II

a) b)

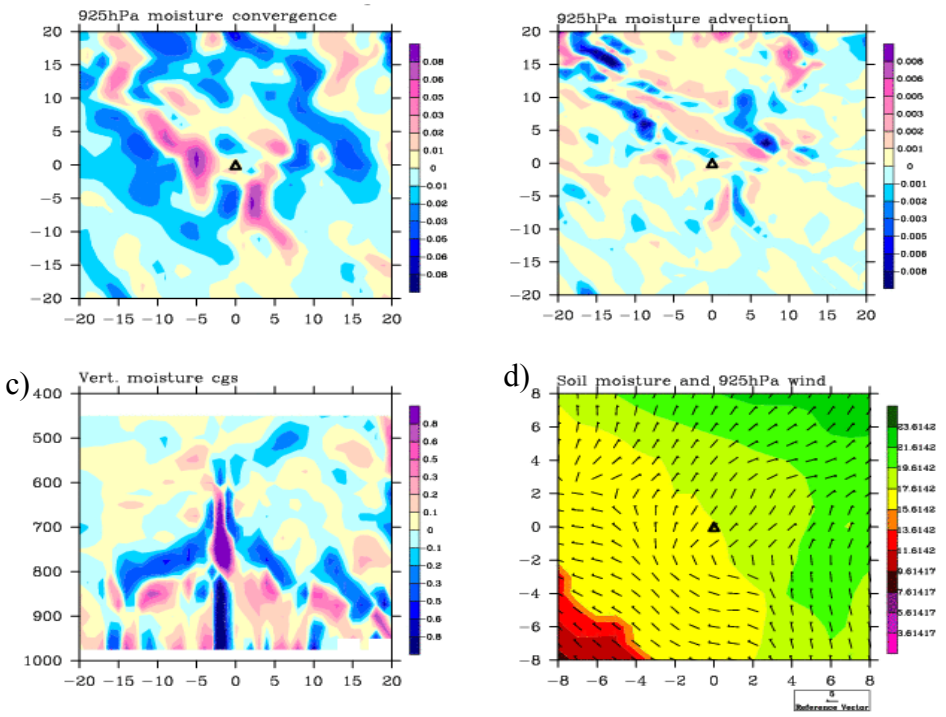

Figure 2.9: same as Figure 2.7, for Case 2

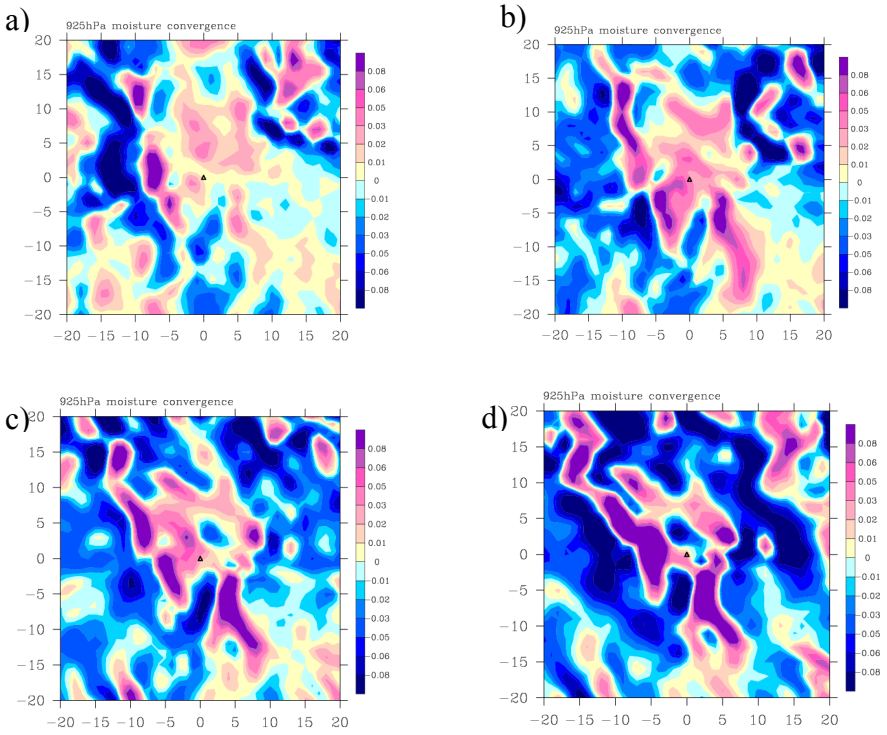

Figure 2.10: 925hPa horizontal wind convergence for Case 2 at times (t-5)h to (t-2)h, (a to d) , where t is the time of rain initiation.

Case 2 is a gradient soil moisture case (Figure 2.9d) of 20 July 2011 of the EMBRACE simulation, where soil moisture decreases in the downwind direction (that is wet to dry

gradient). From Figure 2.9a and Figure 2.9c, a strong linear convergence and vertical moisture convergence is seen close to initiation. Also, here it is worth mentioning that horizontal advection (Figure 2.9b) is weak, thus there is little evidence of synoptic forcing.

If we plot horizontal convergence plots prior to initiation time -5h to initiation time -2h (Figure 2.10 (a-d)) we can see increases in intensity and organization of convergence over the dry soil close to the gradient as the day progresses. This strong linear convergence gives rise to cumulus cloud formation and hence the rain initiation which confirms the dynamic triggering of initiation due to heterogeneous soil moisture conditions. We can say it is a case that has close resemblance with the conditions mentioned in T11 for afternoon convective initiation, but that the gradient is in the opposite direction.

Case 3: Wet case, East domain

This is a case from the East domain, dated 26 July, 2011. This case has high absolute values of soil moisture thus can be referred to as wet case (Figure 2.11d) with no strong horizontal or vertical convergence (2.11a and 2.11b). Figure 2.12c also represents a homogeneous EF field at convective scale and high value of evaporative fraction (0.6< EF <0.8) case. Here the convection appears to initiate by the 1-D profile approach (as mentioned in FE03a), where LFC drops down due to moistening of the boundary layer by surface evaporation, to the level of boundary layer height very rapidly, within two hour, and rain initiates one hour later which is by 0600 UTC, as seen in Figure 2.12d. Here it is worth to mention that there is no sign of dynamic triggering, as horizontal and vertical moisture convergence (Figure 2.11a and 2.11c) is almost negligible.

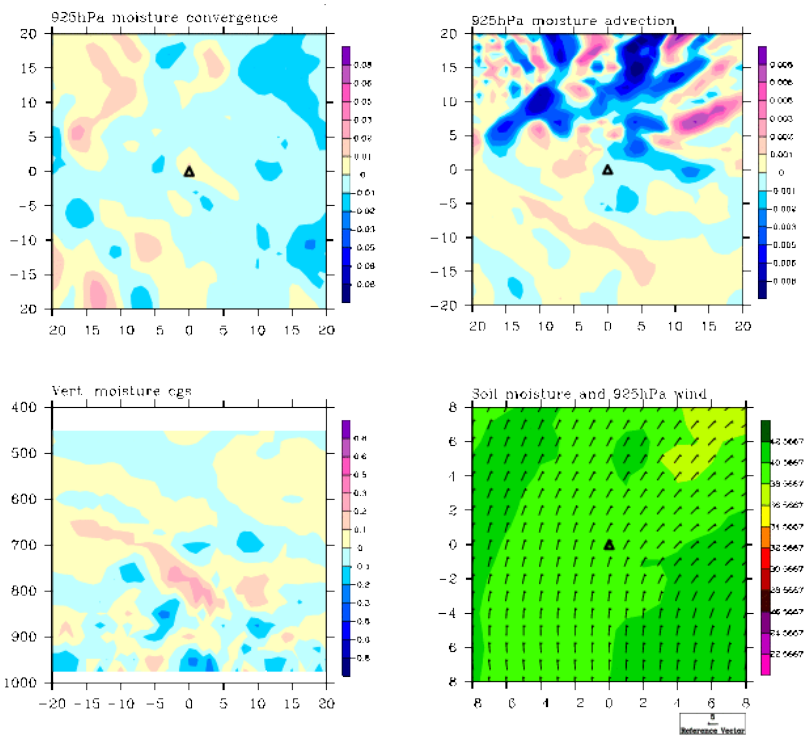

Figure 2.11: Same as Figure 2.7, for Case 3

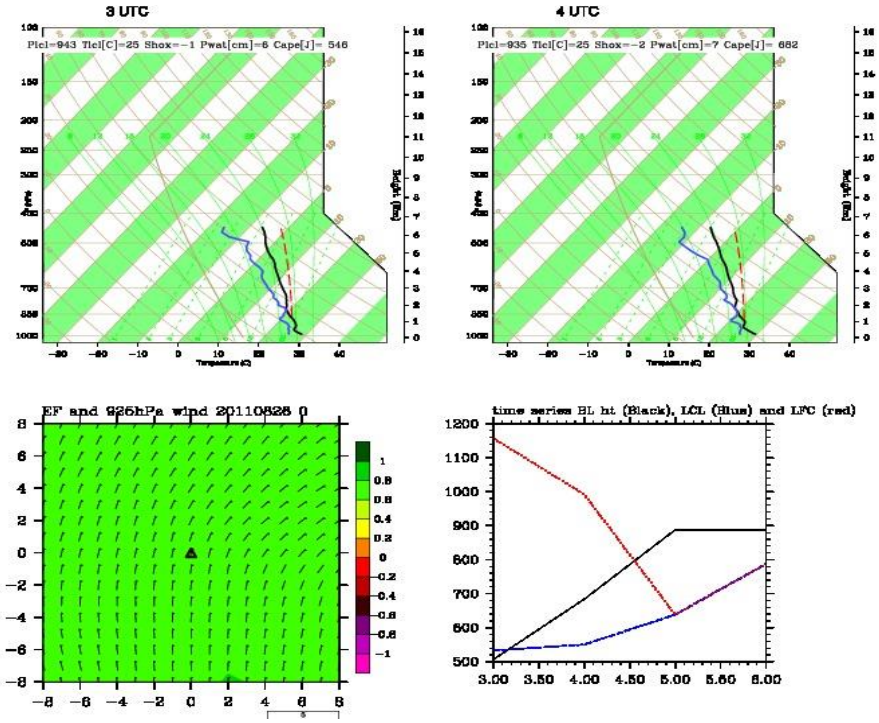

Figure 2.12: same as Figure 2.8, for Case 3

Case 4: Dry soil moisture case

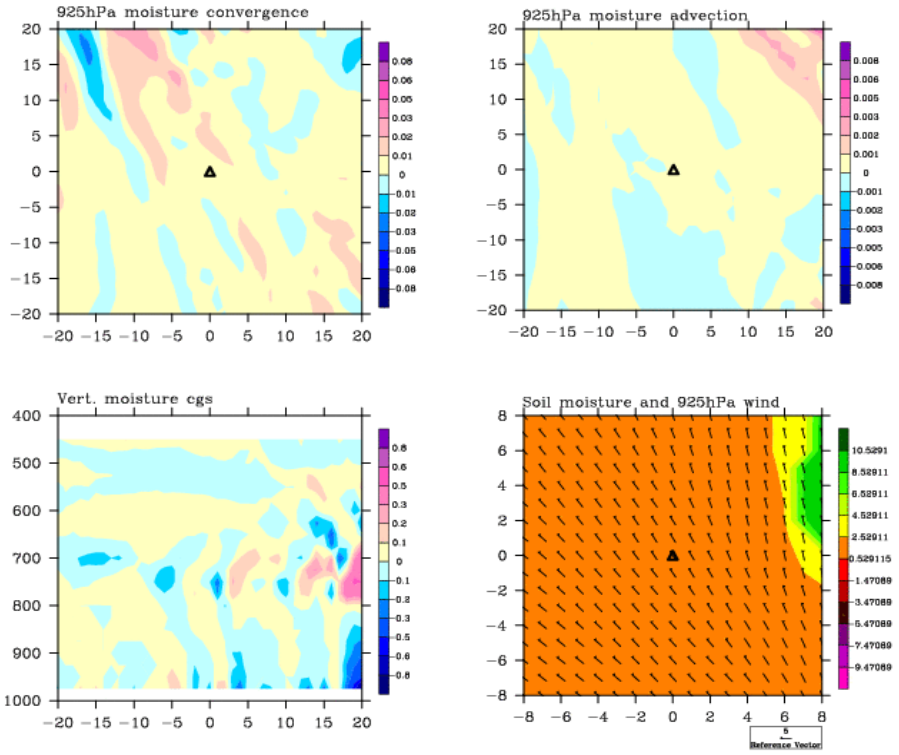

Figure 2.13: Same as Figure 2.7, for Case 4

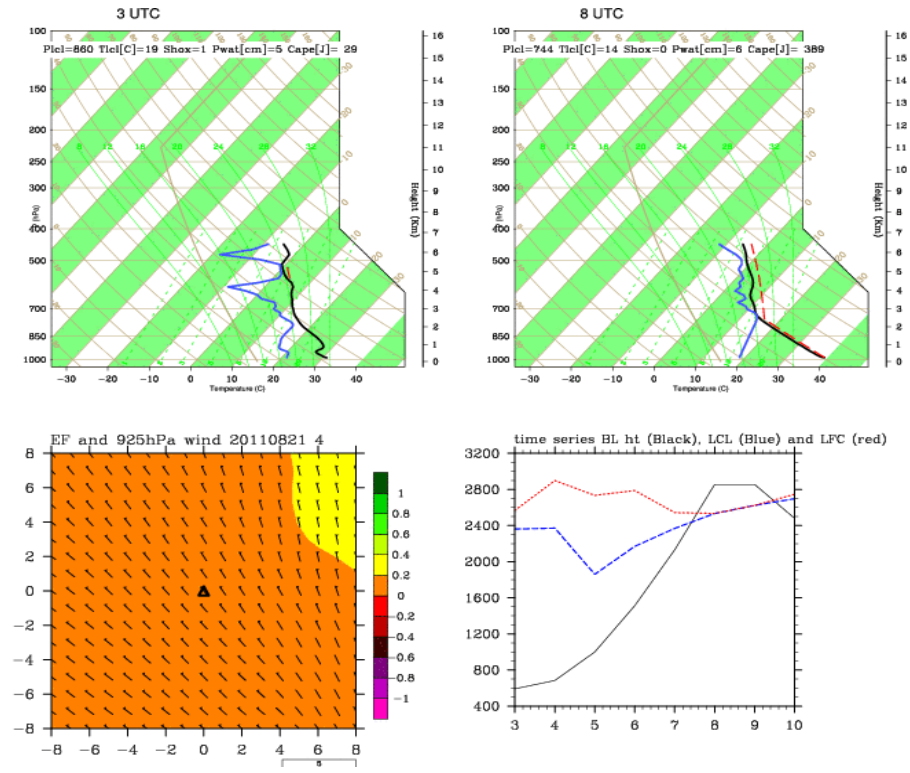

Figure 2.14: Same as Figure 2.8, for Case 4

Case 4 is an example of a very dry soil moisture field homogeneous at convective scale where absolute values of soil moisture (Figure 2.13d) are low, i.e. between 0 and 2.5 kg kg^{-1}. The 925 hPa horizontal and vertical convergence plots don't show any significant convergence (Figure 2.13a and 2.13c). Also, horizontal advection is negligible (Figure 2.13b). However, Figures 2.14b and 2.14d show gradual increase of the boundary layer height by mixing due to high values of the sensible heat flux. This high sensible heat flux is resulted from 5 hours of daytime heating of the surface. Thus at 10UTC when the PBL height reaches the LFC, there is initiation of rain similar to the dry case described in FE03a (Figure 1.8b).

Case 5: Convergence dominant case

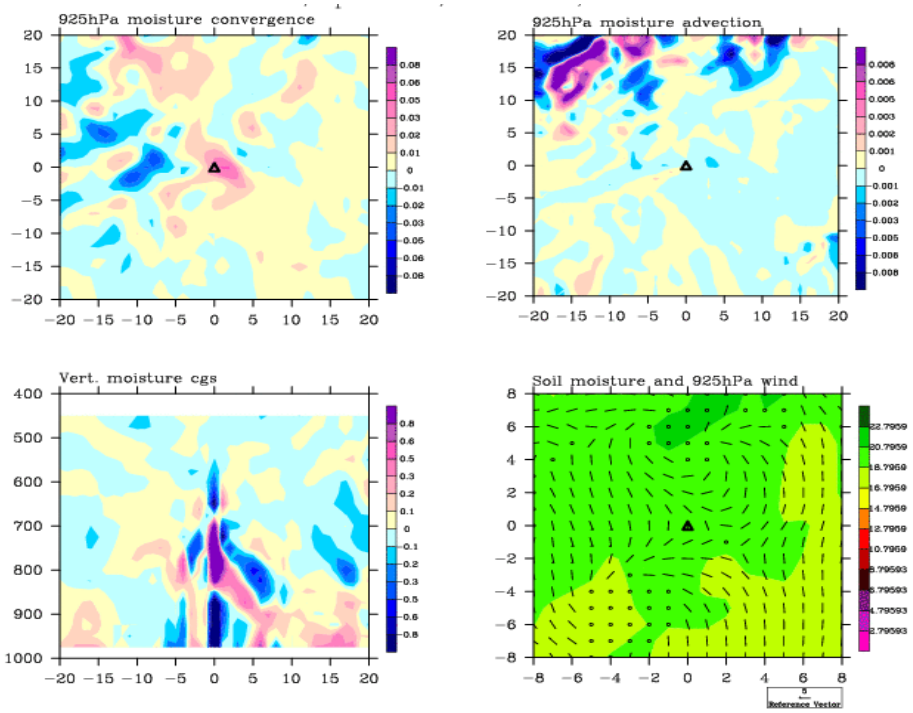

Figure 2.15: Same as Figure 2.7, for Case 5

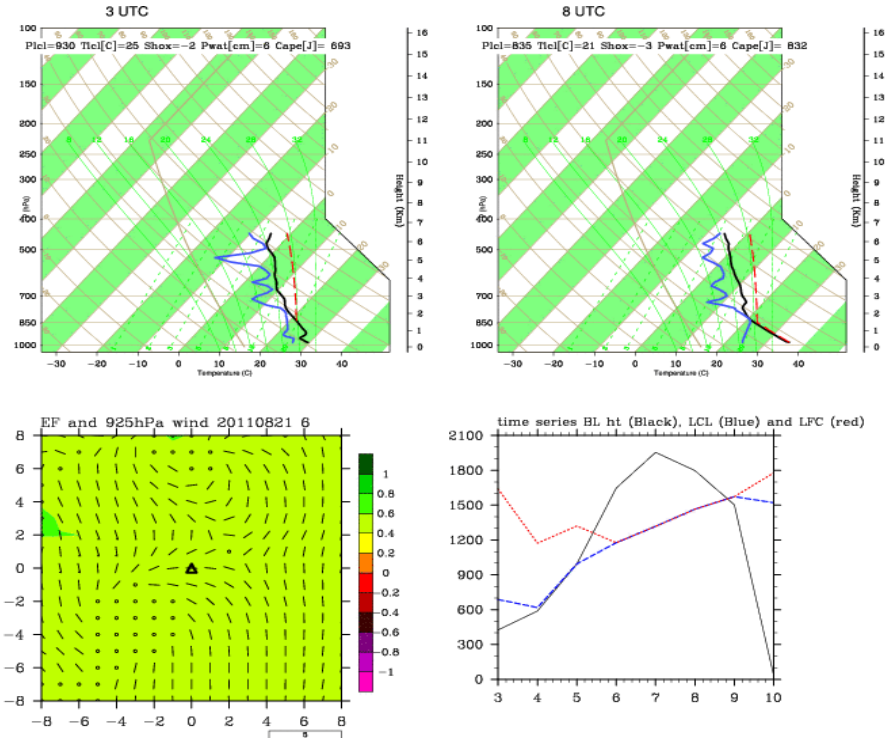

Figure 2.16: Same as Figure 2.8, for Case 5

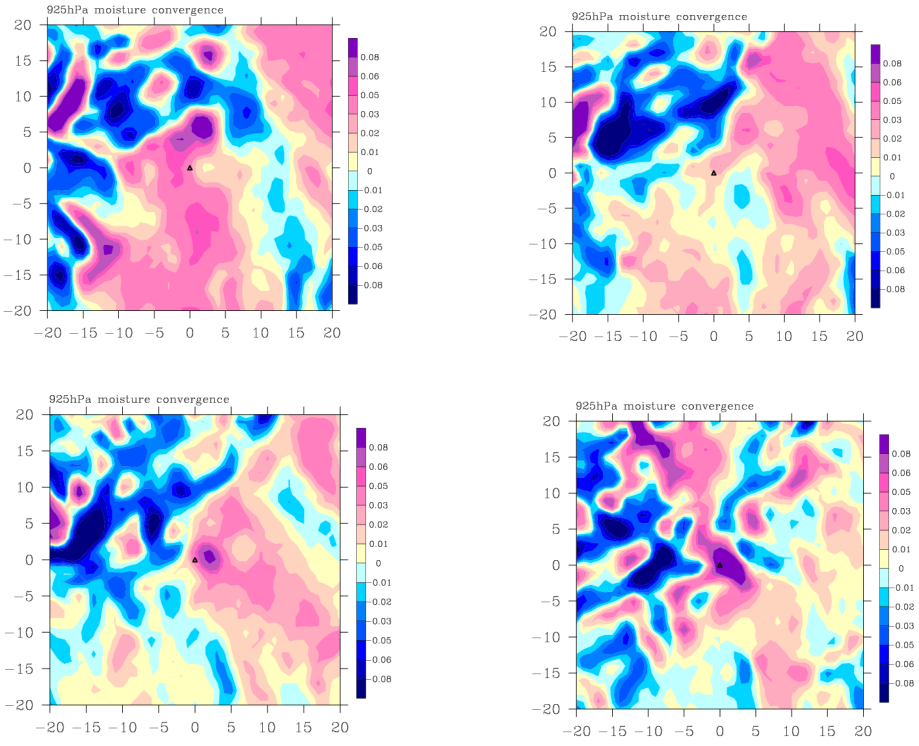

Figure 2.17: Same as Figure 2.10, for Case 5

In case 5 there is localized horizontal convergence (Figure 2.15a) two hours prior to initiation. On closely investigating the 925 hPa wind pattern (Figure 2.15d) there exist a vortex condition which can initiate vertical convergence as seen in Figure 2.15c.

On observing the convergence pattern five hours to two hours prior to initiation (Figure 2.17a to 2.17d) there is a persistence of localized convection which results in an increase in the boundary layer height to overcome morning CIN (Figure 2.16a), and reaching LFC by 0900UTC (Figure 2.16d).

Case 6: Synoptic case

In synoptic case there is a strong soil moisture and evaporative fraction (Figure 2.18d and 2.19c) gradient but no significant convergence is observed at lower levels. Also in Figure 2.19d, boundary layer height does not intersect the LFC at any time prior to initiation. In the tephigram, the low level morning inversion persists (Figure 2.19a and 2.19b). From the observed boundary layer parameters (Figure 2.19d) and 925 hPa convergence (Figure 2.18a) and advection (Figure 2.18b) plots we can see that this rain is not associated with land-atmosphere interaction. However, observing the profile behaviour at 700 hPa (Figure 2.19a and 2.19b), shows the possibility of medium-level cloud formed due to convergence at 700 hPa, as seen in the vertical moisture convergence plot with reddish contours (Figure 2.18c). Thus we can say in this case that rain is probably induced by synoptic convergence at mid-levels.

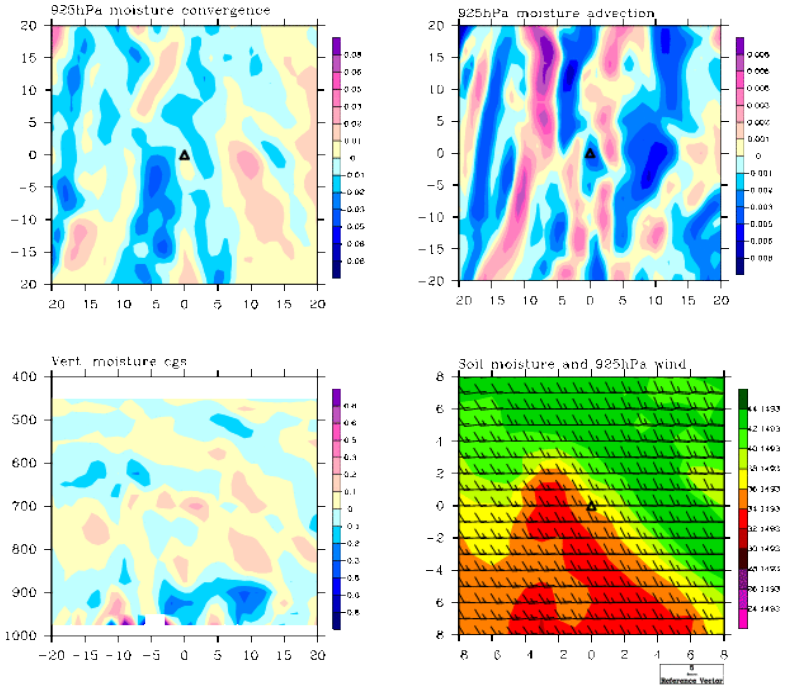

Figure 2.18: Same as Figure 2.7, for Case 6

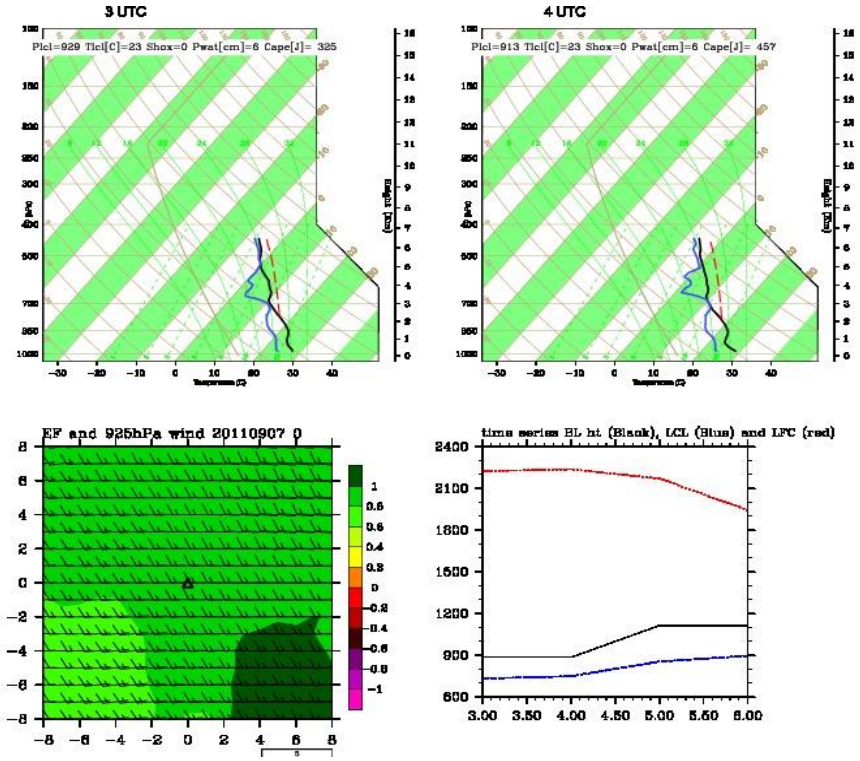

Figure 2.19: Same as Figure 2.8, for Case 6

Case 7: LFC increase as the time approaches initiation

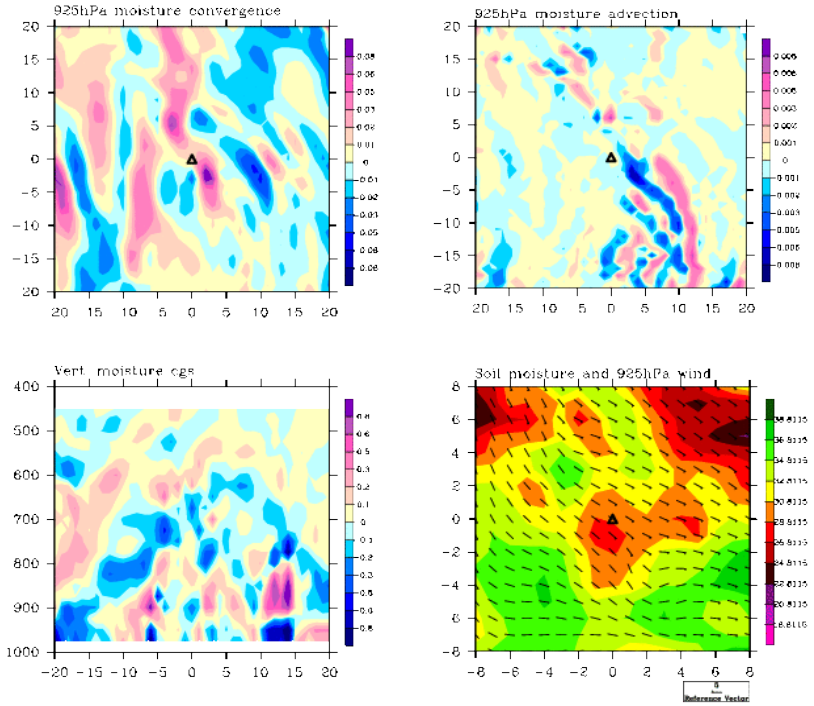

Figure 2.20: Same as Figure 2.7, for Case 7

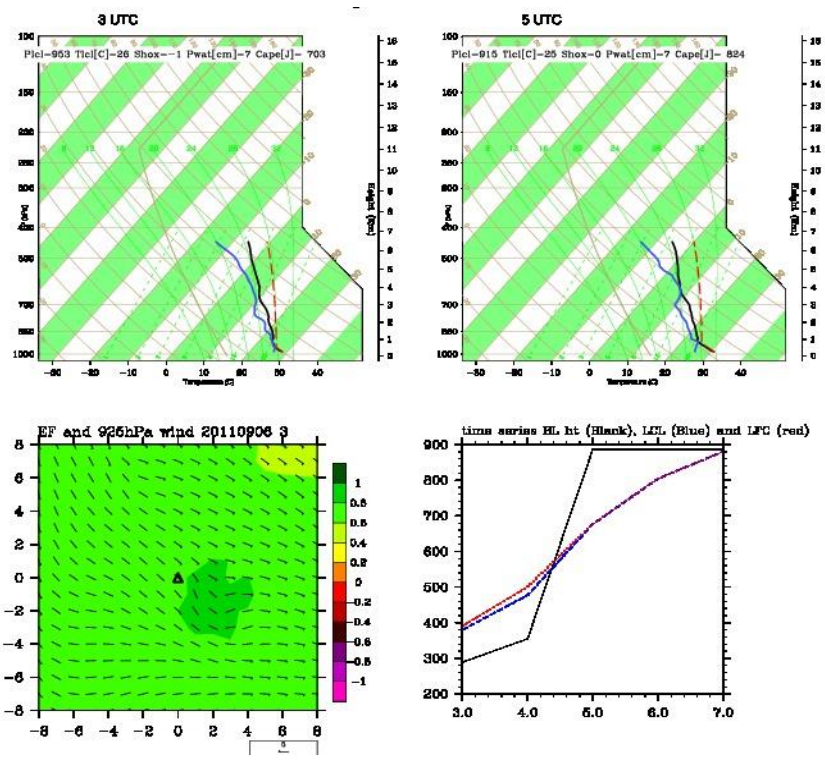

Figure 2.21: Same as Figure 2.8, for Case 7

This is a complex case referenced in Section 4.3.1 of chapter 4, an increasingly dry profile. Here, the difference in humidity between the PBL top and the air above it is increasing in time (Figure 2.21a and 2.21b) which means that the inversion Bowen ratio (see Equation 4.18) is small. Thus, even though the surface is wet, with evaporative fraction > 0.6, the LFC increases at the same time as PBL height increases due to entrainment of dry air from above the inversion, and they meet each other at 7 UTC. Therefore, this is the only case where LFC increases before rain initiation: in all other cases LFC either decreases or remains at the same level before rain initiation. It is worth to note here that this phenomenon, of the LFC increasing in height is not included in the FE03a model.

2.2.4 Summary

In this section case studies are summarized in a tabular format.

Case no.	**Surface Condition**	**Atmospheric Condition**	**Atmospheric Profile**	**Remarks**
1. (Gradient)	Dry to wet soil moisture gradient in downwind direction	Strong vertical convergence	Morning inversion, Deepening of PBL by day time heating.	Rain initiates due to PBL top meeting LFC.
2. (Gradient)	Wet to dry gradient	Lower level (925 hPa) linear and vertical moisture convergence along gradient.	-------	Strong linear convergence gives rise to vertical convergence which in turn gives rise to cumulus formation and hence rain initiation.
3. (Wet)	High soil moisture and evaporative	Calm synoptic and dynamic conditions.	LFC decreases due to	Rain initiates due to rapid

	fraction (0.6<EF<0.8)		moistening of PBL.	fall of LFC to PBL top.
4. (Dry)	Low soil moisture and evaporative fraction (0<EF<0.2)	Calm synoptic and dynamic conditions.	PBL height increases due to strong sensible heating flux and meets LFC.	Rain initiates due to PBL meeting LFC.
5. (Convergence)	Moderate soil moisture	Low-level localized horizontal and vertical moisture convergence (vortex).	PBL height increases due to convergence.	Rain initiates due to PBL meeting LFC.
6. (Synoptic)	Heterogeneous soil moisture	Moisture convergence at 700 hPa.	Appearance of mid-level cloud.	LFC doesn't meet PBL top at any time. Synoptically induced rainfall.
7. (LFC increases in time)	High evaporative fraction	Linear convergence at 925 hPa	Drying of profile	LFC increases as PBL height increases but at a slower rate. Rain initiates when PBL top surpasses LFC.

Table 2.2: Summary of case studies.

Thus from Table 2.2, cases 1, 2 and 5 indicate that afternoon rain initiates due to dynamic triggering which can be explained if we consider the three-dimensional model of the boundary layer growth as described by T11 and others (i.e. due wind convergence near gradients (heterogeneous soil moisture field)). On the other hand cases 3 and 4 appear to be typical examples of one-dimensional boundary layer growth as explored by FE03a. Here it is worth mentioning that case 3 (wet case) and 4 (dry case) have completely opposite soil moisture conditions, apparently following the one-dimensional model, and

the pattern of soil moisture field is homogeneous in the immediate vicinity of rain initiation. However, case 7 (rise in LFC) is not described by FE03a. Also the opposite path taken by LCL and LFC in case 1 is not described by Haiden (1997). Finally, case 6 is a case of synoptically induced rainfall.

This collection of cases seems to show that the different 1-dimensional and 3-dimensional physical mechanisms for initiation both exist, and may have relevance in different atmospheric and surface conditions. In the following Chapter 3, these afternoon rain initiations are tested more systematically in one-dimension and three-dimension model perspectives in order to evaluate the FE03a and T11 models. In Chapter 4 an attempt is made to overcome the limitations of the one-dimensional model's empirical solution method and to understand these advantages systematically.

3 Statistical evaluation of soil moisture-precipitation feedback theories using a convection permitting model over the Indian sub-continent.

3.1 Introduction

As discussed in Chapter 1 soil moisture states are thought to be crucial in modulating patterns of convective activity (FE03a), the monsoon circulation and its rainfall (Niogy *et al.*, 2010; Shukla *et al.*, 2013) and drought conditions (Hong and Kalney 2000; Zampieri *et al.* 2009). Atmospheric interaction with different types of soil moisture conditions can give rise to either negative or positive feedbacks between soil moisture and precipitation (Brubaker and Entekhabi, 1996; Eltahir, 1998). Here negative feedback implies precipitation is favoured over dry soil (i.e. a "dry advantage") whereas if precipitation occurs over wet soil, it is referred to as positive feedback ("wet advantage").

A significant study on the soil moisture-precipitation feedback process was conducted by Koster *et al.* (2004) using GCMs, where they found diagnostically that land-atmosphere interaction is strong over Central India. However, there remain various problems in relation to understanding the soil moisture-precipitation feedback process. The climate models are simulated at comparatively low resolution of a few tens, or usually hundreds of kilometers whereas the horizontal scale of convective clouds is hundreds of meters up to a few kilometers, and as a result the net effect of clouds in the climate model is parameterized. This difference between the scale of convective clouds and resolution of the climate model can induce problems in simulating small scale feedback processes. One such problem is noticed in the Taylor *et al*. (2012) study, where opposite signs of soil

moisture-precipitation feedback were observed in parameterized climate models compared to observations. Attempts to understand the feedbacks theoretically remain relatively limited. The study performed by FE03a developed a predictive framework based on a one-dimensional slab model and morning profiles, to separate the dry and wet advantage rainfall events based on certain threshold values of convective and humidity parameters.

Since the above discussed methods and theories (FE03a, Koster *et al.*, 2004 (K4), T11) are based on different types of modelling studies, and partly using observations, here in this study we have tried to understand and verify these results collectively under a single environment by using a high resolution convection permitting (non-parameterized, or "explicit" convection) model. CASCADE project studies (Taylor *et al*., 2013) with a similar experimental setup have demonstrated that soil moisture patterns close to convective initiation in similar explicit-convection simulations agree with observations. Here we aim to categorize and test the existing theories of land-atmosphere coupling in two different perspectives. The first group can be explained using a vertical one-dimensional boundary layer model. The second group includes consideration of local wind circulation effects as a result of spatially heterogeneous distributions of soil moisture, and surface fluxes.

3.1.1 Vertical perspective

Soil wetness determines the partitioning of the surface heat flux into latent and sensible heat flux (Pielke 2001), which causes moistening or deepening of the boundary layer respectively. FE03a used the difference in height between the LFC and the top of the PBL as a parameter to describe the potential for rainfall, where, if the difference in height approaches zero the likelihood of rainfall increases. Haiden (1997) developed an alternative using LCL instead of LFC for convective triggering and invoked different controlling parameters. According to FE03a this processes of triggering due to LFC approaching the PBL top can occur over both types of soil condition (wet or dry), although the processes involved would be different in each case. Over dry soil, the latent heat flux will be low, and a higher sensible heat flux results in a deeper boundary layer. In this case

the growth of the boundary layer is rapid and may reach the height of the LFC. On the other hand, over wet soil, due to a low sensible heat flux, the boundary layer is shallow but also moist due to higher latent heat flux, and this moistening increases equivalent potential temperature that causes a fall in the LFC towards the height of boundary-layer top. Based on these arguments, FE03a developed a CTP-HI_{low} (Convective Triggering Potential and Humidity Index) framework which uses a morning profile to forecast whether an afternoon rainfall event will depend on different soil moisture conditions or will be atmospherically controlled. Here CTP is an indicator of stability of the atmosphere given by

$$\text{CTP}=\int_{P_{Surf}-100hPa}^{P_{Surf}-300hPa} g\left(\frac{T_{Vparcel}-T_{Venv}}{T_{venv}}\right)dz\,, \qquad (3.1)$$

where T_v represents virtual temperature.

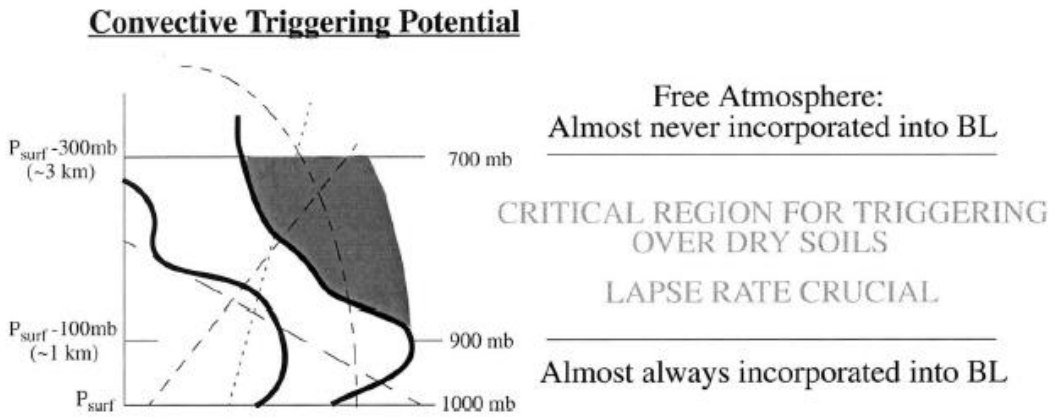

Figure 3.1: "A sketch of the definition of the convective triggering potential on a thermodynamic diagram. Thick solid lines are the temperature and dewpoint temperature profiles; straight long dashed line is a dry adiabat (constant potential temperature); straight short-dashed line is constant temperature; straight dotted line is constant mixing ratio; curved short-dashed line is a moist adiabat (constant equivalent potential temperature). The CTP is determined by integrating the area between the observed temperature sounding and a moist adiabat originating at the observed temperature 100 mb above the surface. The top is bounded by a constant pressure line 300 mb above the surface. Note that the CTP can be negative if the value of the moist adiabat originating from the Psurf -100 mb level is less than the observed equivalent potential temperatures at higher levels. Also, the CTP will be zero if the observed profile is moist adiabatic above the point of origin" as cited from FE03b.

HI_{low} represents lower-level atmospheric dryness. HI_{low} is low when humidity is high in both the planetary boundary layer and lower troposphere:

$$HI_{low} = (T_{950} - T_{d,950}) + (T_{850} - T_{d,850}), \quad (3.2)$$

where T and T_d are temperature and dew point with the subscripts denoting pressure level in hPa. By computing CTP and HI_{low} for early-morning atmospheric profiles, FE03a argued that there are three categories of sounding: i) sounding favouring precipitation over wet soil (positive feedback); ii) precipitation over dry soil is favoured (negative feedback); iii) rainfall irrespective of soil condition (atmospherically controlled).

To test the above hypotheses FE03a forced a slab model with morning atmospheric profiles obtained from radiosondes from Illinois and other parts of the USA under two contrasting soil moisture conditions: one over dry conditions with 20% soil moisture, and the other very wet with 100% soil moisture. They found that for a positive feedback the CTP should be in the range 0-200 J kg^{-1} and HI_{low} in the range 5-10 K, whereas for a negative feedback CTP should be greater than 200 J kg^{-1} and HI_{low} in the range 10-15 K, while other values contribute to atmospherically controlled cases (as shown in Figure 1.6 in Chapter 1). Based on this framework Tuinenburg *et al.* (2011) undertook a study over India and optimized the framework by selecting slightly higher values for HI_{low} (7-12 K and 11-16 K for wet and dry soil respectively) and a cut-off threshold of CTP =250 J kg^{-1}, using the same one-dimensional model and radiosonde observations.

3.1.2 Spatial perspective

The one-dimensional perspective of FE03a ignores triggering due to wind convergence and assumes a constant CIN threshold of the order 0-5 J kg^{-1} that must be overcome before convection is triggered. The spatial perspective improves on this by taking into account the wind convergence that arises due to soil moisture heterogeneity. According to Ookouchi (1984) and Segal and Arritt (1992) spatially heterogeneous soil moisture conditions can give rise to local wind circulations and under favourable atmospheric conditions these local circulations can give rise to focused regions for deep cumulonimbus convection (Pielke, 2001). A large eddy simulation study performed by Avissar and Schmidt (1998) found that under heterogeneous soil moisture conditions, cumulus development tends to occur over pockets of high moisture content (i.e. a wet advantage). Garcia-Carreras *et al.* (2011) in an idealized modelling study of vegetation

patterns found local maxima of equivalent potential temperature, hence high CAPE and minima in convective inhibition (CIN), over vegetation breeze convergence zones i.e. the boundary of forested-deforested (wet-dry) region. This condition (high potential temperature and less hindrance to initiation due to minima in CIN) helps to allow deep and organized convection to occur near convergence zones. At the same time, T11 used satellite data to show that a significant fraction of Sahelian storms are initiated on the warm, dry side of soil moisture boundaries.

Consistently with Garcia-Carreras *et al.* (2011) and T11, Taylor *et al.* (2012) used global satellite observations to suggest there is a preference for afternoon rainfall over dry regions in the vicinity of wetter soil (Figure 1.9 in Chapter 1). According to their explanation based on the observations of Taylor *et al.* (2007), idealized soil moisture-induced flows under light synoptic winds, similar to a sea breeze, create an ascent region where the shallow, strong current opposes the mean wind. The preferred location for convective initiation is within the ascent region induced by the heating gradient at the downwind edge of the dry patch. Additional convergence over the dry patch is provided by a deep, weaker current at its upwind edge, and cross-wind gradients in soil moisture. In other words, afternoon convection's trigged close to the wet-dry boundary, over the dry soil. Taylor *et al.* (2013) also compared parameterized convective simulations with explicit convection simulations at different spatial scales in a limited-area model. The comparison demonstrated opposite signs of soil-moisture precipitation feedback between parametrized and explicit simulations, with the explicit results being similar to observations, but the parametrized model errors being similar to those of climate models.

3.1.3 Synthesis and aims

The discussion of the above studies shows that there remain substantial uncertainties in regard to the important question of how soil moisture modulates rainfall over India. While observationally-based and modelling studies from West Africa (e.g. Taylor *et al.* 2009, Taylor *et al.* 2013) and globally Taylor *et al.* (2012) suggest that afternoon convective rainfall is generally initiated over dry soil, close to boundaries with a wetter surface, the analysis of FE03a implies that initiation over a wet surface is possible in the right

atmospheric conditions. The recent paper by Guillod *et al.* (2015) argues that these two perspectives can be reconciled by the difference between temporal and spatial analysis of the rainfall statistics. Guillod *et al.* (2015) conclude that optimal conditions for afternoon triggering occur in overall wet conditions (temporally), but in drier patches locally. The spatial scale of the analysis is therefore fundamental to the problem, and may depend on the specific regional context.

It is not clear whether the particular climatological conditions pertaining to India may favour soil moisture control of convection in any sense. Notably, the results of Taylor *et al.* (2012) and Guillod *et al.* (2015) fail to show any statistically significant signal of dry advantage over the Indian region, in contrast to other parts of the tropics. Both papers show some evidence (albeit not significant within the confidence intervals) of wet advantage in parts of the subcontinent. With these uncertainties in mind, the aim of this chapter is to evaluate the processes controlling convective rainfall initiation over heterogeneous soil moisture conditions over India. Section 3.1 has broadly categorized the soil moisture – precipitation feedback mechanisms into spatial and vertical perspectives. Section 3.2 presents data and methodology. Sections 3.3 and 3.4 summarise the results and conclusions, respectively.

3.2 Methodology

3.2.1 Classification of study domains and convective rain initiations

(a) An afternoon rain event

An afternoon rain event is diagnosed with a method similar to Taylor *et al.* (2013) using hourly accumulated precipitation between 1130 LT and 2030 LT (where LT is UTC plus 5.5 hours). The afternoon rainfall event is defined where there is no rainfall in the chosen area in the 3 hours preceding 1130LT. The purpose of performing this filtering is to separate stratiform rainfall events (that continued from overnight) from locally initiated convective events which can take place during the afternoon due to local forcing (refer Figure 2.6 in Chapter 2 for location of such initiations). Therefore, the very first step in the method is to identify a continuous rain area (Ebert and William, 2009) using the

flood fill algorithm and thresholding technique. According to this technique all the adjacent pixels exceeding a given threshold value of rainfall are collectively considered as one rain event. The minimum number of pixels to define a rain event as significant, in this study is considered as 3 pixels which is 48 km^2. The minimum rain threshold for all the domains is taken as 3mm accumulated rain in one hour. Then, the location of initiations is traced back to a single grid point, using 10-minute accumulated rainfall.

(b) Study domains

Four sub-domains are defined according to orographic and climatic conditions (shown in Figure 3.2); i) Northern domain (N), red, ii) Centre domain (C), blue, iii) Eastern domain (E), white and iv) Southern domain (S), black. The N and E domains are chosen because the orography is relatively flat and less complex, whereas the orography in the C and S domains is more complex. Also N, C and E lie along the axis of the monsoon trough, whereas S is positioned a little off track.

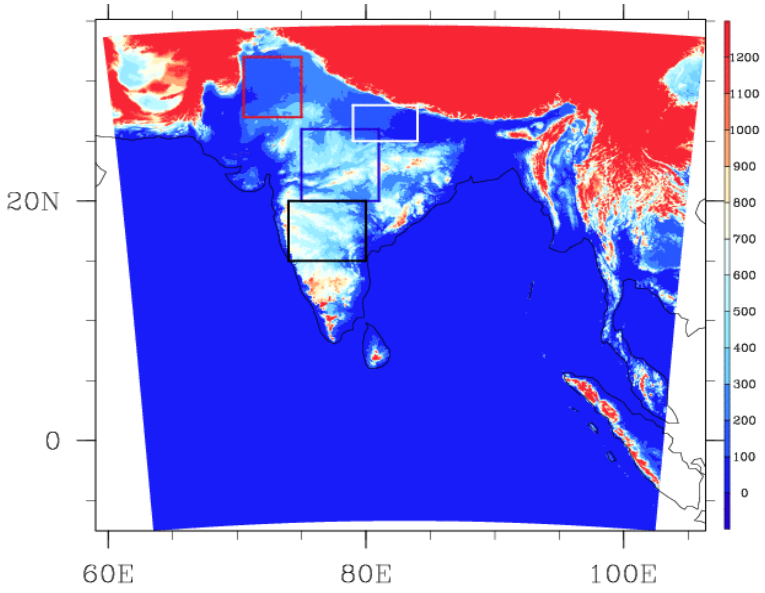

Figure 3.2: Shaded region is the simulated domain and coloured contours represent orographic height in meters from mean sea level. Rectangular boxes represent study domains; North (N, red), East (E, white), Centre (C, blue), and South (S, black).

(c) Soil moisture condition

Figure 3.3 a) shows soil moisture condition within the simulated domains for a randomly chosen date 21 August 2011. It can be observed that surface soil moisture conditions vary

significantly, with extreme high values of 50 kgm^{-2} in the East to 1 kgm^{-2} in the West. It is worth noting here that within each study domain absolute surface moisture value changes very little within the range of 0-4 kgm^{-2}. Thus during the whole study, we have tried to differentiate wet and dry soil relative to surrounding conditions instead of considering absolute values for dryness and wetness.

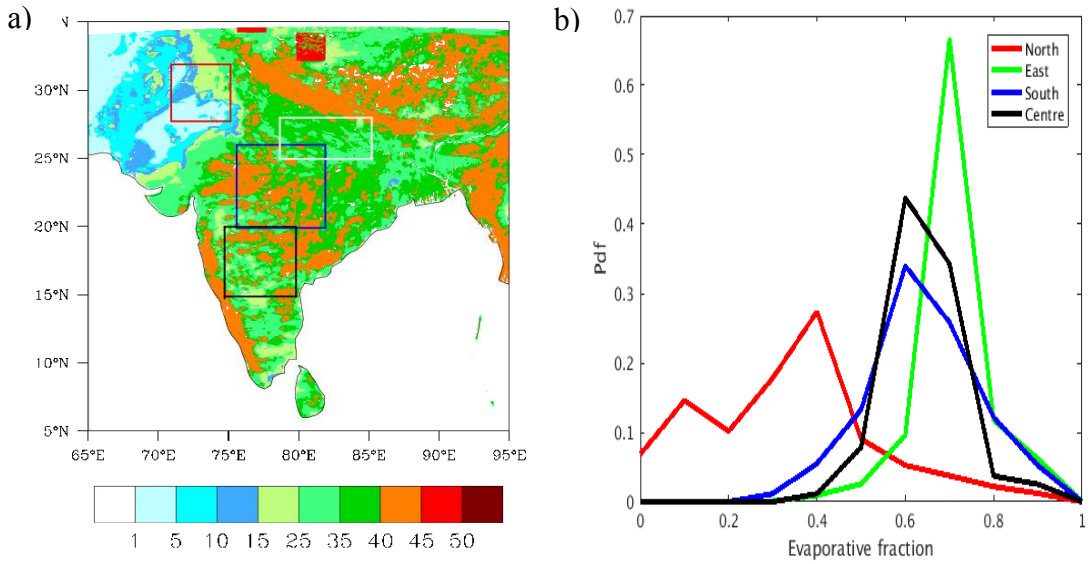

Figure 3.3: a) Map of daily surface soil moisture (kgm^{-2}). b) Probability density function (Pdf) of occurrence of the pixels in each domain under different evaporative fraction category for a randomly chosen date 21 August 2011, 0700 UTC.

From Figure 3.3b) the plotting of probability density function (pdf) of evaporative fraction shows East domain have high values of evaporative fraction for the majority of pixels, implies they belong to humid region. On the other hand, Central and South domains have moderate evaporative fraction values, implies they belong to semi-arid whereas North belongs to transition region from semi-arid to arid regime.

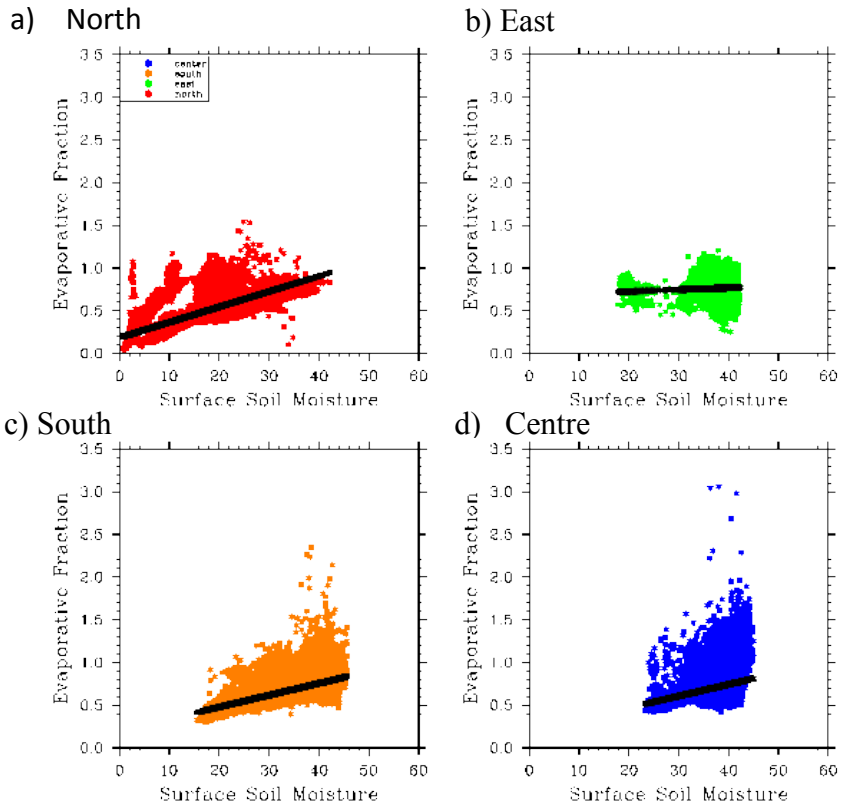

Figure 3.4: Scatter plot of surface soil moisture to that of evaporative fraction for each of four study domains on a randomly chosen date 21 August 2011, 0700UTC. Black line is the best fit line between surface soil moisture and evaporative fraction.

Soil moisture- precipitation feedback mechanisms exist when there exists a soil moisture stress which means soil moisture is a limiting factor to change surface energy balance. To find this relation we have plotted surface soil moisture vs evaporative fraction (factor of surface energy balance).

North domain:- In this domain according to Figure 3.4a) there is very low soil moisture and correspondingly low evaporative fraction values are found. Sometimes there is high evaporative fraction for low soil moisture values, which is possibly due to vegetation. The best fit line in this domain has highest slope compared to other study domains, implying that the evaporative fraction has the highest sensitivity to soil moisture in this domain i.e. soil moisture is a limiting factor. This result is in accordance with result of Figure 3.3 that this domain is semi-arid to arid in nature.

East domain:- From Figure 3.4b) high evaporative fraction values occur for soil moisture values greater than 30kgm^{-2} and minimum soil moisture value starts from 18kgm^{-2}. The best fit line has minimum slope, almost flat which indicates low sensitivity to soil moisture. Also from Figure 3.3a) and b) this region is under humid regime thus soil moisture may not be a limiting factor for moisture supply.

South domain:- Figure 3.4c) shows that the Southern domain has a range of soil moisture values from 16-46 kgm^{-2} . The best fit line shows evaporative fraction has almost linear sensitivity to soil moisture.

Central domain:- Similar to the Southern domain, the slope of the best fit line in this domain (Figure 3.4d) has a linear sensitivity to soil moisture. This result is in accordance with Figure 3.3 a) and b) showing that this is semi-arid regime, and soil moisture is a limiting factor.

To analyze soil moisture conditions, three-hourly average soil moisture prior to rain initiation is computed. All the analyses have been performed in the immediate vicinity of regions that have received afternoon rainfall. Based on identification of these rain initiations, the rest of the study of soil moisture, orography, morning profile (CTP-HI$_{low}$) analysis and wind circulation analysis has been carried out over the four domains.

3.2.2 Statistical analysis of soil moisture gradient

In this method, initially the soil moisture field is rotated according to the domain average 925hPa wind direction and then the soil moisture gradient is calculated in the downwind and upwind directions from the centre to the edges of the surrounding domain by fitting a least squares regression line, similar to the method of T11. In this calculation the location of initiation is 0.1 degrees upstream from the gradient centre in the downwind direction and 0.1 degrees downstream of the gradient centre in the upwind direction as shown in Figure 3.5. A negative gradient implies soil moisture state is transiting from dry (point B) to wet (point A) in the downwind direction and a positive gradient means there is transition from wet (point B) to dry (point A). Thus, there will be four possible combinations of downwind and upwind gradient which can classify the soil moisture state

as i) dry to wet in downwind direction,(DW) ii) wet to dry in downwind direction,(WD) iii) wet patch at centre, iv) dry patch at centre. The possible combinations of gradients are summarised in Figure 3.5. The limitation of this method is when the wind field is converging in the vicinity of rain initiation: this method may not compute the downwind direction of wind correctly. A manual inspection of the cases was made, and this kind of ambiguity in the wind direction was only detected in a small fraction (18%) of cases.

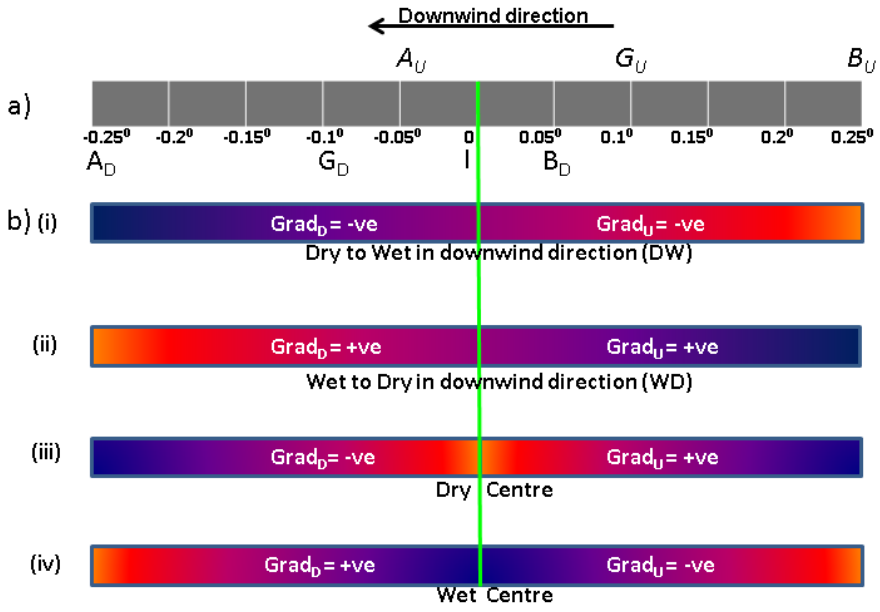

Figure 3.5: Schematic depicting the location of various points for calculation of downwind and upwind gradient. I is the point of convective rain initiation. A and B are points between which gradient is calculated. G is gradient centre. Subscript U and D denote the point for upwind and downwind gradient respectively. Positive gradient implies soil moisture decreasing in the downwind direction, i.e. winds blowing from wet to dry.

3.2.3 Classification of average soil moisture conditions

As the gradient analysis only considers variations in the downwind direction, and soil moisture states affecting the convective rain initiation processes are two-dimensional, it will be useful to describe the average soil moisture state in the vicinity of a rain event at comparatively the same length scale at which the gradient is being calculated. FE03a considered two very extreme soil wetness values, 20% and 100%, to constitute dry and wet regions respectively. In this study a statistical approach has been adopted to quantify

relative wetness, inspired by the study of Taylor *et al.* (2012) which is a relative comparison of the soil moisture at the initiation location to the surrounding soil moisture conditions. For each afternoon initiation, (Figure 3.6) a surrounding area of length L is defined, with the initiation at the centre of this area and event area length defined as l. The mean surface soil moisture over the surrounding area (SM_S) is computed for each initiation and is subtracted from the mean surface soil moisture in the immediate vicinity of the event (SM_E). SM_X is surface soil moisture of any pixel within the surrounding area length L.

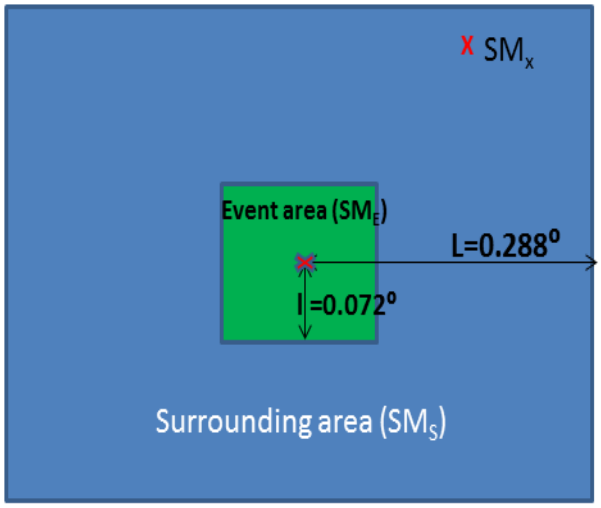

Figure 3.6: Schematic diagram of average soil moisture analysis method.

If the resultant value is negative, the event is termed as dry i.e. it occurred over a relatively dry region compared to surrounding soil moisture conditions; if the value is positive, the event is wet, and if the difference is near zero the event is termed a null event. Here, near zero implies bounded by a small value ϵ that takes into account the scale resolution i.e. at what scale we want to differentiate a event as wet or dry. So mathematically/quantitatively the method can be represented as

1) $SM_E - SM_S < -\epsilon$ (Dry event)
2) $SM_E - SM_S > \epsilon$ (Wet event)
3) $-\epsilon \leq SM_E - SM_S \leq \epsilon$ (Null event)

For whole study the value of ϵ is fixed at ϵ = 1 kg m^{-2} , following the sensitivity test described next.

The method is also sensitive to the choice of surrounding area length (L). If L is very small, it can lead to most of the events being classified in the null category as it limits the effect of surrounding soil moisture conditions. On the other hand, taking L to be too large can cause loss of actual characteristics of the soil moisture in the immediate vicinity of the rain event.

Sensitivity test of L and ϵ

To test the sensitivity of the variables L and ϵ; for each pair of L and l; 4 values of ϵ have been tested using z-test (explained later in Section 3.2.5) significance with the null hypothesis is that there is no relationship between the surface and the initiations at any scale.

i) North domain: -

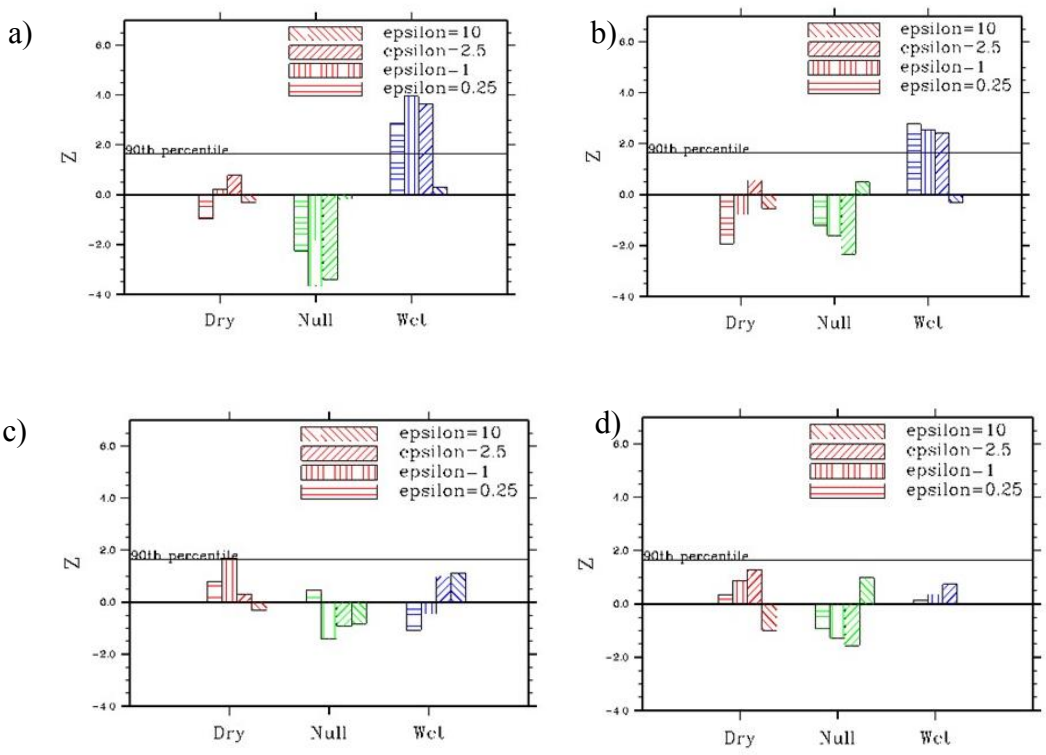

Figure 3.7: Y-axis in each figure denotes z-value for probability of occurrence of afternoon rain event compared to 5000 random events under the three defined categories in x-axis in North domain. a) L=0.288 and l=0.072; b) L=0.5 and l=0.1; c) L=1 and l=0.25 and d) L=2 and l=0.5. All length scales are in degree and ϵ are in kgm^{-2}. The black line at z=1.645 is level of significance at 90^{th} percentile.

On inspecting Figure 3.7 a,b,c and d it is found that Figure 3.7a) demonstrates maximum value of z for different values of ϵ under the wet category. Thus in the North domain values of L=0.288, l=0.072 and ϵ= 1 have highest level of significance, that is maximum probability of occurrence of wet advantage rain event.

ii) East domain:-

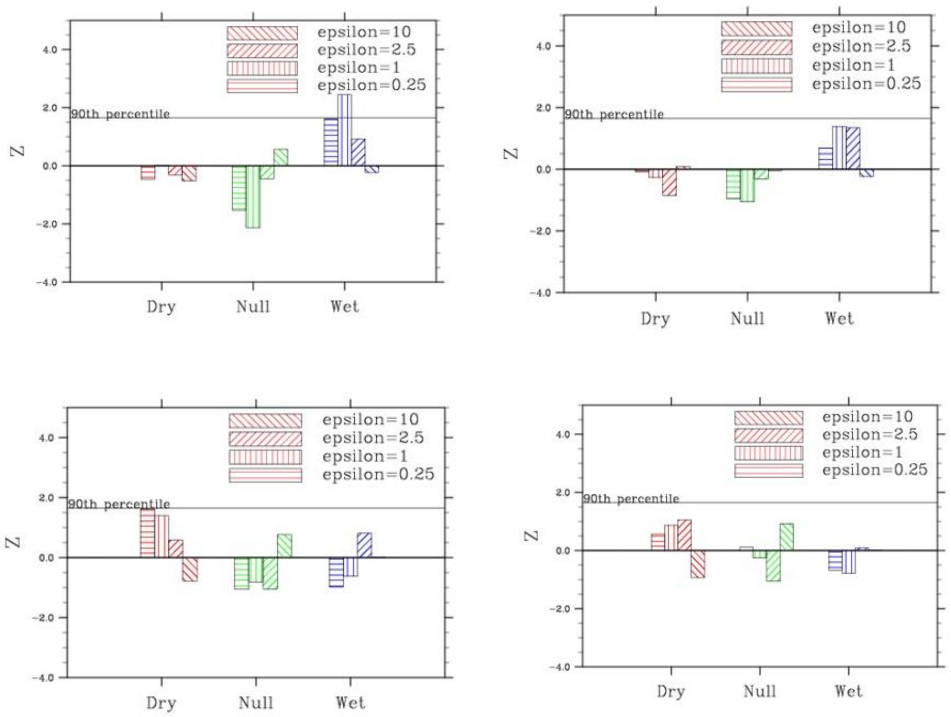

Figure 3.8: Same as Figure 3.7 except that it is for domain East.

Similar to domain North, here in the East domain the maximum value of significant wet advantage afternoon rain events occurs for the combination of L=0.288, l=0.072 and ϵ= 1.

iii) South domain: -

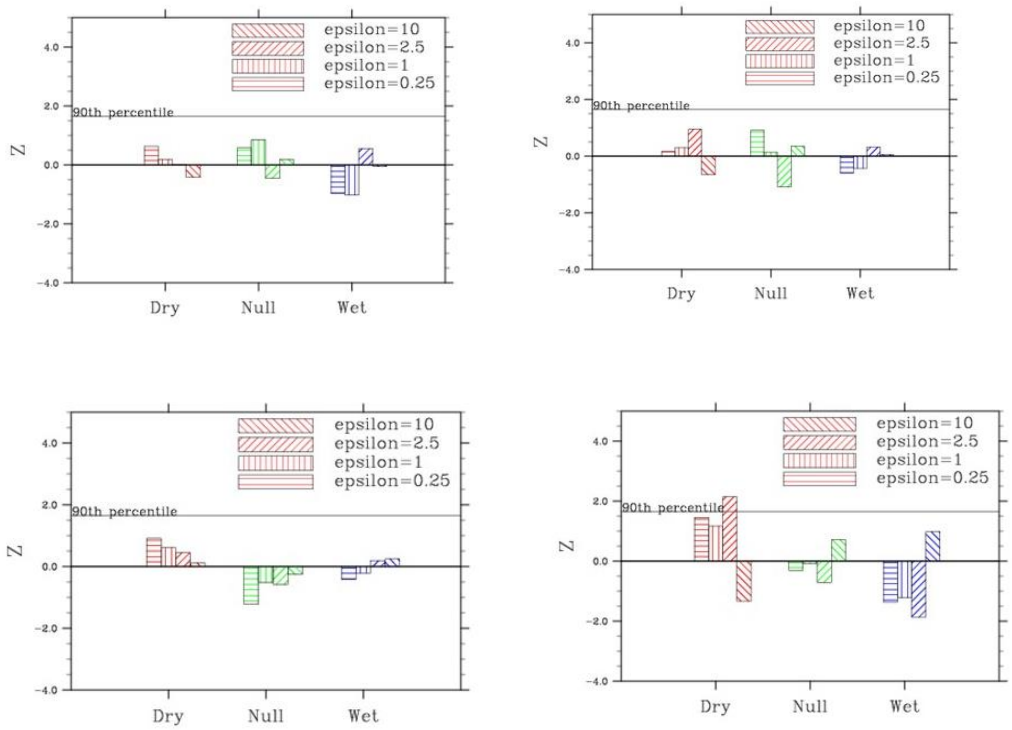

Figure 3.9: Same as Figure 3.7 except that it is for domain South.

In contrast to North and East domain, none of the events are statistically significant at small length scales up to L=1 degree for any of the ϵ values. However, Figure 9d) shows that for comparatively higher value of L=2, l=0.5 and ϵ=2.5 there is statistically significant number of dry advantage afternoon rain events. Higher values of L and l suggest occurrence of large scale mesoscale events like squall lines or organized mesoscale convective complexes whose investigation is beyond the scope of present study.

iv) Centre domain:-

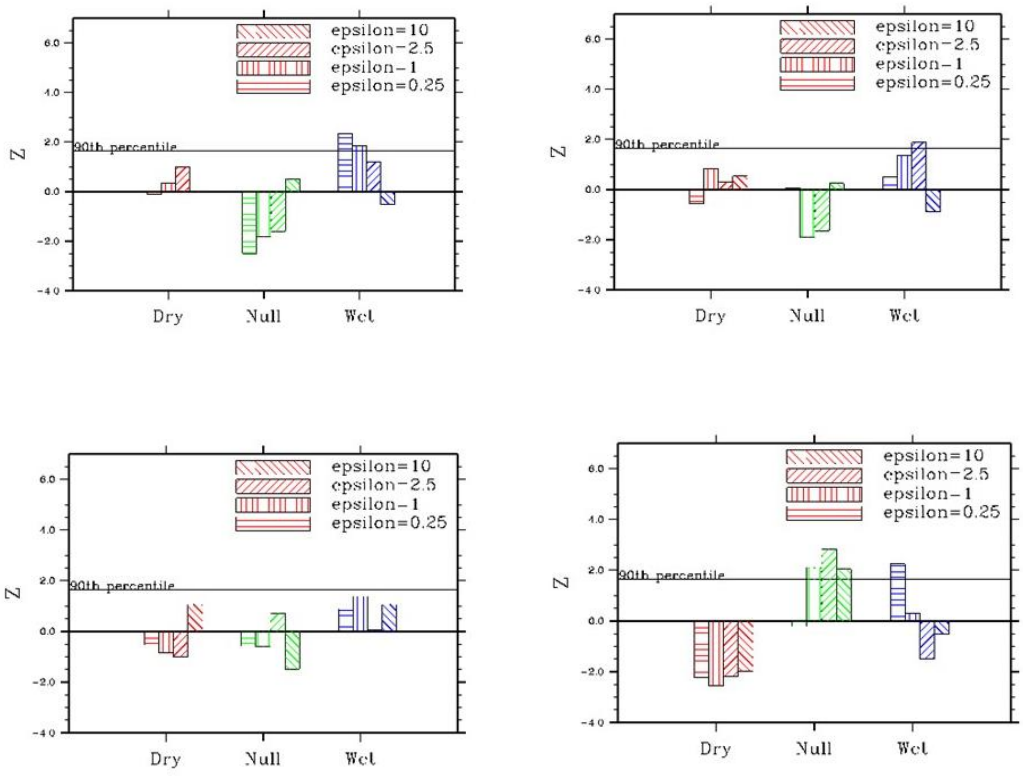

Figure 3.10: Same as Figure 3.7 except that it is for domain Centre.

In the Centre domain the statistically significant wet advantage rain events occur for L=0.288 or L=2 and ϵ=0.25.

Thus after experimenting with different values of L and l, for this study L is fixed at a values of L=0.288 degrees and l=0.072 degrees, which is close to the length scale (10-40 km) suggested by T11 for significant land atmosphere interaction at the mesoscale. Also the ϵ = 1 kgm^{-2} value is fixed to distinguish between wet and dry pixel as suitable for the N, E regions. Here it is worth mentioning that this method is not so useful if the soil moisture field is very patchy. However, at the relatively small scale of 0.288 degree there are very few cases with a considerably large number of wet and dry patches within one case.

3.2.4 Statistical analysis of orography

In order to analyse orographic conditions in the vicinity of rain events in complex terrain domain C and S, we split the analysis over low and high topography. To achieve this, the probability density function of orographic height in the surrounding area of length L is calculated for 10 equally spaced percentile categories i.e. heights falling under 10^{th} percentile value is referred as category 1 (low orography). Then the average height of the rain event region is computed and compared with the 10 percentile categories; and accordingly given the index of the matched category.

3.2.5 Significance test

To test the significance of statistical analysis i.e. what is the chance that an event cannot occur by random chance, a difference of portion 2-tail z-test is performed. Five thousand random points were chosen, taken from the 20 days of model simulation during the afternoon period for each domain. Then the same parameters, of dryness/ wetness, soil moisture gradient, CTP and HI_{low} were computed using equation 3.1 and 3.2, as for the actual initiation events. Then the probability density functions were computed, as for the initiation events, and a z-test performed under the null hypothesis that the probability of occurrence of events under a certain category is the same as that for probability of occurrence of random cases.

P_1 = portion of random event falling under given category
N_1 = number of random events
P_2 = portion of rain event falling under given category
N_2 = number of rain events

$$P = \frac{P_1 N_1 + P_2 N_2}{N_1 + N_2}$$

$$S = \sqrt{\left\{ \frac{P(1-P)}{N_1} + \frac{P(1-P)}{N_2} \right\}}$$

$$Z = \frac{(P_2 - P_1)}{S}$$

$Z > 1.645$ for 90^{th} percentile confidence level.

3.3 Results of various analyses of soil moisture patterns around initiation events

3.3.1 Diagnosis of soil moisture state

To look at the physical state of soil moisture conditions around rainfall initiation a composite analysis has been performed. In this analysis normalized soil moisture difference has been computed for each pixel by subtracting the average 0.072-degree event-box soil moisture; $[(SM_x-SM_E)/ (SM_x+SM_E)]$, where SM_x and SM_E are defined in Figure 3.6. Then every frame is rotated to the domain average 925 hPa with temporal average $t_2 - t_1$= (rain initiation time-3) - (rain initiation time-1) in downwind direction

Here downwind direction is considered from Cartesian east to west (Figure 3.11).

u_{avg}=average wind direction towards x-axis

v_{avg}=average wind direction towards y-axis

where th_{e1}= average meteorological angle of the event in radian

$\theta_{E1} = \text{atan2}(-u_{avg},-v_{avg})$; radian

$\theta_E = \theta_{E1} * 180/\pi$; average meteorological angle of the event in degrees

$\theta_{d1} = \text{mod}(90- \theta_E, 360^\circ)$; degree (Rotated meteorological coordinate with respect to Cartesian east to west direction)

$\theta_d = \theta_{d1} * 3.14/180^\circ$; radian

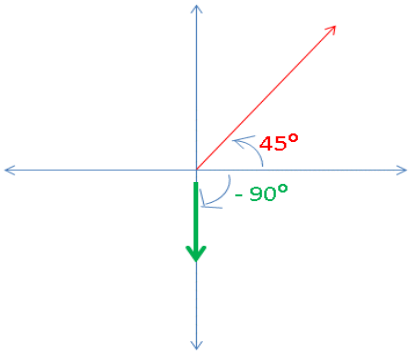

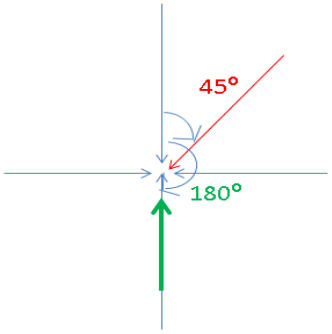

a) Cartesian (θ_d) Meteorological (θ_E)

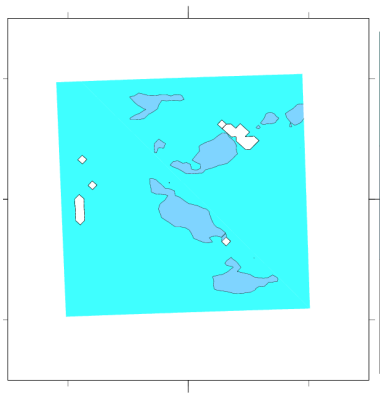

Original

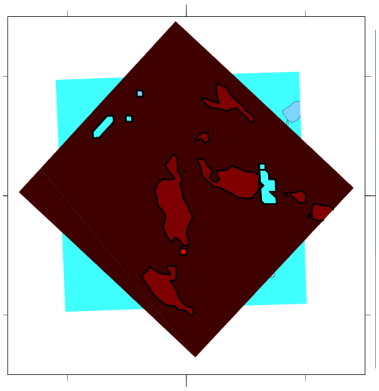

$\theta_E = 45°$

$\theta_d = 45°$

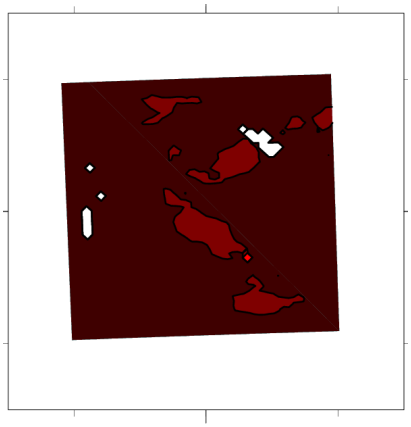

$\theta_E = 90°$

$\theta_d = 0°$

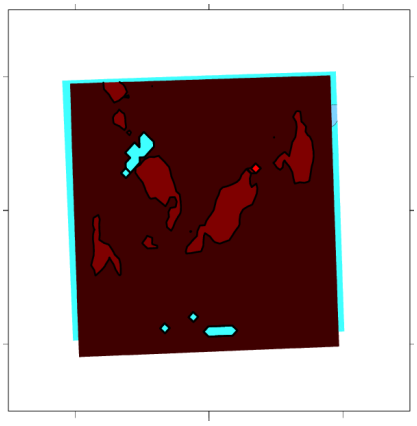

$\theta_E = 180°$

$\theta_d = -90°$

b)

Figure 3.11a) Schematic of rotated meteorological angle with respect to Cartesian angle. b) Examples of rotated meteorological angles with respect to Cartesian east to west direction.

A composite of all events has been made (Figure 3.12), similar to T11. Here it worth mentioning that Taylor *et al.* (2012) looked at spatial contrasts in temporal anomalies of soil moisture whereas we have compared spatial anomalies. Since some events could occur over a strong gradient and some over weak, to give equal weighting to every event the difference values are normalized. Thus a negative difference (red shaded region) implies the surrounding pixel is drier than the event average soil moisture conditions and if it is positive (blue shaded region), the surrounding pixel is wetter.

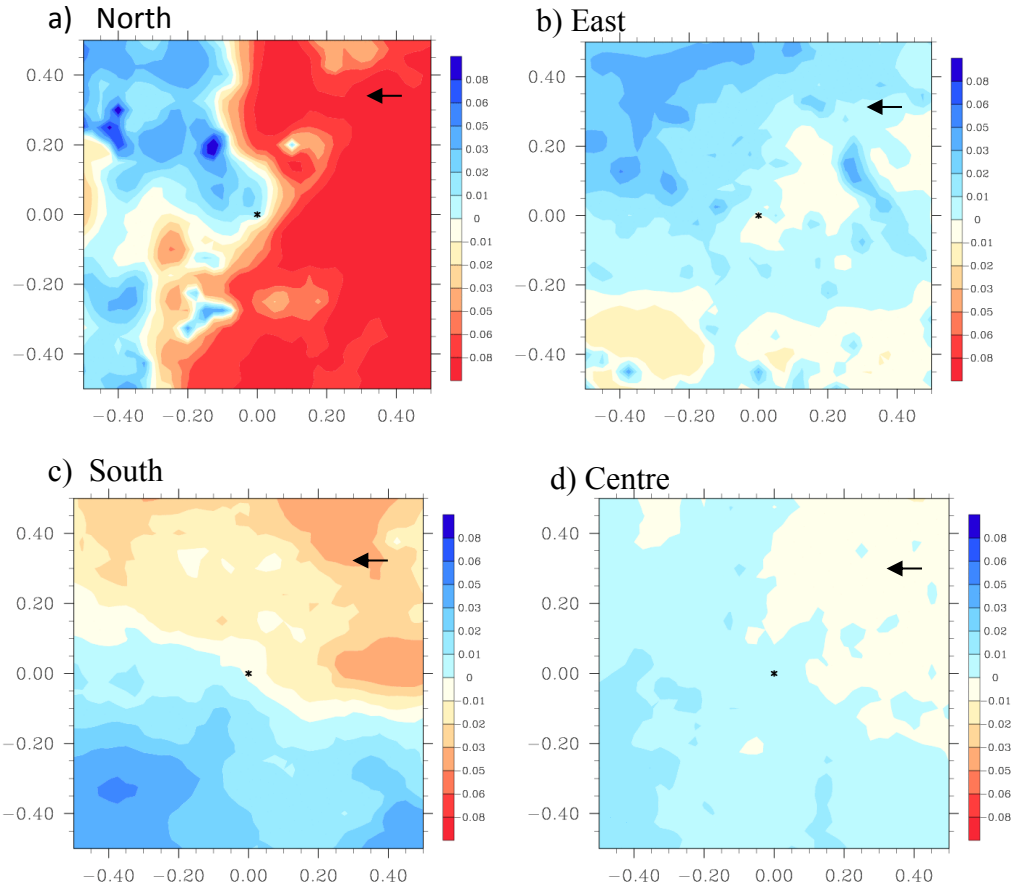

Figure 3.12: Normalized soil moisture difference, frame of reference rotated in downwind direction (the rotated wind is east to west(Black Arrow)). Here the black marker at the centre (0,0) is the location of rain initiation. Length scale of plotting is 0.5 degree on either side of centre. a) North domain,b) East domain, c) South domain, d) Central domain.

Figure 3.12 a) shows that in the Northern domain rain initiations are close to steep east to west, dry to wet gradients in the downwind direction. In the East domain Figure 3.12b) afternoon rain initiations are again close to a dry to wet gradient but the strength of gradient is quite weak in this domain. In the South domain i.e. Figure 3.12c) there is an inclined east to west gradient and afternoon rain initiations tend to initiate over a dry to

wet gradient similar, to the North and East domains. In the Central domain, afternoon rain initiates a few kilometres downwind from a dry to wet gradient over the wet surface as shown in Figure 3.12 d).

a) Statistical analysis of soil moisture gradient

In order to quantify the composite soil moisture gradient (i.e. Figure 12) objectively, the method described in Section 2.2 has been applied to each rain initiation. The soil moisture gradient is calculated in upwind and downwind directions and the categories are summarized in Figure 3.5 under the four categorized states.

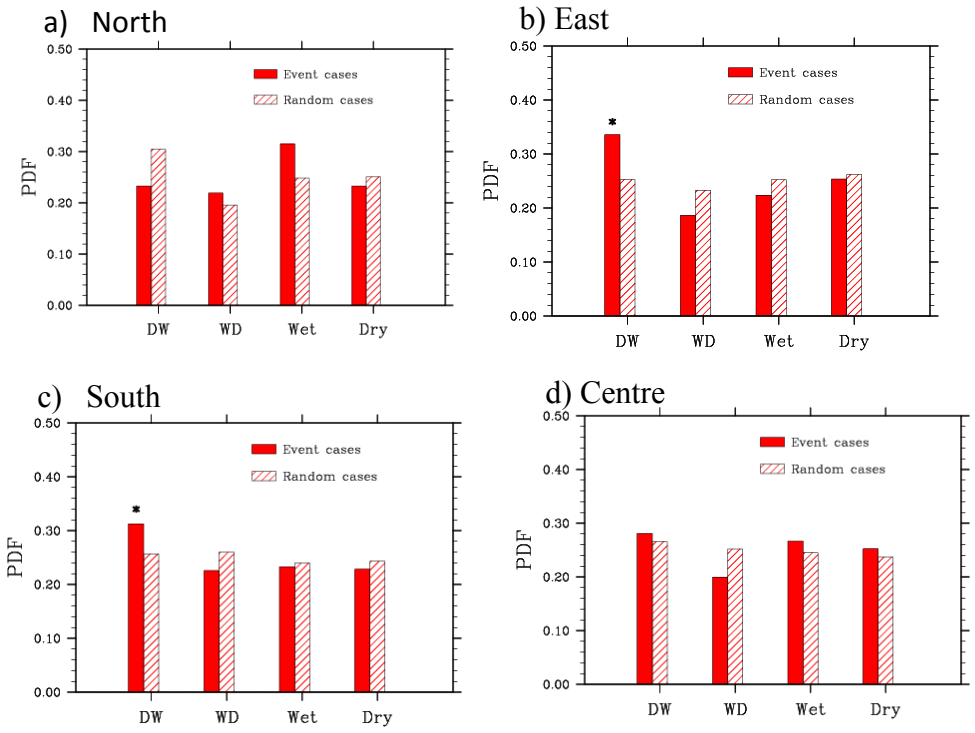

Figure 3.13: Probability density function of occurrence of rain initiation under different soil moisture categories as computed from downwind and upwind gradient sign combinations (refer to Figure 3.5 for categories denoted in x-axis). The solid bar represents rain initiation events and hatched bar represents pdf of random cases. The black asterisk over the bar denotes the category significantly different from random cases at or above the 90th percentile. a) North domain,b) East domain, c) South domain, d) Central domain.

In the East and South domains (Figure 3.13 b and 3.13c) the occurrence of events are statistically significant at the 95th percentile for dry to wet (DW) downwind gradient consistent with Figure 3.12 b and c. However, over the North and Central domain the number of events occurring under the wet category is statistically significant at the 80th and 85th percentile. There is slight disagreement in the composite and gradient analysis

results in the North domain; the composite analysis shows an appearance of strong moisture gradients whereas in the statistical analysis the gradient appears insignificant. This happens because the position of the North domain is over a strong climatological soil moisture gradient and the number of random cases with a gradient is also very high, as demonstrated in the graph with hatched bars (Figure 3.13(a)). This disagreement also highlights the importance of two-dimensional statistical analysis of soil moisture for more robust conclusions which are presented in the next section.

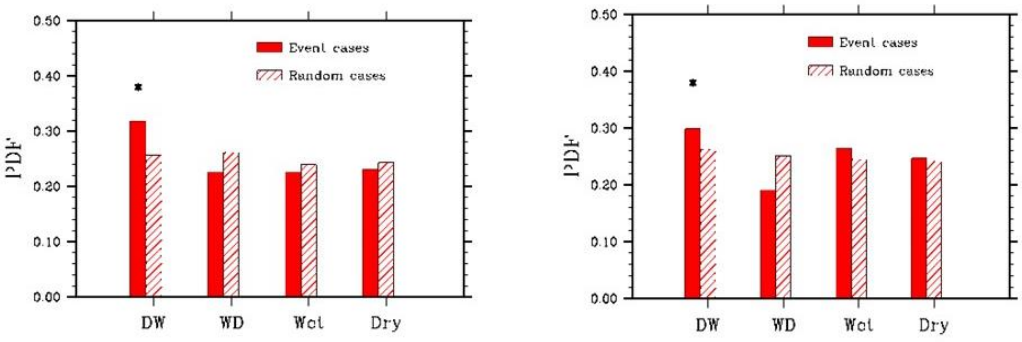

a) South b) Centre

Figure 3.14: Same as Figure 3.13 except that high orographic events with orographic contrast greater than 300 m are filtered out.

Since domain South and Centre have complex orography, to filter out the effect of higher orography the afternoon rain initiation events and random events whose difference between 10th percentile and 90th percentile of orographic value in surrounding area is greater than 300 m (300m is used as describe in Taylor *et al.* (2012)) are omitted from the calculation of significance test. Using this criterion the gradient category DW is statistically significant over the South and Central domain at 99th and 95th percentile (Figure 3.14a and b).

In summary, we principally find significant signals of DW in E, S and C domains.

b) Statistical analysis of average soil moisture state

The relative average soil moisture state described in Section 3.2.3 has been applied to the four different domains and results are presented in Figure 3.15. Since evaporative fraction

is an important coupling parameter (Dirmeyer *et al.*, 2009) between land and atmosphere so we have applied similar analysis to this parameter with $\epsilon_{EF} = 0$.

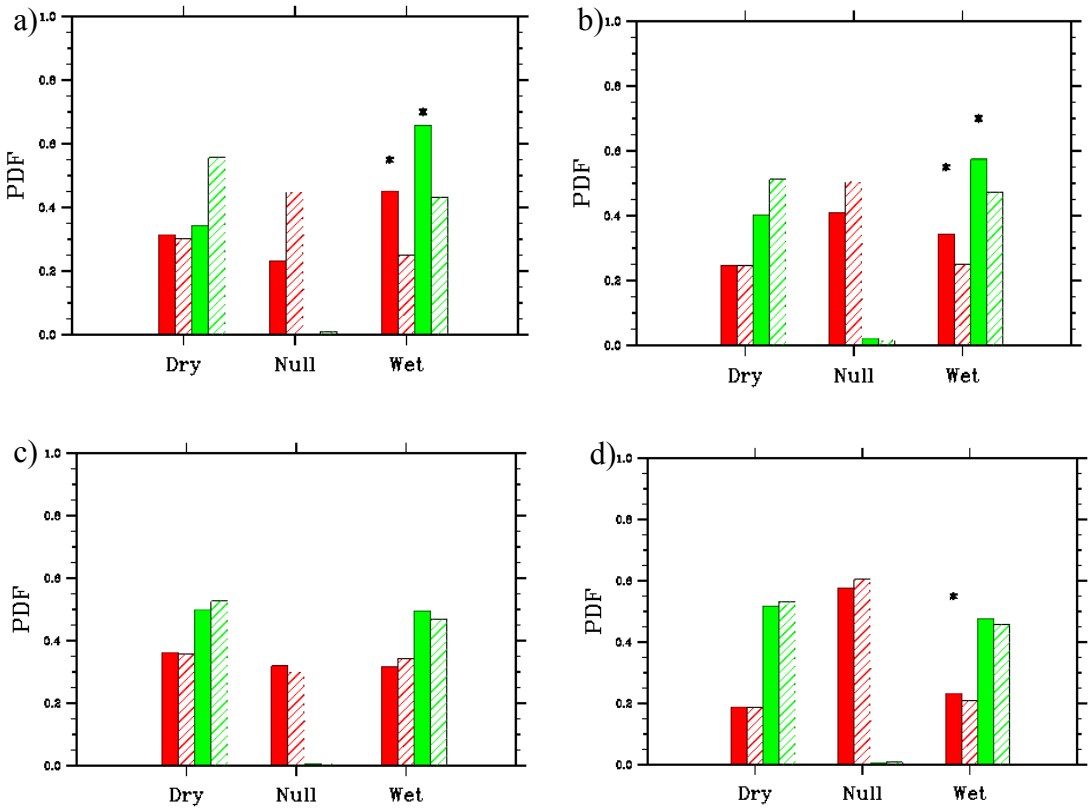

Figure 3.15: Normalized frequency (probability density function (pdf)) of occurrence of rain. Horizontal axis denotes the rain event soil moisture category; dry, null or wet. The red bar represents soil moisture analysis whereas the green bar represents analysis based on evaporative fraction. A solid bar represent statistics of actual rain events whereas a hatched bar represent statistics of 5000 random cases to compute statistical significance of the events. The black asterisk over the bar denotes the category significantly different from random cases at or above the 90th percentile. a) North domain,b) East domain, c) South domain, d) Central domain.

From Figure 3.15, over the North, East and Central domains soil moisture and evaporative fraction have similar statistics that afternoon rain initiations have the preference to occur over wet soil. The occurrence of wet advantage is statistically significant at 99th, 95th, 90th percentile for North, East and Centre respectively, whereas over domain S there is no significant result. For the complex orographic domain South and Centre, the result remains the same even after filtering out higher orographic cases of height difference 300 metres. The reason for statistically significant wet cases in the Central domain is discussed later in detail with the orographic effect.

On comparing results of the composite analysis, gradient analysis and average soil moisture analysis we can make some general conclusions regarding the relationship between initiations and the soil moisture. The most significant signals in Figure 3.13 (b and c) and 3.14 (a and b) indicate, in the East, South and Central domains, initiations occurring preferentially on dry to wet gradients, significant at or above the 90th percentile level when orographic events are removed. However, for the North domain, the only, weakly significant patterns are a tendency for initiations over wet centres. The results of the average soil moisture state in Figure 3.15 are more conclusive, with the North, East and Centre domains all showing preference for wet advantage, significant at the 99th , 95th and 90th percentiles. Combining these conclusions, we can say that we have evidence for afternoon initiation to occur on dry-to-wet gradients, and preferentially over wetter surfaces in general.

In terms of the preference for initiation over gradients, this pattern is consistent with the composite analysis of Figure 3.12 and with the general results of T11. In terms of the surface state (wet advantage), these results differ from previously published analyses (e.g. Taylor *et al.* (2012)) which showed dry advantage to be most prevalent worldwide. One explanation for this discrepancy in the Centre domain is the presence of significant orography (analysed in Section 3.3.2). For the North and East domains, orography is low: here, the discrepancy of these model results with previously published papers could be due to the timing of rainfall relative to surface gradients, meaning that rainfall is delivered at a different location to that of the first initiation. Close to a gradient, a small shift of the rain could change the underlying surface conditions significantly. This issue is further discussed in Section 3.4.

3.3.2 Orographic analysis

In this section, domains with complex orography, that is, the Centre and South domains, are further analysed using an additional parameter, 925 hPa wind convergence.

a) Statistical analysis of orography

In this section, for the complex terrain domains, Centre and South, the probability density functions (PDF) of occurrence of rain events is plotted according to different height

categories classified in Section 3.2.3, and results are presented in Figure 3.16. Following the aim to separate rain initiation events according to orographic conditions, it has been observed that for the Centre domain, there is a peak of wet events at comparatively higher orography. On the other hand, for the South domain there exist two peaks, one over lower topography, having a large number of dry advantage events and the second over higher orography, with more wet advantage events.

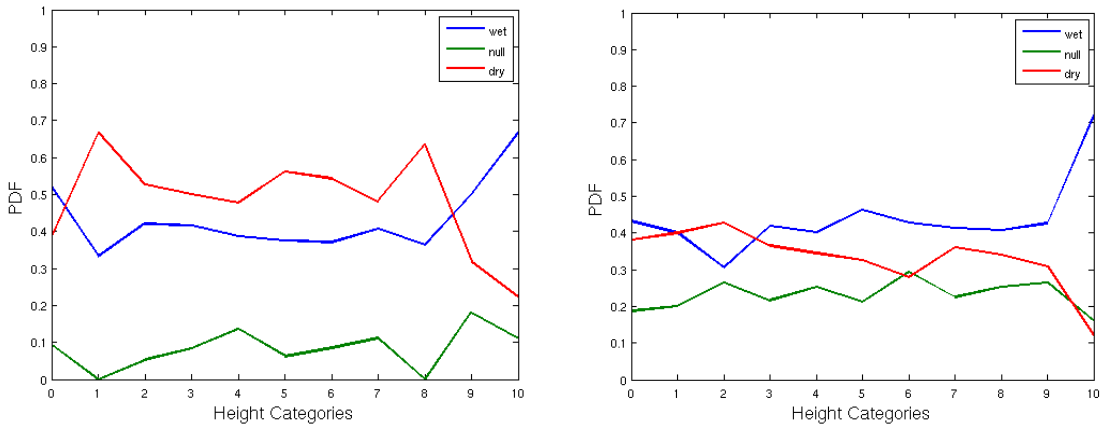

(a) South (b) Centre

Figure 3.16: Probability density function (Pdf) of rain events over different orographic heights, according to different soil moisture conditions. The blue line indicates distribution of wet advantage rain events over different orographic heights. Similarly red and green lines are for dry advantage and null case respectively.

b) Subjective analysis of wind convergence and orography

A spatial approach is adopted in this section to observe any orography-driven synoptic conditions persisting over the complex South and Centre domains. The 925 hPa, 20-day average wind convergence is plotted, overlaid by hourly average rainfall of the afternoon period. Over the Southern domain orography is very complex and average plotting of wind convergence and hourly rainfall at a spatial scale of 5 degree could not reveal any significant association of wind convergence with orography and rainfall whereas over the Central domain there is significant association of rainfall with convergence zones arising due to higher orography, as shown in Figure 3.17.

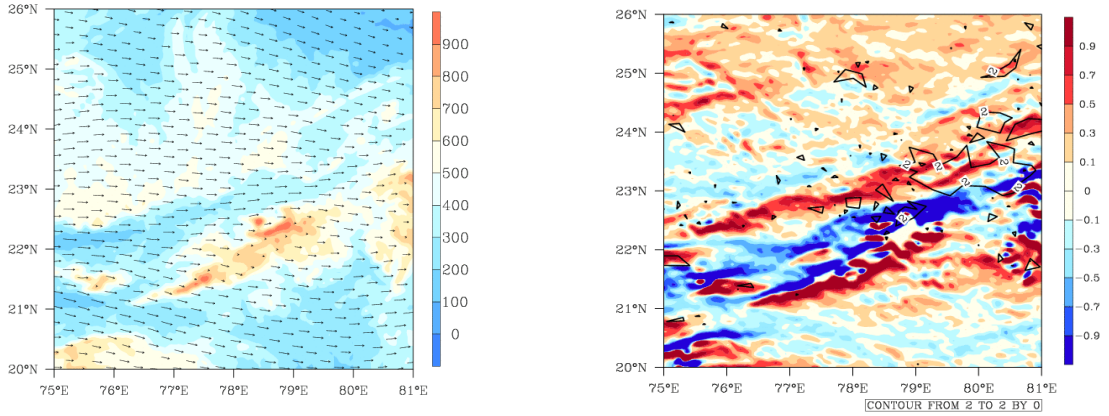

Figure 3.17: a) Hourly mean 925hPa wind superimposed on orographic height in m. b) Coloured filled contours are 20 day hourly average of 925 hPa level wind convergence (10^{-4} s^{-1}) for afternoon period. The thick black unfilled contour shows 20-day hourly average of afternoon rainfall. Both plots are for the Central domain.

On comparing the Figure 3.17(b) convergence plot with the 3.17(a) orography plot, it can be observed that over the Central domain the convergence pattern is strong near higher orography and is followed by rain. Also, analysis of events based on soil moisture conditions and height (Figure 3.16b) indicates that, for the Central domain, there are more wet advantage cases for higher orographic conditions. It can be explained in conjunction with subjective wind convergence analysis (Figure 3.17b) and orographic analysis (Figure 3.16b) as there is serial occurrence of rainfall over the same place again and again due to fixed orographic triggers which results in wet soil at the initiation locations. For this reason, Taylor *et al.* (2012) excluded higher orographic regions in their analysis. Thus on reanalysis of the Central domain (Figure 3.14), if rain initiations associated with orographically induced wind convergence are excluded, the dynamic land atmosphere interaction near DW gradient is significant.

3.3.3 CTP-HI_{low} analysis

We tested the results of the FE03a study using the high resolution convection permitting model instead of a one-dimensional slab model. For the study we have computed values of CTP-HI_{low} over the rain event initiations, for 0000UTC model atmospheric profiles, and tried to categorize wet and dry events according to CTP-HI_{low} threshold values given

by FE03a, Tuinenburg *et al.* (2011) or any other value. In this study, we have used the methods of Section 3.2.3 to categorise wet and dry events, rather than the absolute extreme soil moisture conditions imposed by FE03a in their experiment.

The CTP-HI_{low} values computed from the morning 0000 UTC profiles of afternoon rain events are presented in Figure 3.18 for each of the 4 domains.

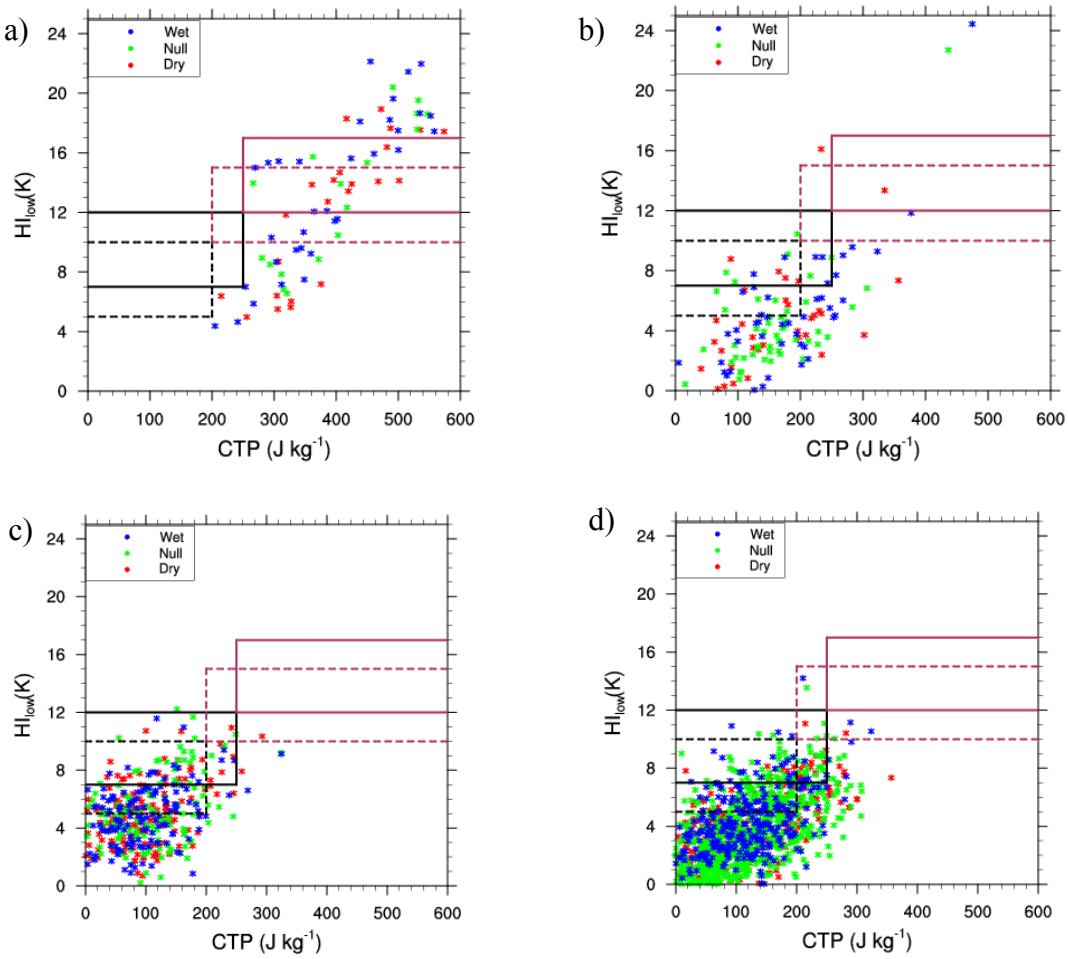

Figure 3.18: CTP-HI_{low} plot for the (a) North, (b) East, (c) South, and (d) Centre domains, for early morning model profiles (0000 UTC) at the initiation location of afternoon rain events. Here, a red points implies the rain event is over dry soil, blue points implies rain event occurred over wet soil and green points means rainfall occurs over a region where the soil moisture contrast condition is relatively insignificant i.e. a null case. Solid and dotted Purple line shows regions of predicted dry advantage according to Tuinenburg *et al.* (2011) and FE03a respectively. Similarly, the black line is indication of predicted wet advantage region.

At first inspection, there is little evidence of CTP-HI_{low} differentiating the likelihood of wet or dry advantage. However, subjectively, looking at the plots suggests a slight

separation of dry and wet advantage events in the North arid to semi-arid region (Figure 3.18a).

By applying the statistical significance z-test, it is found that there is preference for dry advantage events for FE03a threshold of CTP greater than 200 J kg^{-1} and HI_{low} in the range 10 to 15 K in the semi-arid North and South domain, significant at the 80th percentile but in the South domain there are only three events. In the humid East and Central domains, the results are mixed and it is difficult to separate dry and wet advantage events based on any CTP-HI_{low} threshold value.

Our results appear to contradict the Tuinenburg *et al.* (2011) thresholds. The ranges of CTP greater than 250 J kg^{-1} and HI_{low} between 12 and 17 K are proposed by Tuinenburg *et al.* (2011) to exhibit dry advantage but we find in the North domain there is a preference for wet advantage, significant at the 90th percentile, in this range.

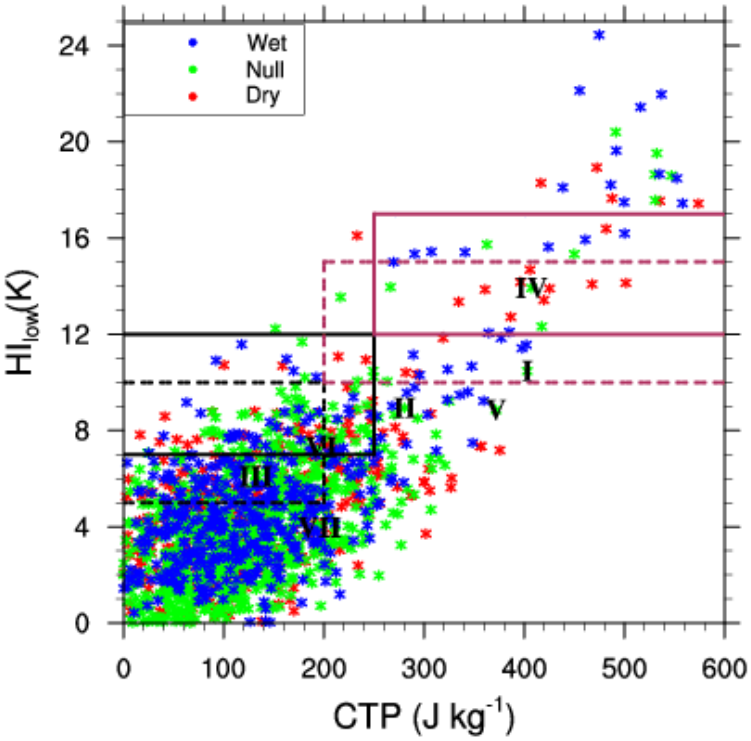

Figure 3.19: The CTP-HI_{low} plot for all four study domain combined, having relatively flat orography i.e. height difference for rain event considered are less than 300 m. Here roman numbers are case studies described in Chapter 2.

Again to reduce the effect of orography, events with height difference greater that 300m are excluded from both random as well as rain initiation cases and the significance test is applied for the FE03a and Tuinenburg *et al.* (2011) thresholds. From subjective analysis it is apparent that the prediction of the dry advantage event is significant (Figure 3.19, refer purple solid line). However, the combined domain computation results in a statistically insignificant value for both thresholds over dry as well as wet advantage events.

Figure 3.19 also illustrates that our choice of case-studies span the range of CTP-HI_{low}. From qualitative analysis in Chapter 2, Case III is wet and Case IV is dry 'homogeneous' case at convective scale whereas according to quantitative (statistical analysis) both fall under null category with ϵ =-0.379 and ϵ =- 0.583 respectively and appeared within the dry and wet threshold limit of CTP-HI given by FE03a. But on their own they are not significant.

3.4 Discussion and Conclusions

In this study, afternoon rain initiations over different orographic and climatic conditions have been categorized objectively according to soil moisture conditions. As the South and Central domains have complex orography, they are further analyzed using orographic and subjective wind convergence analysis.

Over the domains with relatively flat orography (North and East), soil moisture analysis shows that afternoon rainfall tends to initiate over wet soil, and close to dry-wet boundaries (increasing soil moisture in the downwind direction). Although Taylor *et al.* (2012) and Taylor *et al.* (2013) found that afternoon rainfall is more likely to occur over the same kind of soil moisture gradient (increasing in the downwind direction), these earlier papers identified initiations occurring over drier soil, on the upwind side of that gradient, whereas we have found initiation to be preferred on wet soil of the downwind side. However, it is worth mentioning here that Taylor *et al.* (2012), based on the Taylor *et al*. (2011) study, considered convective initiation in terms of the first appearance of cold cloud, whereas our results are for convective rain initiation, which occurs some time, perhaps 30 minutes, after the first cold cloud tops appear. If the clouds are moving with

the mean wind toward the wet side of the gradient, it is natural that there should be a shift from dry to wet, in the analysis of first convection followed by rainfall. Hence, in spite of convection being initiated over dry soil, rain may initiate over the wet soil a few kilometres downwind.

The preliminary analysis of wind convergence (not shown here) over all the domains indicates that rainfall is more likely to occur near convergence zones. This aspect of vertical uplift and moisture advection needs to be quantified in detail, which is currently proposed for future study, taking into account the Birch *et al.* (2014) study on wind convergence patterns.

Taylor *et al.* (2012) and Guillod *et al.* (2015) also found, globally, that spatial analysis of rainfall indicates greater prevalence of triggering over locally dry surfaces. This result is apparently at odds with the results we have found for the EMBRACE model over India. However, it should be noted that both Taylor *et al.* (2012) nor Guillod *et al.* (2015), in their global analyses, found a signal of dry advantage over India, and there is in each paper a signal of wet advantage over some locations in India. While the wet advantage found for parts of India may not be statistically significant (for instance, in Taylor *et al.* (2012) a 10% significance level is used, meaning that globally, 10% of regions will have wet advantage by chance), it is also possible that the particular climatological conditions prevailing in the Indian Summer Monsoon may favour the boundary / wet advantage described here.

In our model results, the subjective analysis of CTP-HI_{low} plots over the semi-arid North and South domains indicates the possibility of slight separation between wet and dry advantage in the events, but the behaviour is not very clear. The occurrence of dry events with the given values i.e. CTP=200 J kg^{-1}/250 J kg^{-1} and HI_{low} 5/7 K -10/12 K for wet and HI_{low}=10/12 K – 15/17 K for dry advantage (FE03a and Tuinenburg *et al.*, 2011) thresholds is statistically significant in these North and South domains, but only at the 80% level, and it is not easy to find clear regions of wet advantage in this parameter space. The previously quoted CTP-HI_{low} values in the East and Central domains are unable to separate the behaviour of rain initiation based on initial surface moisture conditions

during monsoon season. Even filtering of the high orographic events did not yield any statistically significant result.

We have tried to quantify the CTP-HI_{low} framework in a three-dimensional atmospheric model where the role of advection, orography and flows that originate from land surface heterogeneity (i.e. two-dimensional soil moisture condition close to practical scenario instead of one-dimensional point observation) are considered with respect to rainfall, but the framework predictive parameters are limited to the one-dimensional atmospheric profile approach. Over the semi-arid North and South regions, the mechanism for initiation of dry advantage events, based on the CTP-HI_{low} framework, is that convection initiates when the PBL top rises rapidly to meet LFC. This may be enhanced by the mechanism demonstrated by Garcia-Carreras *et al*. (2011) in that due to surface moisture heterogeneity there could be rapid formation of fronts that lead to strong upward motion and thus increase the height of the boundary layer rapidly to meet the LFC (Case I and II in Chapter 2).

Orographic analysis of the South and Central domain confirms that over higher orography, rainfall tends to initiate over wet soil. Comparison of the average wind convergence plot with the orographic plot in the Central domain shows that there exists a dominant zone of convergence and divergence near higher orographic regions and this region is prone to afternoon rainfall. The orographic analysis shows more wet advantage over this region which can be linked to orographic induced rainfall, as the rain occurs over the same place again and again, so the rain event region is relatively wet all the time. However, the gradient analysis excluding higher orography in Central India shows preference for DW events implying land atmospheric coupling exists in this region, which is a region mentioned by Koster *et al.* (2004) for strong land- atmosphere coupling in climate models. Our findings show that at the mesoscale, dynamic land-atmosphere coupling is significant in this region only for low lying orographic events. The CTP-HI_{low} analysis over this domain cannot separate out dependence of rainfall on surface moisture conditions.

As this study has been carried out for the monsoon season, in order to generalize the conclusions, pre-monsoon, monsoon onset period and post monsoon seasons should also

be analysed and compared, as these are the periods of significant moisture-limited cases, to explore better understanding of the soil moisture-precipitation feedback mechanism over India.

4 Thermodynamic analysis of the sensitivity of afternoon deep convective initiation to surface Bowen ratio.

4.1 Introduction

We have seen in the literature review in Chapter 1, it is likely that land atmosphere heterogeneity at the mesoscale (2 to 200 km) can significantly affect the initiation of convective rainfall. In Chapter 2 it has been observed in Figure 2.7d and 2.9d, that heterogeneous soil moisture conditions can give rise to convergence and hence rain initiation. Figure 2.12d shows initiation by lowering of LFC over wet soil and Figure 2.14d, a case where initiation occurs due to elevation of the PBL top. In Chapter 3 we have tried to investigate suitability for prediction of convective rainfall over different soil state based on two prevailing theories which are the dynamic (T11; Garcia-Carreras *et al.*, 2011; Segal and Arritt, 1992) and the 1-D thermodynamic model (Findell and Eltahir 2003a; Haiden, 1997). In 3-D models, the variation in the thermodynamics is not studied in detail whereas the 1-D model fails to offer a universal solution. Now in this chapter we try to readdress some of the problems in one-dimensional models (to find a solution based on physical principles rather than empirical as described by FE03a), starting from first principles.

The mechanism proposed to control impact of soil state on precipitation is through the partitioning of surface energy flux as accounted by Bowen ratio i.e. ratio of the sensible heat flux to the latent heat flux. Changes in surface Bowen ratio thus impact changes in temperature and moisture content of the PBL, which in turn impact growth of the PBL and other thermodynamic properties. The presence of vegetation and moisture in the surface reduces the Bowen ratio. If rainfall occurs over such lower Bowen ratio surfaces,

it is called wet advantage. In contrast if rainfall occurs over high Bowen ratio it is called dry advantage.

In the past few decades much progress has been made to understand the response of boundary layer to surface Bowen ratio in different atmospheric profiles, using one-dimensional models. Haiden (1997) addressed the question of cumulus onset by analytically solving the boundary layer evolution equation, to access the point where boundary layer height reaches the LCL. Here it is worth to note that this is a different problem to deep convection which uses the LFC instead of LCL (FE03a). Parker (2002) analysed the tendencies in CAPE and CIN according to surface Bowen ratio and atmospheric profiles but failed to compile the results in a form that enabled the question to be addressed in "wet and dry advantage" form.

FE03a explained the mechanism of convective rain initiation as the process by which boundary layer height top approaches LFC, to have very low CIN under different soil moisture conditions. Over a wet surface, Bowen ratio is low, and boundary layer depth is relatively low, because the sensible heat flux is low but moistening due to high latent heat flux increases the moist static energy and therefore deep convection occurs by descent of the LFC (as the assumed cloud parcel from the boundary layer increases its equivalent potential temperature). In contrast, over a dry surface Bowen ratio increases rapidly and the rate of increase of boundary layer height depends upon the stability of the profile just above the capping inversion (quantified as a "convective triggering potential", or CTP, which is inversely proportional to stability). Thus under low stability conditions (high CTP) over a dry surface, the dry boundary layer grows rapidly and may approach the LFC for deep convection. Based on the above mentioned theory FE03a proposed to use the parameter CTP, and a humidity index HI_{low}, which is the sum of dew point depression in and just above the boundary layer. They argued that values of these two parameters can predict whether a given morning profile will rain over dry soil or over wet soil, or whether rain is independent of profile parameters.

The CTP-HI_{low} approach has been quite influential and has been applied in a number of context, namely Tuinengburg *et al.* (2011), and Ferguson and Wood (2011). Although this model provides useful understanding of the problem, it also have some drawbacks.

Primarily, why these two parameters are thought to be the only and right parameter to characterize the conditions is not justified. Secondly, the parameter CTP, based on stability of the profile to describe depth of boundary layer is understandable, the dependence on HI_{low} is not so obvious. In fact, observations and models of the boundary layer (Betts and Ball, 1995; Parker, 2002) suggest that the role of dry air above boundary layer is important in controlling likelihood of deep convection, which implies that a difference in humidity within and above the boundary layer should be used to measure convective development. Furthermore, there is a question in regard to the generality of this parameter space. The similar study conducted over India by Tuinengburg *et al.* (2011) showed a requirement of slightly higher values of CTP-HI_{low} with respect to the Continental USA. This apparent lack of generality suggests either that additional parameters are required, or these two are not the optimal ones.

Thus in this chapter, using the basic idea of FE03a i.e. that there is likelihood of rain when boundary layer top reaches LFC over different soil states (Chapter 2; Figure 2.12d and 2.14d), we have redeveloped the model from first principles using the boundary layer growth model of Betts (1973), Carson (1973) and Tennekes (1973). Here it is also shown that this model can be solved exactly, which yields three parameters which are all needed to find whether there will be a dry or wet advantage. In section 4.4, this new analytical solution is tested against the EMBRACE initiations.

4.2 Development of the one-dimensional model

Following Betts and Ball (1995), we define the pressure-depth of the mixed layer to be

$$P_i = p_s - p(z_i),$$

where z_i is the inversion height and p_s the surface pressure. The pressure difference between the inversion and the level of free convection is

$$\Delta p = p(z_i) - p_{LFC}. \qquad (4.1)$$

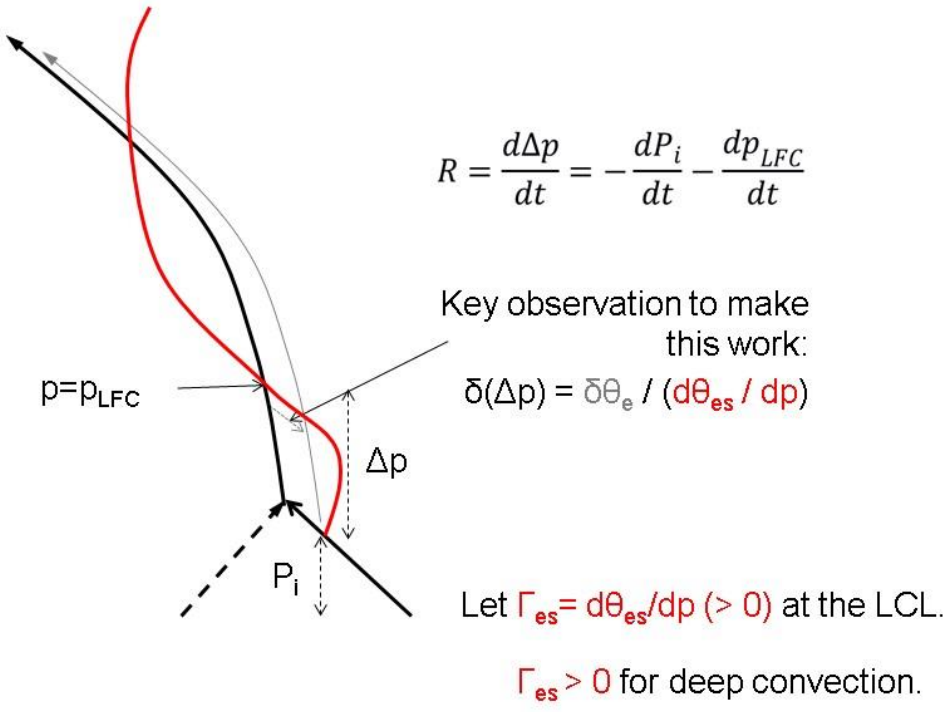

Figure 4.1: Schematic of the profile on a tephigram, and definition of LFC, stabilities.

Therefore, the rate of change of Δp with time is

$$R = \frac{d\Delta p}{dt} = \frac{-dP_i}{dt} - \frac{dp_{LFC}}{dt}. \qquad (4.2)$$

For a transition to deep convection by one-dimensional boundary layer growth, we require that the LFC and the inversion approach each other, and R < 0.

The first term in (4.2) can be calculated with good accuracy using well-known bulk formulae for the growth of a convective boundary layer (Betts (1973), Carson (1973), Tennekes (1973), in the form given by Betts and Ball (1995).

$$\frac{d\theta}{dt} = \frac{g(R_n - G)\beta}{c_p P_i(\beta+1)}\left[1 + \frac{\beta_i}{\beta} A_r \frac{(\beta-\beta_v)}{(\beta_i-\beta_v)}\right] \qquad (4.3a)$$

$$\frac{dP_i}{dt} = \frac{1}{\Gamma_+}\frac{d\theta}{dt} = \frac{g(R_n - G)\beta}{\Gamma_+ cP_i(\beta+1)}\left[1 + \frac{\beta_i}{\beta} A_r \frac{(\beta-\beta_v)}{(\beta_i-\beta_v)}\right] \qquad (4.3b)$$

where $\Gamma_+ = -d\theta/dp|_i$ (4.3c)

is the stability of the profile just above the boundary layer capping inversion, g is acceleration due to gravity, (R_n-G) is the net surface heat flux, β is the surface Bowen ratio, β_i is inversion Bowen ratio defined later, c_p is the specific heat at constant pressure, and $\beta_v \approx -0.07$ is the slope of the dry virtual adiabat. We note that in normal circumstances, $\Gamma_+ > 0$. The right hand side of (4.3a, 4.3b) has a singularity at $\beta_i = \beta_v$: this corresponds to the situation in which the boundary layer inversion corresponds to a virtual adiabat (Betts (1992)), and therefore we expect $\beta_i < \beta_v < 0$, on physical grounds[1].

The second term in (4.2) can be related to the development of equivalent potential temperature in the boundary layer by inspection of the parcel ascent curve in the vicinity of the LFC. From Figure 4.1, in which we assume that the parcel equivalent potential temperature, θ_e, is equal to that of the well-mixed boundary layer, it can be seen that

$$\frac{dp_{LFC}}{dt} = \frac{d\theta_e/dt|_{PBL}}{d\theta es/dp|_{LFC}} \qquad (4.4a)$$

and we can use

$$\frac{d\theta_e}{dt}|_{PBL} = \frac{g(R_n-G)}{P_i c_p}\left[1 + A_r \frac{(\beta_i+1)(\beta-\beta_v)}{(\beta+1)(\beta_i-\beta_v)}\right] \qquad (4.4x)$$

(Betts and Ball (1995)), to obtain

$$\frac{dp_{LFC}}{dt} = \frac{g(R_n-G)}{\Gamma_{es}\, P_i\, c_p}\left[1 + A_r \frac{(\beta_i+1)(\beta-\beta_v)}{(\beta+1)(\beta_i-\beta_v)}\right], \qquad (4.4y)$$

in which

$$\Gamma_{es} = d\theta es/dp\,|_{LFC}. \qquad (4.4z)$$

For a conditionally unstable atmosphere in which convective showers may occur, we require $\Gamma_{es} > 0$. Putting (4.3b) and (4.4b) in (4.2) yields

[1]Otherwise the inversion would be unstable in terms of θ_v.

$$R = -\left[\frac{g(R_n-G)\beta}{\Gamma_+ c_p P_i\,(\beta+1)}\left\{1+\frac{\beta_i}{\beta}A_r\frac{(\beta-\beta_v)}{(\beta_i-\beta_v)}\right\}\right] - \left[\frac{g(R_n-G)}{P_i\,c_p\,\Gamma_{es}}\left\{1+A_r\frac{(\beta_i+1)(\beta-\beta_v)}{(\beta+1)(\beta_i-\beta_v)}\right\}\right] \quad . \qquad (4.5)$$

In this one-dimensional model, the question of whether a given atmospheric profile offers a wet or dry advantage in terms of convective initiation comes down to a question of whether the rate of change of pressure difference between the top of the boundary layer and LFC, R, is higher over a wet (low β) or dry (high β) surface. Given that R is negative if any initiation is to occur, wet advantage implies that R is an increasing function of β, or $\Delta R > 0$, and dry advantage occurs when R decreases with β, or $\Delta R < 0$.

Equation (4.5) can be rearranged as follows, to clarify the dependence on β:

$$R = \frac{g(R_n-G)}{\Gamma_+ c_p P_i\,(\beta+1)}\left\{-\beta-\beta_i A_r\frac{(\beta-\beta_v)}{(\beta_i-\beta_v)}\right\} - \frac{g(R_n-G)}{P_i\;c_p\,\Gamma_{es}(\beta+1)}\left\{(\beta+1)+A_r\frac{(\beta_i+1)(\beta-\beta_v)}{(\beta_i-\beta_v)}\right\},$$

$$R = \frac{g(R_n-G)}{\Gamma_+ c_p P_i\,(\beta+1)}\left[\left\{-\beta-\beta_i A_r\frac{\boldsymbol{\beta}}{(\beta_i-\beta_v)}+\beta_i A_r\frac{\beta_v}{(\beta_i-\beta_v)}\right\} - \frac{\Gamma_+}{\Gamma_{es}}\left\{(\beta+1)+A_r\frac{(\beta_i+1)\boldsymbol{\beta}}{(\beta_i-\beta_v)} - A_r\frac{(\beta_i+1)\beta_v}{(\beta_i-\beta_v)}\right\}\right],$$

$$R = \frac{g(R_n-G)}{\Gamma_+ c_p P_i\,(\beta+1)}\left[\beta\underbrace{\left\{-1-A_r\frac{\beta_i}{(\beta_i-\beta_v)}-\frac{1}{\gamma_{es}}\left(1+A_r\frac{(\beta_i+1)}{(\beta_i-\beta_v)}\right)\right\}}_{b} - \underbrace{\left\{-\beta_i A_r\frac{\beta_v}{(\beta_i-\beta_v)}+\frac{1}{\gamma_{es}}\left(1-A_r\frac{(\beta_i+1)\beta_v}{(\beta_i-\beta_v)}\right)\right\}}_{a}\right],$$

in which

$$\gamma_{es} = \Gamma_{es}/\Gamma_+ \; . \qquad (4.6)$$

so that we can write R in the form

$$R = \frac{(b\beta-a)}{\gamma_+(1+\beta)} \; , \qquad (4.7)$$

in which a,b and γ_+ are all independent of β. γ_+ is the only dimensional parameter given by

$$\gamma_+ = \frac{\Gamma_+ c_p P_i}{g(R_n - G)} \quad , \qquad (4.8)$$

on right hand side of equation (4.7) and is positive definite:

The non-dimensionalised parameter a and b are given by,

$$b = -1 - A_r \frac{\beta_i}{(\beta_i - \beta_v)} - \frac{1}{\gamma_{es}}\left(1 + A_r \frac{(\beta_i + 1)}{(\beta_i - \beta_v)}\right), \qquad (4.9)$$

and

$$a = -\beta_i A_r \frac{\beta_v}{(\beta_i - \beta_v)} + \frac{1}{\gamma_{es}}\left(1 - A_r \frac{(\beta_i + 1)\beta_v}{(\beta_i - \beta_v)}\right) \qquad (4.10)$$

To establish the dependence of R on surface state, we differentiate R with respect to β, from equation (4.7), to find

$$\frac{dR}{d\beta} = \frac{(b+a)}{\gamma_+} \frac{1}{(1+\beta)^2}. \qquad (4.11)$$

Equation (4.11) tells us that the sign of $\frac{dR}{d\beta}$ is independent of β itself. This is a powerful result, because it means that the question of wet or dry advantage is universal in terms of surface Bowen ratio; its sign is independent of Bowen ratio. Furthermore, since γ_+ is a positive definite function in convective conditions, the sign of $\frac{dR}{d\beta}$ (and hence the separatrix between wet and dry advantage, $\frac{dR}{d\beta} = 0$) is determined by the sign of b+a. If $b + a > 0$ then we expect wet advantage, and if $b + a < 0$, we expect dry advantage.

Once it is seen that the function R(β) is monotonic, the question of wet or dry advantage can alternatively be found by comparing the wet (low β) and dry (high β) limits of R

$$R(0) = -\frac{a}{\gamma_+} \qquad (4.12)$$

$$R(\infty) = \frac{b}{\gamma_+} \qquad (4.13)$$

And the difference is

$$\Delta R = \frac{(b+a)}{\gamma_+} \qquad (4.14)$$

Expanding these terms we find

$$(b+a) = \left[\left\{-1 - A_r \frac{\beta_i}{(\beta_i-\beta_v)} - \frac{1}{\gamma_{es}}\left(1 + A_r \frac{(\beta_i+1)}{(\beta_i-\beta_v)}\right)\right\} + \left\{-\beta_i A_r \frac{\beta_v}{(\beta_i-\beta_v)} + \frac{1}{\gamma_{es}}\left(1 - A_r \frac{(\beta_i+1)\beta_v}{(\beta_i-\beta_v)}\right)\right\}\right]$$

$$(b+a) = -1 - A_r \frac{\beta_i}{(\beta_i-\beta_v)} - \frac{1}{\gamma_{es}} - \frac{1}{\gamma_{es}} A_r \frac{(\beta_i+1)}{(\beta_i-\beta_v)} - \beta_i A_r \frac{\beta_v}{(\beta_i-\beta_v)} + \frac{1}{\gamma_{es}} - \frac{1}{\gamma_{es}} A_r \frac{(\beta_i+1)\beta_v}{(\beta_i-\beta_v)}$$

$$(b+a) = -1 - A_r \frac{\beta_i}{(\beta_i-\beta_v)} - \frac{1}{\gamma_{es}} A_r \frac{(\beta_i+1)}{(\beta_i-\beta_v)} - \beta_i A_r \frac{\beta_v}{(\beta_i-\beta_v)} - \frac{1}{\gamma_{es}} A_r \frac{(\beta_i+1)\beta_v}{(\beta_i-\beta_v)}$$

$$(b+a) = -1 - A_r \frac{\beta_i}{(\beta_i-\beta_v)}\{\beta_v + 1\} - \frac{1}{\gamma_{es}} A_r \frac{(\beta_i+1)}{(\beta_i-\beta_v)}\{\beta_v + 1\} \qquad (4.15)$$

or, setting $A'_r = A_r(\beta_v + 1)$,

$$(b+a) = -1 - A'_r \frac{\beta_i}{(\beta_i-\beta_v)} - \frac{1}{\gamma_{es}} A'_r \frac{(\beta_i+1)}{(\beta_i-\beta_v)} \ . \qquad (4.16)$$

Putting (4.16) back into (4.11) gives

$$\frac{dR}{d\beta} = \frac{\Delta R}{(1+\beta)^2} = -\frac{1}{\gamma_+(1+\beta)^2}\left\{1 + A'_r \frac{\beta_i}{(\beta_i-\beta_v)} + \frac{1}{\gamma_{es}} A'_r \frac{(\beta_i+1)}{(\beta_i-\beta_v)}\right\}. \qquad (4.17)$$

Unlike FE03a, who devised two parameters (CTP and HI_{low}) to categorise the behaviour of the system, we find that the progression of the boundary layer towards triggering over surfaces of differing Bowen ratio is controlled by three parameters derived from the ambient profile, namely β_i, γ_+ and γ_{es}. However, we are fortunate that the separatrix between wet and dry advantage given by b+a =0 depends only on the two non-dimensional parameters, β_i and γ_{es}, and is independent of dimensional parameter γ_+.

The equations can now be used to determine the conditions yielding wet or dry advantage according to the three controlling parameters.

4.3 Sensitivity of convective development functions, R and ΔR, to controlling parameters

The strength of the gradient of R with β, ΔR, which quantifies the degree of wet or dry advantage, depends only on the functions a, b and γ_+. Since γ_+ is positive definite, this reduces to two statements.

I. b+a determines the sign of ΔR, and therefore controls wet or dry advantage. Remarkably, this only depends on two non-dimensional external parameters, β_i and γ_{es}.
II. (b+a)/γ_+ determines the strength of the sensitivity (the amplitude of ΔR), and depends on all three parameters, β_i, γ_+ and γ_{es}.

Making sense of these relationships requires some appreciation of physically-relevant values of the external parameters. The inversion level Bowen ratio can be estimated in terms of the humidity and potential temperature gradients across the boundary layer inversion, according to

$$\beta_i = \frac{c_p}{L}\frac{\delta\theta}{\delta q}, \qquad (4.18)$$

where L is the latent heat of vaporisation and q the mixing ratio. Betts and Ball (1995), in presenting data from the FIFE project, suggests that βi may take a wide range of values, though for most of the FIFE experiment βi lay in the range $-0.7 < \beta i < -0.3$. For physical reasons we require $\beta_i < \beta_v \sim -0.07$.

The stability just above the boundary layer inversion, Γ_+, may take a wide range of values, from very low stability associated with a residual boundary layer, to stable values associated with subsidence. However, for any cumulonimbus to occur, the stability is unlikely to be very high. High values can be of the order of $\Gamma_+ \sim 10^{-3}$ KPa, which corresponds to isothermal layer near ground. In deep convective conditions, γ_{es}, can also

take a wide range of values, from close to zero to much larger than unity. Note that value of R~ -1 Pa s^{-1} would be a reasonably rapid rate of decrease of Δp of about 360 m hr^{-1} .

Now, considering (4.7) and (4.11) we can see that the shape of R(β) is relatively simple, as illustrated by Figure 4.2. From consideration of Figure 4.2, we can summarise the conditions for wet or dry advantage as follows:

- If $\Delta R = (b+a)/\gamma_+$ is small, then there is no significant wet or dry advantage. (Illustrated by grey curves in Figure 4.2)
- If $\Delta R = (b+a)/\gamma_+$ is not small[2], and R is negative for some β, then
    - If b+a > 0 there is wet advantage (blue curves).
    - If b+a < 0 there is dry advantage (red curves).

The numerical evaluation of these rules can be seen on Figure 4.3 in which ΔR is plotted as a function of (β_i , γ_{es}), for a range of values of Γ_{es}.

From inspection of Figure 4.3 and consideration of equation (4.11), the sensitivity of triggering to surface type and atmospheric profile can be explained in the following ways.

4.3.1 Dependence of separatrix between wet and dry advantage on β_i and γ_{es}

If it is the case that R is sufficiently large and negative for one-dimensional triggering to be a possibility, then we can then consider the conditions which determine the sign of b+a in (7), as a function of just the two parameters β_i and γ_{es}.

The inversion Bowen ratio, β_i, controls the rate of drying of the PBL air by entrainment, and in most circumstances, where the air above the PBL is drier than the air in the PBL,

[2]Note that we do not know a priori how large ΔR needs to be, for significant wet or dry advantage, and this in practice is likely to depend on the magnitude of convective triggers in the boundary layer.

this process reduces θ_e, and therefore restricts the rate of descent of P_{LFC}. For these reasons, the PBL over the dry surface normally has lower θ_e than the air over the wet surface, and in extreme cases, θ_e can fall with time over the dry (Betts and Ball 1995). Whether this process is significant depends then on the ***difference*** in humidity between the PBL and the air above it (not, as in FE03a, a measure of the sum of these humidities, HI_{low}). When the humidity difference between PBL air and the air above is small, β_i is very large and negative, and we should expect a dry advantage: the LFC behaves similarly over the wet and dry ground because there is little reduction of θ_e due to entrainment, P_{LFC} is similar over the wet and dry surfaces, but the boundary layer grows deeper more rapidly over the dry surface. In contrast, when the difference in humidity between the PBL and the air above it is large, β_i is very small and negative, and θ_e in the PBL is significantly reduced by entrainment. In this case, while the boundary layer over the dry surface may be deepening rapidly, P_{LFC} over this surface may also be rising less rapidly (or even possibly falling) relative to p_{LFC} over the wet surface, which will always fall in cases of conditional instability. So in summary, for large-negative β_i, we expect dry advantage, but for small negative β_i, wet advantage is possible.

The ratio of stabilities, $\gamma_{es} = \Gamma_{es}/\Gamma_+$, represents the degree to which p_{LFC} and P_i are responsive to the surface heat fluxes and attendant changes in PBL thermodynamics, and could be termed a "stiffness ratio". If Γ_{es} is high, then the LFC is in some sense "stiff" in relation to the changes in θ_e in the boundary layer, meaning that the descent of the LFC with increasing boundary layer θ_e is slow. If Γ_+ is high, then the PBL grows relatively slowly over both wet and dry surfaces. If the stiffness ratio γ_{es} is high, the LFC remains relatively fixed while the PBL is more mobile and may grow more rapidly (particularly over dry surfaces, where sensible heating is significant). If γ_{es} is low, the LFC moves more freely in response to PBL θ_e, but the boundary layer depth grows more slowly, and in these circumstances wet advantage is possible.

Combining the effects of the controlling parameters, we find wet advantage to be increased when β_i is small negative and when γ_{es} is low. In this case, p_{LFC} descends rapidly over the wet surface, and is also more highly sensitive to θ_e in the PBL. Although PBL growth may be relatively slow if there is high stability, Γ_+ contributing to low γ_{es}, θ_e is

lower over a dry than a wet surface, and therefore p_{LFC} is also lower (higher altitude) over the dry.

4.3.2 Amplitude and sign of R: is wet or dry advantage significant?

Now it has been seen that the possibility of wet or dry advantage is determined by Figure 4.3, but we still require the sensitivity of R to Bowen ratio, ΔR, to be large, for any advantage to be significant. We can say that ΔR, which is proportional to $(b+a)/\gamma_{+}$, will be large in magnitude when the magnitude of (b+a) is large, and/or γ_{+} is small.

If, Γ_{+} is large (γ_{+} is large and lower γ_{es}), CBL growth is slow over both wet and dry surfaces. In this case, there is little entrainment of dry air from aloft, over both surfaces, and the development of θ_e and LCL is very similar over the wet and dry. Consequently there can only be weak advantage between wet and dry surfaces. In fact, this is probably a high-CIN environment in which dynamic triggering is dominant.

The dimensional stability, γ_{+}, also depends on the net heat flux, (R_n-G): the rates of PBL growth and θ_e tendency are controlled by the magnitude of surface fluxes, and if these fluxes are weak, there will be little tendency for convective development through this one-dimensional process. Similarly, the dependence of γ_{+} on P_i can be explained quite easily: when P_i is small, the rate of boundary layer growth is much more rapid (heat is added to a smaller mass) and therefore there can be much greater difference between wet and dry environments.

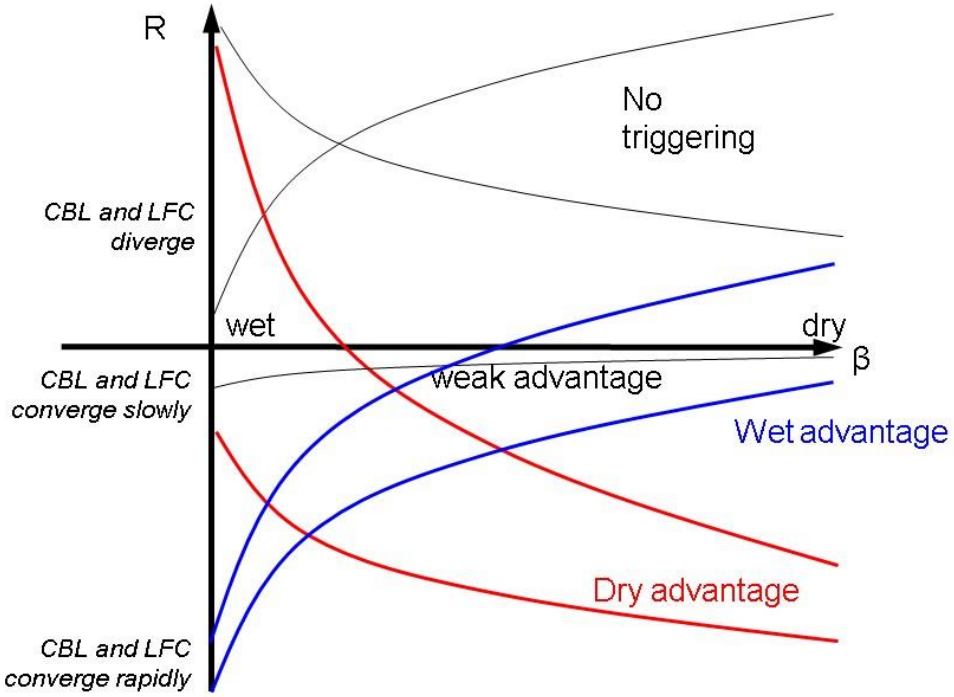

Figure 4.2: Typical curve of R(β) for dry and wet advantage.

Finally, we require R to be significantly negative somewhere, for any advantage between dry and wet surfaces to be significant. In considering this, we separately treat the regions of dry and wet advantage and consider the possible curves in Figure 4.2.

- In regions of wet advantage (low β) we require R(0) = $-\frac{a}{\gamma_+}$ to be large and negative for R to be sufficiently negative over a wet surface.
- In regions of dry advantage (high β) we require R(∞) = $\frac{b}{\gamma_+}$ to be large and negative, which only fails when β_i is very small and negative (when we expect wet advantage) i.e. case 7 in Chapter 2 where β_i is very small, means large enterainment, so BL and LFC both increases. Thus when rate of increase of BL is greater than rate of increase of LFC (i.e over wet surface), convection occured.

These conditions were tested in the plotting of Figure 4.3 and the condition of large negative R in cases of wet or dry advantage was always fulfilled.

4.3.3 Summary of sensitivity of wet or dry advantage to controlling parameters.

This model predicts location and strength of wet and dry advantage on β_i and γ_{es} space based on values of ΔR. The conditions are seen in Figure 4.3 below. In Figure 4.3, results are derived for a boundary layer of initial conditions Ar=0.4, P_i= 5000 Pa, R_n-G(Surface energy input)= 500Wm^{-2}, Γ_+ = 0.001 K Pa^{-1}, β_v= -0.07, g=9.81 ms^{-2}, c_p = 1004. In the figure, a range of solutions are shown for 0 < stiffness ratio (γ_{es}) < 8.

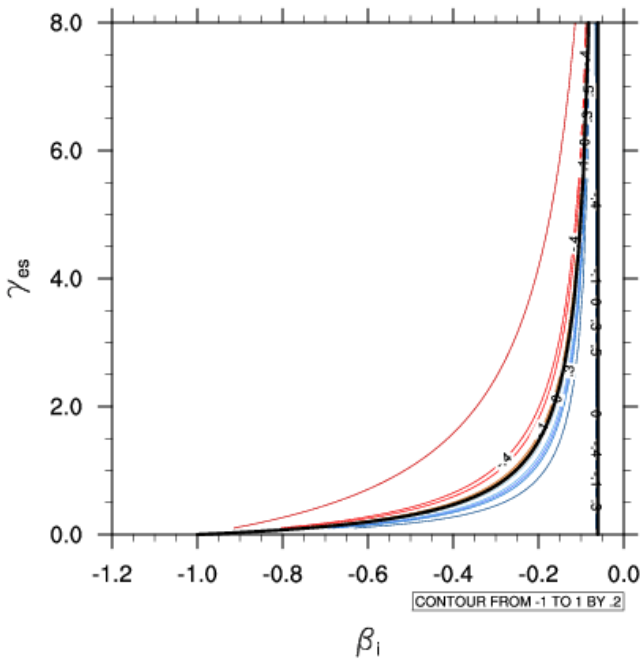

Figure 4.3: Contour plot of ΔR (~ Pa s^{-1}) as a function of (βi,γ_{es}) for different values of γ_+. Here red contour represent conditions favourable for dry advantage and blue contours are region favourable for wet advantage in the plot. The black contour is the separatix curve i.e. ΔR=0.

Wet advantage is favoured when β_i is small and negative (θ_e reduces by entrainment) and stiffness ratio γ_{es} small i.e. P_{LFC} is more mobile than PBL top and P_{LFC} approaches PBL top. This condition is satisfied in lower right side of the plot in Figure 4.3, shown by blue curve.

Whether this wet advantage is significantly strong depends on γ_+ being sufficiently small (in (4.11)). There is a connection between the conditions on γ_{es} and γ_+, in that inversion stability Γ_+ appears in both parameters. High Γ_+ will tend to decrease γ_{es}, generally increasing the likelihood of wet advantage, but by increasing γ_+, will tend to reduce the amplitude of this wet advantage.

Similarly for dry advantage β_i is comparatively large and negative and stiffness ratio γ_{es} also large. Large Γ_{es}, γ_{es} obstructs the free movement of LFC and make it constant over the period of time. This condition is shown by red curves in Figure 4.3.

Thus, in this section we are able to find analytical solutions of the physical one-dimension convective initiation model suggested in FE03a. According to this solution, there is a seperatix curve whose value depend only on β_i, which distinguish whether an event will have the wet advantage or dry advantage. In the next section we have tested these solutions against EMBRACE output which is a convection-permitting, limited area simulation.

4.4 Model Evaluation

This section presents analysis of EMBRACE simulation output for the rates at which the boundary layer top and the LFC approach each other over a given surface; we here attempt to evaluate this analysis against the numerical solutions.

4.4.1 Computation of parameters

This analysis is based on the conceptual approach of FE03a, in which an early morning sounding is studied in order to assess the subsequent profile evolution. Of the controlling parameters in the system, Γ_+ and γ_+ are reasonably standard quantities to calculate or estimate from EMBRACE simulation.

a) Calculating Γ_{es}

In practice it is a two-stage process: Firstly the LFC should be determined through computation of a moist parcel ascent (Normand's construction): Where LFC is the level where parcel saturated profile meets environment profile and this computation is a

standard element in routines to compute CAPE, for instance. Once the LFC is identified, Γ_{es} can be computed as the vertical gradient of θ_{es}, using equation (4.4z), but for instance the precise value of Γ_{es} at the LFC may be very sensitive to local thermodynamic anomalies in the profile. Also sometimes, during the morning the LFC does not exist so we applied bulk estimates of relatively broad layer between fixed pressure levels to compute Γ_{es}. The reference levels for bulk estimate are found based on the test given below.

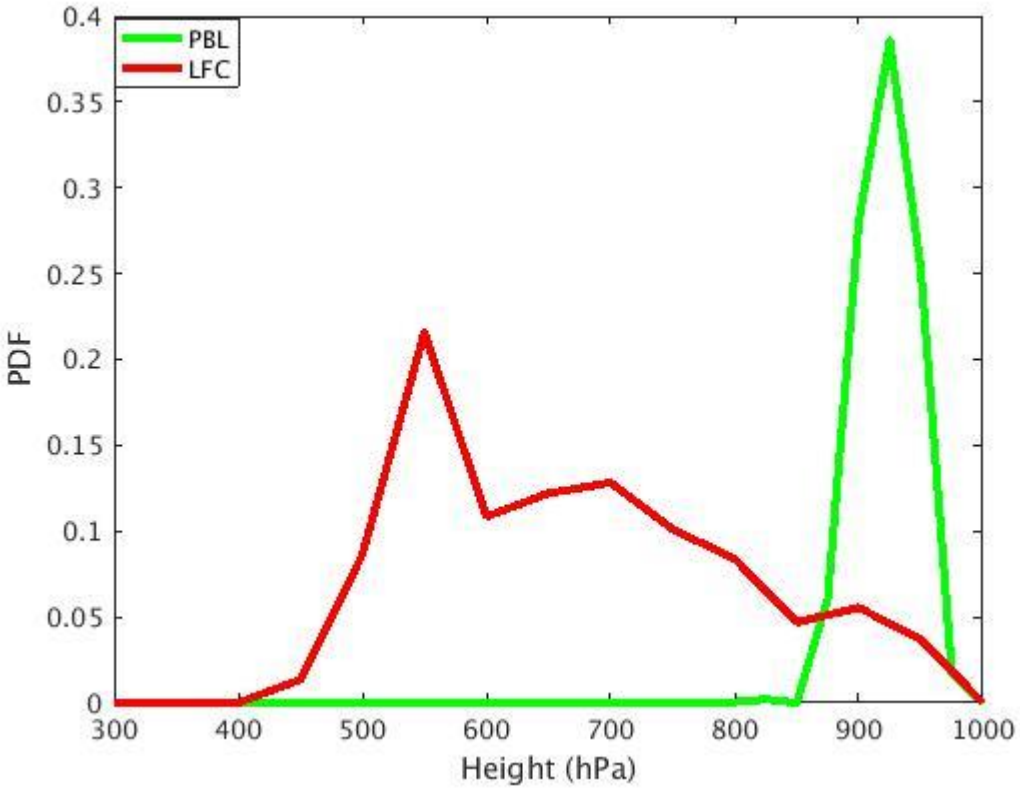

Figure 4.4: To show average height of LFC and PBL top at 0300UTC (morning) in EMBRACE simulation.

Figure 4.4 shows that the inversion height (PBL top) has quite a narrow range between 875 to 975 hPa whereas the LFC can take a wide range of values. The majority of values of LFC fall within the range 550 hPa to 850 hPa, thus during bulk estimates of LFC we have chosen these levels as reference levels. Here it is worth to mention that in the morning LFC exists for only 811 cases out of 1961 subsequent initiations.

b) Calculating β_i and Γ_+

To find these two quantities is also two stage process: at first the inversion level is identified. Inversion layer above PBL often called as capping inversion, which is the layer that has temperature higher than boundary layer. Thus, β_i could be computed based on the differences in specific humidity and potential temperature using nearest possible layers across the inversion level, using (4.18). And Γ_+ can be computed as the vertical gradient of θ just above capping inversion, using equation (4.3c).

4.4.2 Evaluation of results

In Figure 4.3 we have idealised numerical solution of equation (4.17). In this section we have computed βi , Γ_{es} and ΔR from EMBRACE output for afternoon convective initiations (as defined in section 2.2.2 of Chapter 2) for four defined domains, and compared them with Figure 4.3.

a) Comparison with idealized numerical solution as shown in Figure 4.3

i) All domains combined

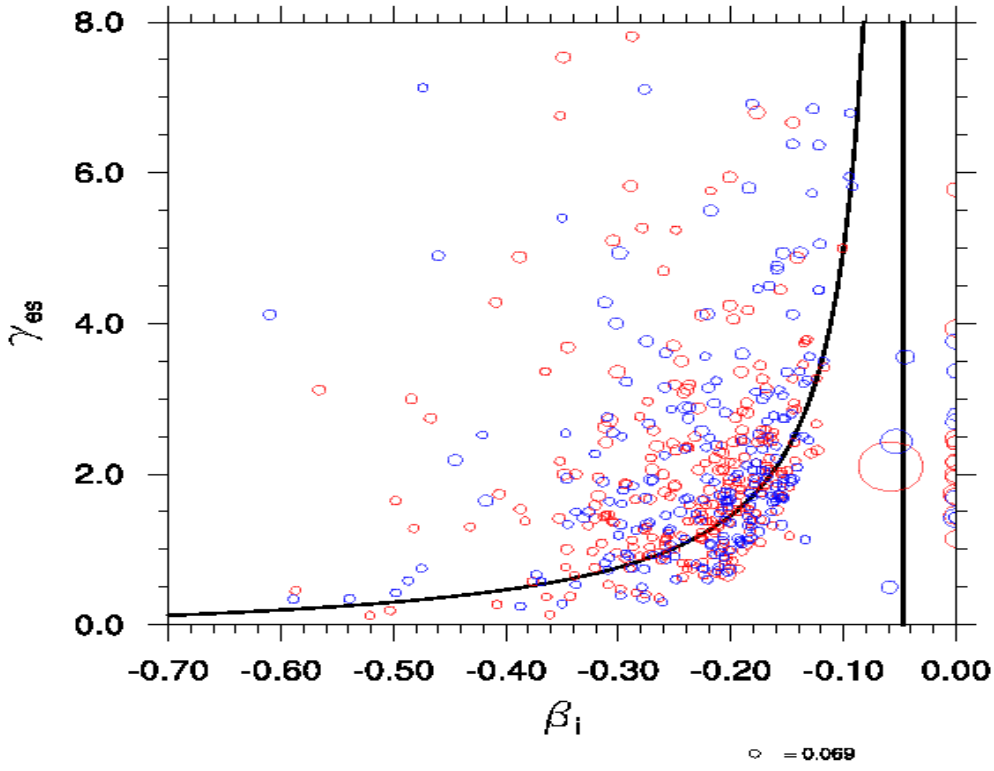

(a)

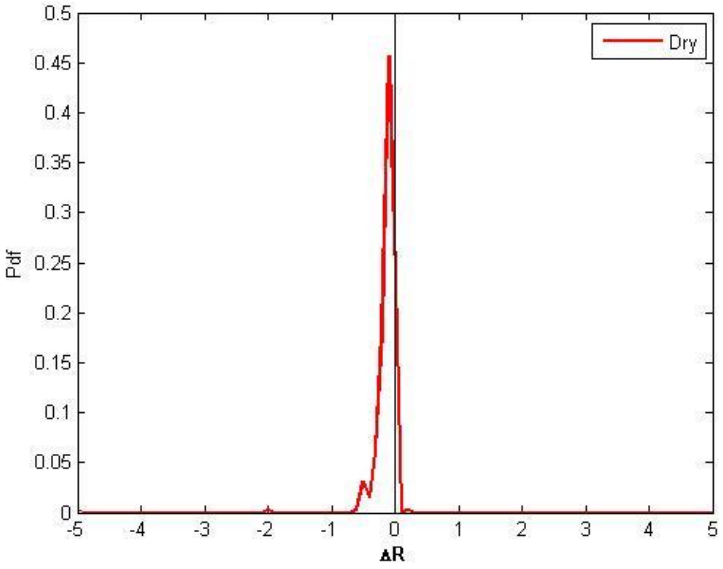

(b)

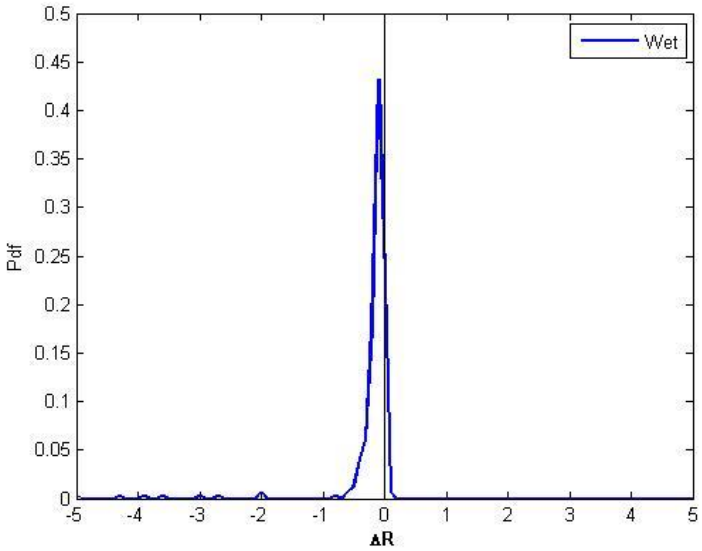

(c)

Figure 4.5a) Reconstruction of Figure 4.3 for observed wet (blue circle) and dry (red circle) event (as described in Section 3.2.3 of Chapter 3) in EMBRACE output for all study domains combined, where size of circle denotes magnitude of ΔR. Here only those events are included for which R < 0. Black line is the theoretical separatix curve. b) and c) are the probability density function of dry and wet events having different values of ΔR.

Figure 4.5a) evaluates the observed value of ΔR for dry and wet events against the numerical solution. In this figure red and blue circles represent dry and wet advantage events as observed in EMBRACE simulations using the method described in Section 3.2.2 of Chapter 3. The location of circles shows theoretical prediction of wet and dry advantage i.e. if event position is below black curve it is forecasted as wet advantage whereas if the position is above black curve the initiation should be favoured over dry soil.

There is no statistically significant difference between curve (4.5(b) and 4.5(c)), nor the mean and median, but it is worth mentioning here that the majority of events have ΔR less than 0. Thus, it shows that even in the wet period of the monsoon season, the majority of observed morning profiles do commonly occupy the broad band of phase space in Figure 4.3 corresponding to dry advantage (red contours in Figure 4.3) and rarely the narrow band corresponding to wet advantage (blue contours in Figure 4.3). Alternatively, we can say, our model offers some theoretical (thermodynamic) basis for the observation of Taylor *et al*. (2012), showing preference for dry advantage. However, our data do show wet advantage in many cases.

It should also be noted that the values of ΔR in Figure 4.5b and 4.5c are relatively low, implying only a small difference in likelihood of triggering of convection, between wet and dry surfaces. Note that the median value of $\Delta R \sim 0.05$ Pa s^{-1} corresponds to a difference in height from boundary layer to LFC of only 18 metres per hour in difference between a wet and dry surface. This is insignificant relative to the magnitude of other convective triggers, and for this reason it is unsurprising that there is little difference between the pdfs of Figure 4.5b and 4.5c.

In Section (b) below, an attempt is made to consider only the much smaller class of events in the dataset for which ΔR has a larger value.

Here it is worth to mentioning that Case 1 and 2 in Chapter 2 (which has similar features to that of the Taylor *et al.* (2011) explanation), shows strong vertical moisture convergence at the point of initiation which lowers the LFC at the location whereas thermodynamic forcing over the dry surface rapidly lifts the PBL top to the LFC. So, in

these cases the thermodynamic aspect of boundary layer meeting the LFC is fulfilled using the dynamic condition.

Finally, it should be remembered that the apparent disagreement between theoretical prediction (position of circles) and observed type of feedback (color of circle) in Figure 4.5a could be due to our method of deciphering wet and dry soil.

(ii) Domain wise evaluation

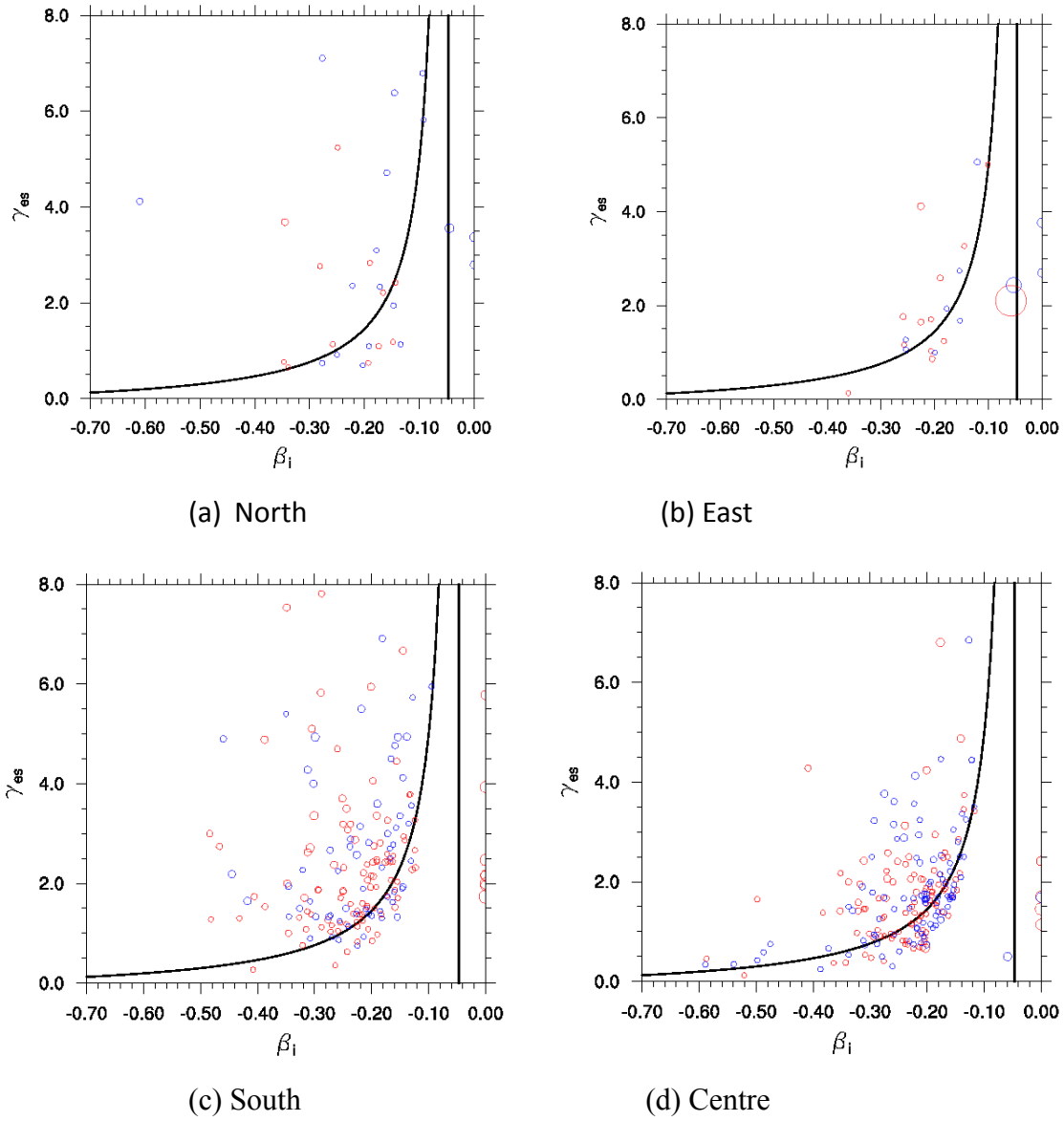

Figure 4.6: Same as 4.5(a) but for different study domains separately. Also for South and Centre domain higher orographic events (height difference >300) are excluded.

Figure 4.6 shows statistics of observed dry and wet advantage convective initiation compared to theoretical separatrix curve, over different study domains. The East domain (Figure 4.6b) shows the minimum number of convective initiations based on thermodynamic model. Since it is an active spell of the monsoon season, rain initiation could be synoptically induced by mid-level moisture convergence (Case 6, Chapter 2) and the primary condition of LFC meeting PBL top is not fulfilled. The Central domain (Figure 4.6d) excluding higher orographic events shows the maximum number of thermodynamically driven initiations.

(iii) Statistics of events excluding gradient cases

In Figure 4.7 events with soil moisture pattern of gradient and higher orography are excluded and reanalyzed. From statistical analysis there is no statistically significant difference between mean and median of the two curves shown in Figure 4.7b.

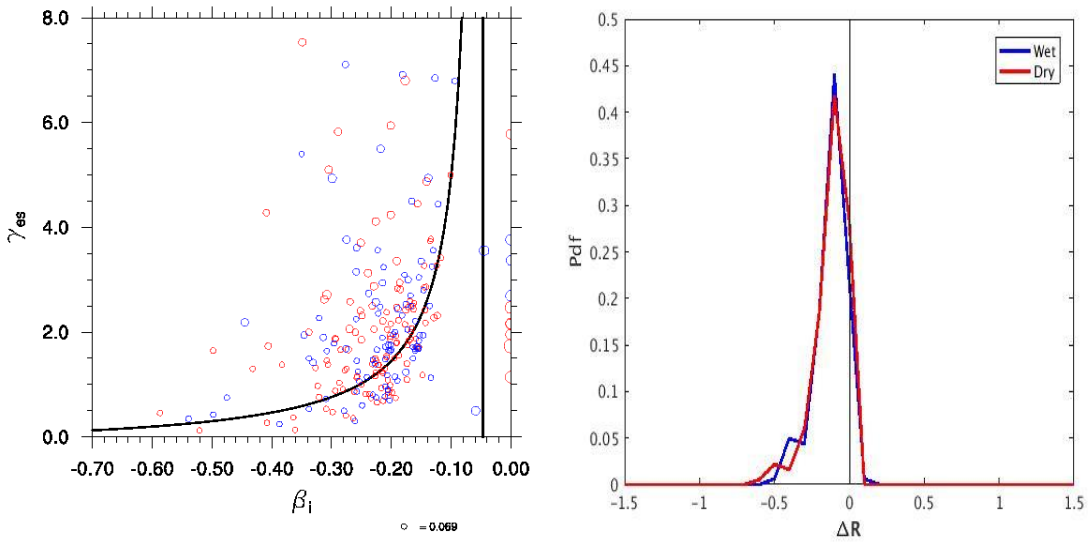

Figure 4.7: a) Same as 4.5a except that gradient cases (as defined in Section 3.2.2) and orographic case with height difference > 300m are excluded. b) The probability density function of dry (red curve) and wet (blue curve) events having different values of ΔR.

b) Probability of occurrence of dry or wet advantage event

It has been noted that for the great majority of events shown in Figure 4.5, the ΔR is extremely low, implying insignificant difference in the likelihood of thermodynamic 1D triggering between wet and dry surface. To account for this in the statistics, a new

category of data with low magnitude of ΔR is defined where |ΔR|< delta. Significant values of delta are chosen from delta=0.1 Pa s^{-1} (~ 36 metres per hour) upwards as shown in Table 4.1. The contingency table shows that for theoretically favorable conditions for dry advantage i.e. ΔR negative, only 1 in 3.7 theoretical initiation showed an actual dry advantage event. Similarly, out of 3.6 theoretically predicted wet advantage cases (ΔR > 0), only 1 event showed observed wet advantage. Thus, there is less than or equal to 1/3rd chance for theoretical forecast to match observed type of initiation. Of course this method is subjected to depend on our method of deciphering wet and dry advantage in practice.

	ΔR < δ				**ΔR > δ**			
δ =	0.0	-0.1	-0.3	-0.5	0.0	0.1	0.3	0.5
Dry (%)	246 **(26.79)**	96 **(29.81)**	19 **(24.36)**	4 **(10.25)**	74	1	-	-
Wet (%)	239	103	30	13	68 **(21.79)**	2 **(33.33)**	-	-
Null	433	123	29	22	170	3	-	-
	918	322	78	39	312	6	-	-

Table 4.1: Contingency table shown, for the fraction of dry, null and wet events (defined in Section 3.2.3) for different cutoff (δ) values of ΔR. This is the result for all study domains combined.

4.5 Discussion

4.5.1 Relationship to FE03a

Unlike FE03a, we find the dynamics of the convective system initiation to depend on 3 parameters. Out of these, only two parameter, β_i and γ_{es}, are needed to distinguish whether the initiation occurs over wet or over the dry surface but it is not the sufficient condition. It is also necessary that $(a+b)/\gamma_+$ should be large enough for any advantage to exist

therefore the third dimension parameter γ_+ cannot be neglected. A comparison of the controlling parameter in this system with those of FE03a (CTP-HI_{low}) follows.

a) Representation of profile stability

The parameter CTP in FE03a is inversely related to stability just above the boundary layer inversion (Γ_+). FE03a have argued that high value of CTP leads to likelihood of dry advantage. High value of CTP corresponds to low Γ_+ and high Γ_{es}, meaning high γ_{es} which implies dry advantage. The decrease in value of parameter Γ_+ in γ_+ (equation 4.8), enhances the strength of dry and wet advantage Thus the behaviour of γ_{es} is in accord with that of FE03a's derived CTP.

b) Representation of humidity parameter

Both of the models have a humidity parameter: in FE03a it is named as HI_{low} which is sum of dew point depression in and above the boundary layer, whereas in our model humidity parameter is inversion Bowen ratio β_i, which is difference of humidity between the same layers. The inversion Bowen ratio controls the evolution of θ_e as a boundary layer growth and therefore it controls the behaviour of P_{LFC} . In FE03a if HI_{low} is high, high surface Bowen ratio (changes in latent heat flux/moisture is fairly constant thus no change in θ_e) leads to fairly constant P_{LFC}, whereas high sensible heat flux corresponds to rapid growth of boundary layer, and hence dry advantage is likely. However if β_i is small and negative over the dry surface, this leads to a decrease in θ_e by entrainment, and the height of the LFC may increase (as noted in the behaviour of EMBRACE model Case 7, in Chapter 2), thus the likelihood of dry advantage is reduced.

4.5.2 Limitations

In applying these results to real-world situations, a number of important limitations must be considered. The model is restricted to describing initiation of convective systems through daytime growth of the convective boundary layer, and not the important class of convective rainfall events occurring at night, nor convective events dynamically triggered, at cold fronts for instance. The distribution of rainfall by organised convective systems (MCSs) is also not likely to be captured by this model: such systems usually

involve intense mesoscale flows (gravity currents and gravity waves) which trigger convection dynamically, somewhat independent of the underlying boundary layer state. For these reasons there is evidence that MCSs deliver more precipitation to a surface of low Bowen ratio, where there is simply more water vapour in the boundary layer available for precipitation (Taylor and Clark, 2001; Hartley *et al.*, 2016).

An additional, and fundamental drawback of the model presented here is that its one-dimensional setup ignores mesoscale dynamic flows which are also driven by the differences in boundary layer state over adjacent wet and dry surfaces. Such flows have been shown in observational (Taylor *et al.* 2011; Kang *et al.*, 2007; Dixon *et al.*, 2013) and modelling (Roy and Avissar, 2002; Roy, 2009; Garcia-Carreras *et al.*,2011) papers to be significant under conditions of reasonably light winds. The very question of whether wet or dry surfaces trigger convection first in a given atmospheric profile implies that these surfaces are in some proximity, and therefore will tend to drive their own circulations on the boundaries. These circulations are thermally direct, with hot air rising, and tend to give the greatest convective triggering on the warm and dry side of a surface boundary (specifically, on the downwind side of a warm/dry surface). Garcia-Carreras *et al.* (2011) also showed that this location is where, due to interactions of mixing and advection, the boundary layer θe is maximised, giving an additional advantage for convective triggering close to the boundaries. Taylor *et al.* (2012) in a global analysis found dry advantage at almost every location where a significant signal appeared, and argued that this is consistent with dynamic triggering on the warm side of boundaries. It remains to be seen whether the one-dimensional model has any value at all, given its lack of representation of mesoscale dynamics, although our brief evaluation of high resolution simulation in section 4, and case studies in Chapter 2 shows that one-dimension evolution of boundary layer is possible where the boundaries between contrasting wet and dry surfaces are relatively smooth transitions, meaning that pressure gradients and the resulting circulations may be weak.

A further limitation of the method developed here is that it is (like FE03a) based on the early-morning thermodynamic profile, and does not follow the full transition through several hours towards the eventual point of convective initiation. A number of functions of the system will necessarily change during this evolution, differently over wet and dry

surfaces, including the inversion Bowen ratio. The analysis shown here indicates the sense of the tendency towards deep convection early in the morning, but does not tell us whether that tendency is maintained consistently in the following hours. Whether the method does consistently capture wet and dry advantage must be tested in practice.

Finally, the presence of modestly strong winds will break down the coupling between surface and boundary layer state. Although Dixon *et al.* (2013) demonstrated significant patterns of boundary layer thermodynamics coupled with West African surfaces in ambient winds up to 5 ms^{-1}, the strength of this signal weakens with ambient wind speed.

In this section, a number of physical processes have been listed, which offer challenges to the implementation of one-dimensional model. However, in condition of relatively calm synoptic condition and weak mesoscale forcing such as seen in Figure 2.12 and 2.14 of Chapter 2, one-dimension boundary layer model can reasonably describe physical basis of convective initiation

Apart from challenges due to physical basis there are some limitations that arise due to practical application. For instance, the comparison of the sign of predictive feedback with observational initiation depends on our method of deciphering wet and dry surface in practice. Here wet and dry advantage events are based on wet patch or dry patch patterns in the soil moisture field. However we have seen in Chapter 2 that homogeneous dry and wet soil patterns at convective scale also play an important role in application of the one-dimensional model. Keeping in view this factor, it might be interesting to see behaviour of null events (described in Section 3.2.3) with high and low average evaporative fraction in β_i and γ_{es} phase space.

4.6 Conclusions

Based on the conceptual framework of FE03a, we have developed a thermodynamic model which describes the different one-dimensional pathways towards convective triggering. The equations provided in this chapter represents, first analytical solution to the model proposed by FE03a, which has been widely used.

Unlike FE03a, we find the system to be governed by 3 parameters. However, fortunately, only two of these are needed to separate the possible conditions of wet and dry advantage. This leads to the separatrix curve shown in Figure 4.3. Although the separatrix divides conditions of wet or dry advantage, whether this advantage is relevant depends on the amplitude of the signal, and in order to determine this amplitude, all three controlling parameters need to be taken into account. As a future work it will be interesting to find strength of this amplitude to surpass any synoptical forcing in this region, which is driven by synoptic scale monsoon dynamics.

The cutoff values in parameter space of CTP-HI_{low} to separate dry and wet advantage in FE03a has been found empirically whereas the threshold to differentiate between wet and dry advantage in this model is based on physical principles. Since in FE03a values are found empirically it changes its value based on region, like over Indian subcontinent its values are higher than that of the continental USA.

The first testing of this one-dimension model against numerical model simulations from EMBRACE over four domains combined, as described in Chapter 3, indicates existence of cases existing in both dry and wet advantage regimes (Figure 4.5 and 4.6). However, Figure 4.5 and Table 4.1 show that the prediction of prevailing dry advantage events is the most common occurrence in morning profiles, and this conclusion may lend support to the observational dominance of dry advantage, found by Taylor *et al*. (2012). It is worth to mention here that the considered simulation includes the region, where the results of Taylor *et al.* (2012) are not statistically significant for dry advantage over India. Although the first testing over the Indian sub-continent shows some linkage between previously defined one-dimensional and three-dimensional models through thermodynamics, more testing is required in other places like Sahel and Great Plains of USA. Thus the equation provided in this chapter offers a quantitative prediction of the possibility of wet and dry advantage occurring systematically, which is of great importance for climate analysis, to weather and climate forecast especially over the regions with limited water availability.

5 Conclusions and proposed future work

5.1 Conclusions

The pathways to solve the long-standing problem of soil-moisture-precipitation feedback have been addressed in various part of the world such as The Great Plains of USA and Sahel. In these regions progress has been made. However, there is a lack of studies over the Indian sub-continent. This thesis tries to understand the underlying processes which drive land-atmosphere interactions (here in particular soil moisture – precipitation feedbacks) to give rise to the convective initiation over different soil moisture conditions over the Indian sub-continent during the monsoon period.

In this thesis, each chapter approaches the problem in a different way to tackle the different aspects of the soil moisture-precipitation feedbacks. In Chapter 2 indirect observational evidence of land-atmosphere interaction has been presented. In this chapter, case studies from EMBRACE model output which is simulated from operational data have been presented to illustrate and understand the important boundary layer processes that cause convective initiation. Chapter 3 took a statistical approach to evaluate the existing soil moisture-precipitation feedback theories and find their limitations in a mesoscale non-parameterized convection-permitting simulation. Finally, in Chapter 4 a one-dimensional conceptual model is developed and briefly tested, to offer deeper physical understanding of the problem.

5.1.1 Problem overview

In the literature review in Chapter 1 it has been seen that there are two branches of explanation for the land-atmosphere feedback processes. According to the first group,

convective initiation can be explained using a one-dimensional boundary layer- level of free convection (LFC) model as described by FE03a. According to this theory there is a probability of rain initiation when the boundary layer top meets the level of free convection by heating or moistening of the boundary layer. Thus this theory emphasises the thermodynamic aspects of the problem. The second group explains convective initiation as dynamic triggering i.e. triggering due to wind convergence (Ookouchi, 1984; Segal and Arritt, 1992; Garcia-Carreras *et al.*, 2011; Taylor *et al.*, 2011). Spatially heterogeneous soil moisture conditions can give rise to local wind circulations which under favourable condition can be organized into convection near convergence zones. Thus, the second theory takes into account three-dimensional dynamics. Therefore, this thesis has tried to evaluate which theory best explains the feedback processes over India. It has also quantified the limitations of the existing models and provided an analytical solution to the FE03a quantitative model derived from sound physical relationships instead of empirical solutions (FE03a).

5.1.2 Insight gained from observations and case-studies

Chapter 2 tries to find the evidence of soil moisture-precipitation feedback from existing observations and mesoscale modelling. The above mentioned one-dimensional model requires radiosonde and in situ data to test the thermodynamic model but it is difficult to get both the data at the same place and at same time. It is more difficult to validate three-dimension models using the present state of observational data over India. Therefore, in first part of the chapter synoptic observations are used to find indirect evidence of land-atmosphere interaction. Here, rainfall is taken as a factor which changes the soil moisture and characteristics of boundary layer parameters. This study showed that changes in the value of the boundary layer parameters due to rainfall, take several hours to recover to the mean trend of the season.

The second part of the chapter is a qualitative study of the boundary layer processes like one-dimension profile changes, vertical and horizontal convergence through convection permitting mesoscale modelling data. Seven case studies have been presented.

The presented case studies and subjective analysis of all the afternoon rain initiation cases over two low orography domains show that a core condition that needs to be satisfied in the majority of cases for rain initiation by land-atmosphere interaction, is the meeting of the boundary layer top with the LFC. In particular, the model of Haiden (1997) analysing LCL and boundary layer top, is not applicable to deep convective initiation in these cases. Now the condition of boundary layer top meeting the LFC can be satisfied by changes in thermodynamic or dynamic conditions of the boundary layer. The thermodynamic consideration shows the possibility of occurrence of ***both*** wet and dry advantage as postulated by FE03a. Wet advantage can occur by moistening of the boundary layer by increase of the latent heat flux which causes the LFC to descent, whereas the dry advantage is probable by gradual heating and thus lifting of the boundary layer top by high sensible heat flux. Recall that, the three-dimensional dynamic model shows probability of ***only*** dry advantage near wet to dry soil moisture gradients by local wind convergence. In this case there is a generation of local wind circulation near the heterogeneous surface which give rise to the convective initiation that are favoured on the dry surfaces (low EF), close to wetter surfaces (high EF).

Thus in summary, it appears that mesoscale thermodynamic triggering occurs for the extreme low and high soil moisture values under homogeneous soil moisture conditions at convective scale whereas dynamic triggering happens under heterogeneous soil moisture conditions.

5.1.3 Evaluation of existing models

The purpose of Chapter 3 is to test the applicability of various existing theories in the context of feedback mechanisms between soil moisture and precipitation over the Indian sub-continent during the monsoon season. To test existing theories, various relationships between soil moisture, fluxes and rainfall in a high resolution convection-permitting atmospheric model (UK Met Office Unified Model) have been evaluated. Triggering by 3-D circulations over soil moisture anomalies is explored, as well as the effects of 1-D profile stability measures, which are thought to confer “wet advantage” (triggering of rain

over wet surfaces) or “dry advantage” in different conditions. The impact of topography is also examined.

In Chapter 2 it was seen that characteristics of the soil moisture anomaly has direct impact on the pathway that leads to different types of feedback. Gradient and very dry homogeneous patches can give rise to dry advantage under different conditions. Similarly, for the wet advantage, high evaporative fraction plays an important role under the calm synoptic conditions. So, to identify the characteristics of the underlying soil moisture conditions associated with triggering, three statistical methods have been developed, named as composite analysis, gradient analysis and average soil moisture analysis. The composite analysis is a composite of the soil moisture field drawn, to see the average soil moisture structure in the vicinity of rain initiations for different domains.

The gradient analysis is effective to find gradient or patchy characteristics in soil moisture field, like dry-to-wet (DW), wet-to-dry (WD), wet patch at event centre, or dry patch in downwind direction. It is worth to mention here that the gradient analysis is a one-dimensional analysis so can have bias/error if there is noise (i.e very patchy soil moisture conditions) in the soil moisture field. Gradients in the soil moisture field usually have gradual transitions so may be easy to depict, but finding wet or dry patches using one-dimensional regression analysis could be erroneous, thus a two-dimensional average soil moisture analysis has been performed to characterize the soil moisture structure. The average soil moisture analysis method has 3 variables, ϵ, l, L which can be useful to optimize different moisture scenarios such as different seasons and scale-dependent studies.

From the composite and gradient soil moisture analysis, it has been found that the afternoon convective rainfall tends to initiate over comparatively wet soil near, and slightly downwind of soil moisture gradients, with dry soil just upwind of the initiation. Orographic analysis of the Central and Southern Indian domains, which have complex orography, showed that rainfall over high-lying orography has a greater preference over wet soil. Here it is worth mentioning that excluding events having orographic difference greater than 300m from the South and Central domain leads to significant preference for DW cases in the gradient analysis. The subjective wind-field convergence and orographic

analysis shows that in the Central domain near higher orography, dynamic land-atmosphere interaction is weak, compared to orographically initiated precipitation. Overall, it appears that rainfall dynamically triggered by orography leads to serial correlation of rainfall with high soil moisture in these areas.

Therefore, if we summarize soil moisture analysis domain wise, it is seen that

- the North domain has preference for wet advantage.
- The East domain has statistically significant preference for wet soil near DW gradients.
- The Southern domain has the preference for dynamic triggering near the soil moisture DW gradient for both low and high lying orographic events.
- The high orographic rain initiation in the Central domain has the preference for the orographically induced wet advantage which is caused by serial correlation between the rain and higher values of soil moisture whereas comparatively flat locations in this domain have the preference for the dynamic triggering near DW gradients.

To evaluate the predictive capability of the 1-D "convective triggering potential – humidity index" (CTP-HI_{low}) framework, a reverse experiment was designed using generalized soil moisture conditions and the three-dimensional atmospheric model instead of the one-dimensional Slab model used by FE03a and Tuinenburg *et al.* (2011). It is found that there is no evidence of consistent predictability of wet or dry advantage within the parameter ranges suggested by previous authors. It seems that there is a requirement for a more generalized or modified framework, to have universal threshold values to distinguish between dry and wet advantage rain events, and that 1-D boundary-layer evaluation may not be sufficient to address all atmospheric conditions.

5.1.4 A new theoretical model

The problem of one-dimensional boundary layer development over wet and dry surfaces is analysed, in order to quantify the tendency for deep cumulonimbus convection to first initiate over the wet or the dry surface. Well-known integral models for the

thermodynamic evolution of the convective boundary layer were used to provide the rate of ascent of the boundary layer top. The associated changes in equivalent potential temperature in the boundary layer determine the rate at which the level of free convection descends, as a function of the ambient profile, the thermodynamic forcing, and the surface Bowen ratio. In combination, algebraic equations are derived for the rate at which the boundary layer top approaches the level of free convection. The behaviour of these equations is controlled by three parameters. Two non-dimensional parameters, the Bowen ratio at the boundary layer top, and the ratio of the vertical gradient of saturated equivalent potential temperature at the level of free convection to the profile stability just above the boundary layer, determine whether there is wet or dry “advantage". A dimensional function, dependent on the surface fluxes, the boundary layer depth and the profile stability, describes the magnitude of the response, and is needed to assess whether the wet or dry advantage will have significant amplitude. Collectively, these relatively simple algebraic equations, which have been derived from sound physical relationships, provide a quantitative model to explain and predict the feedback of rainfall initiation with a heterogeneous surface.

In Section 4.4 the new model is briefly evaluated against EMBRACE data over the pre-defined four study domains. The primary condition $R<0$ shows that there is some thermodynamic tendency for 1-D triggering, and separates synoptic events from land surface initiations to some extent.

The ΔR analysis in Figures 4.5 and 4.6 shows the existence in the model of a tendency for both dry and wet advantage as predicted by the β_i and Y_{es} phase space diagram. However, predicted dry advantage is predominant. Regardless of the sign, the values of ΔR are found to be very small, with a median corresponding to only a few metres of difference per hour of boundary layer development, between a wet or dry surface. The corresponding analysis of the actual events shows that there is no significant separation of wet or dry advantage events by their ΔR values: this is unsurprising given the low values of ΔR.

The small values of ΔR which have been found, could be said to correspond to an "atmospherically controlled" situation, in the terminology of FE03a and Tuinenburg *et al.*

(2011). Note that Tuinenburg *et al.* (2011) found 81% of their cases over India also to be atmospherically controlled. In this case, we can ask whether "atmospherically controlled" situation is one in which the mesoscale circulations induced by the land surface may themselves provide the locations for triggering: if so, this would explain the results of Chapter 3, in which initiation on DW boundaries was dominant.

The ΔR analysis has also shown that there is less than or equal to 1/3rd chance for the theoretical forecast to match the observed type of initiations depending on the present method of segregation between wet and dry soil moisture conditions (which is a heterogeneous condition).

Even though the chosen period of the simulation is a wet monsoon period, the atmospheric profiles have prevailing (weak) dry advantage prediction. If this is a more general result globally, with stronger values of ΔR, it could help to reconcile the two apparently different (FE03a and T11) theories (described in Section 4.4.2a): dry advantage may in fact be the dominant thermodynamic condition.

In summary, the results of the EMBRACE testing cannot be used to test to the value of the model as a predictor of wet or dry advantage, because the values of ΔR are too weak. However, we can state with some confidence that these values do indicate that thermodynamically, this Indian monsoon study region and period do not show significant preference for wet or dry advantage. This observation may help to explain the fact that Taylor *et al.* (2012) and Guillod *et al.* (2015) found an insignificant signal of wet or dry advantage over India in their analyses.

Future work should apply the new method to other parts of the world or other seasons in India, to see whether significant preferences are found.

5.1.5 Limitations of present work

The present study is mainly focused on analysis of the modelling data initialized from operational model output. To test a hypothesis, it is easier to use a modelling framework as all the required variables (some of which are unknown at the beginning) are available

simultaneously. As this study has established a new predictive framework describe in Chapter 4, this study needs to be reassessed using observations. Some of the limitations of the new model are already described in Section 4.5.2, but considering the whole study, in view of the data and methods used in this study, we can count on a few more limitations.

EMBRACE simulations provided a first quantitative testing of the new model over India during a short period of the wet monsoon season. Thus extend the testing of the new model in different seasons, like the pre-monsoon and post-monsoon, and including a whole monsoon season will add weight to its validation.

Also, this model needs to be evaluated on other parts of the world like the Sahel and the Great Plains of the USA using CASCADE-like simulations and observations (because its general basis should be applicable everywhere).

5.2 Future Work

5.2.1 Exploit satellite and field data

Satellites like INSAT-3D with imagers and sounder have the capability to provide the data simultaneously for surface state as well as the atmospheric profile. Satellite data also have wider spatial and temporal coverage of the region. So, tests of new predictive parameters like stiffness ratio, inversion Bowen ratio and $dR/d\beta$ for dry and wet advantage, using satellite data will evaluate the framework better. This could be combined with radiosondes 0000UTC data. A global study similar to Ferguson and Wood (2011) using satellite data can be done for new proposed model.

The in-situ and flight data collected during field campaign like INCOMPASS can be used to evaluate new model. Models can be initialized and assessed using in-situ and remotely sensed data for refinement of land cover and boundary layer characteristics.

5.2.2 Extend period of EMBRACE kind of simulation

To extend the period of EMBRACE-like simulations would enhance the study for different seasons. In terms of seasonality, apart from the variations in the meteorology, it is particularly interesting to look at the impact of the development stage of the vegetation, particularly in relation to the rapid change in crops which causes dominant changes in the surface fluxes from the beginning to the end of the monsoon season. Wide-spread irrigation practices in the Ganges plain cause significant changes in soil moisture patterns, which opens another aspect of future study.

5.2.3 Further analysis of threshold values

In this study in Chapter 3 we defined the variables ϵ, l, L. Here ϵ is the cutoff value to distinguish between wet and dry soil. So, its optimum value can be found for different seasons for the soil to be categorized as significantly wet or dry. Variables l and L can play an important role in scale analysis.

Evaporative fraction is found out to be another important parameter that needs to be analysed in more detail as its behaviour is dependent on climatic condition also. In other words, analysing in terms of evaporative fraction would also embrace the effects of vegetation or soil type as well as soil moisture, in influencing the boundary layer and the convective initiation.

In Chapter 4, the sign of $dR/d\beta$ predicts the feedback sign but the value of $dR/d\beta$ is equally important to find the strength of the feedback. Larger strength of feedback means more probability of occurrence. Thus to put an optimum cut-off on $dR/d\beta$ remains an open challenge to be computed. It will also be interesting to see observationally that how far new model prediction stands under different climatic regimes.

In summary this study has attempted to evaluate different existing theories over India under one environment for the first time. Quantitative analysis suggested that examples can be found to illustrate all the prevailing theories. In the process of statistical evaluation

and understanding of the boundary layer processes in light of soil moisture-precipitation feedback, the thesis has identified limitations of the one-dimensional predictive framework and developed a new framework having analytical solutions. In evaluation of the new predictive framework with comparison to case studies in Chapter 2 revealed some connection between two theories. Or alternatively we can say some thermodynamic basis to dynamically triggered model (Garcia Carreras *et al.*, 2011; Taylor *et al.* 2011). Overall, there is a lot more scope for validation, evaluation and extension of testing regions for the new model framework. However, it is hoped that information given in this thesis will enhance the understanding of the interaction of the boundary layer parameters to predict wet and dry advantage for convective rain initiation.

References

Agro climatic classification of the Indian sub-continent. http://www.imdagrimet.gov.in/node/287 [Accessed on 24 April 2013]

Asharaf, S., Dobler, A., and Ahrens, B.,2012: Soil Moisture-Precipitation Feedback Processes in the Indian Summer Monsoon Season., J. of Hydrometeorology Vol 13,5,1461-1474.

Avissar, R., and Schmidt, T., 1998: An evaluation of the scale at which ground-surface heat flux patchiness affects the convective boundary layer using large-eddy simulations. J. Atmos. Sci., 55, 2666-2689.

Banacos, P.C., and Schultz, D.M., 2005: The Use of Moisture Flux Convergence in Forecasting Convective Initiation: Historical and Operational Perspectives. Weather and Forecasting, 20, 351-366.

Betts, A. K., 1973: Non-precipitating cumulus convection and its parametrization. Q. J. R. Meteorol. Soc., 99, 178–196.

Betts, A.K., 1992: FIFE atmospheric boundary layer budget methods. J. Geophys. Res., 97., 18,523-18,531.

Betts, A.K. and Ball, J.H., 1995: The FIFE surface diurnal cycle climate. J. Geophys. Res., 100, 25679–25693.

Betts, A. K., Ball, J. H., Beljaars, A. C. M., Miller, M. J. and Viterbo, P. A., 1996: The land surface–atmosphere interaction: A review based on observational and global modelling perspectives. J. Geophys. Res., 101, 7209–7225.

Birch, C.E., Parker, D.J., Marsham, J.H., Copsey, D. and Garcia-Carreras, L., 2014 : A seamless assessment of the role of convection in the water cycle of the West African Monsoon, J. Geophys. Res. Atmos., **119**, doi: 10.1002/2013JD020887.

Birch, C.E., Marsham, J.H., Parker, D.J., Taylor, C.M., 2014b: The scale-dependence and structure of convergence fields preceding the initiation of deep convection, Geophys. Res. Lett., doi: 10.1002/2014GL060493.

Blanford, H. F., 1886, "Dirunal period of rainfall at Calcutta", Indian Meteor Memoirs, IV, 39-46.

Bollasina, M.A., and Ming, Y., 2013: The role of land-surface processes in modulating the Indian monsoon annual cycle. Clim Dyn., **41**, 2497-2509, doi:10.1007/z00382-012-1634-3.

Boos, W.R., Hurley, J.V. and Murthy, V.S., 2015: Adiabatic westward drift of Indian monsoon depressions. Q.J.R. Meteorol. Soc., **141**, 1035–1048. doi:10.1002/qj.2454.

Brubaker, K.L., and Entekhabi, D.,1996: Analysis of feedback mechanisms in land–atmosphere interaction. Water Resour. Res., **32**, 1343–1357.

Carson, D.J., 1973: The development of a dry inversion-capped convectively unstable boundary layer. Q. J. R. Meteorol. Soc., 99, 450–467.

Charney, J.G., Quirks, W. J., Chow, S.H., and Kornfield, J., 1977: A comparative study of the effects of albedo change on drought in semi-arid regions. J. Atmos. Sci., 34, 1366–1385.

Das P.K., Chakraborty A., Seshasai M.V.R., 2014: Spatial analysis of temporal trend of rainfall and rainy days during Indian Summer Monsoon season using daily gridded rainfall data for the period 1971-2005. Meteorol. Appl., **21**,481-493.

Dirmeyer, P.A., 2000: Using a global soil wetness dataset to improve seasonal climate simulation. J. Clim., **13**, 2900-2922.

Dirmeyer, P. A., Schlosser, C.A.and Brubaker, K.L., 2009: Precipitation, recycling, and land memory: An integrated analysis, J. Hydrometeorol., **10**, 278–288, doi:10.1175/2008JHM1016.1.

Dixon, N.S., Parker, D.J., Garcia-Carreras, L., Taylor, C.M., Harris, P.P., Marsham, J.H., Polcher, J., Woolley, A., 2013: The effect of background wind on mesoscale circulations above variable soil moisture in the Sahel, Quarterly Journal of the Royal Meteorological Society, 139, 1009–1024.. doi: 10.1002/qj.2012.

Douglas, E., Niyogi, D., Frolking, S., Yeluripati, J.B., Pielke Sr., R.A., Niyogi, N., Vo¨ro¨smarty, C. J. and Mohanty, U.C., 2006: Changes in moisture and energy fluxes due to agricultural land use and irrigation in the Indian Monsoon belt, Geophys. Res. Lett., 33, L14403, doi:10.1029/ 2006GL026550.

Douglas, E.M., Beltra´n-Przekurat, A., Niyogi, D., Pielke Sr., R. A., and Vo¨ro¨smarty, C.J., 2009: The impact of agricultural intensification and irrigation on land-atmosphere interactions and Indian monsoon precipitation: A mesoscale modeling perspective, Global Planet. Change, 67, 117– 128, doi:10.1016/j.gloplacha.2008.12.007.

Ebert, E.E. and William, A. Gallus Jr., 2009: Toward Better Understanding of the Contiguous Rain Area (CRA) Method for Spatial Forecast Verification. Wea. Forecasting, **24**, 1401-1415.

Eltahir, E.A.B., 1998:A soil moisture–rainfall feedback mechanism. Theory and observations. Water Resour. Res., 34, 765–776.

Ferguson, C.R., and Wood, E.F., 2011: Observed Land–Atmosphere Coupling from Satellite Remote Sensing and Reanalysis, Journal of Hydrometeorology,12, 6, 1221.

Findell, K.L and Eltahir, E.A.B., 2003a: Atmospheric controls on soil moisture – boundary layer interactions. Part I: Framework development. J. Hydrometeor., 4, 552–569.

Findell, K.L and Eltahir, E. A.B., 2003b: Atmospheric controls on soil moisture–boundary layer interactions. Part II: Feedbacks within the continental United states. J. Hydrometeor., 4, 570–583.

Findell, K.L., Gentine, P., Lintner B.R. and Kerr, C., 2011: Probability of afternoon precipitation in eastern United States and Maxico enhanced by high evaporation. Nature geoscience,4,434-439.

Gadgil, S., 2003: The Indian monsoon And Its Variability. Annu. Rev. Earth Planet. Sci. 2003. 31:429–67, doi: 10.1146/annurev.earth.31.100901.141251.

Gantner, L. and Kalthoff, N., 2010: Sensitivity of a modelled life cycle of a mesoscale convective system to soil conditions over West Africa. Quart. J. Roy. Meteor. Soc., 136(s1): 471–482.

Garcia-Carreras, L., Parker, D.J. and Marsham, J.H., 2011: What is the Mechanism for the Modification of Convective Cloud Distributions by Land Surface-Induced Flows?, J ATMOS SCI, **68**, pp.619-634.

Genuchten M.T., Van, 1980: A closed-form equation for predicting the hydraulic conductivity of unsaturated soils. Soil science society of American journal 44 (5), 892-898

Guillod, B.P., Diego, B., Miralles, D.G., Teuling, A.J., and Seneviratne, S.I., 2015: Reconciling spatial and temporal soil moisture effects on afternoon rainfall. Nature Communications, 6, Article number: 6443, doi:10.1038/ncomms7443.

Guo, Z., and Coauthors, 2006:GLACE: The global land–atmosphere coupling experiment. Part II: Analysis. J. Hydrometeor., 7, 611–625.

Haiden, T., 1997: An analytical study of cumulus onset. Quart. J. Roy. Meteor. Soc., **123**, 1945–1960.

Hartley, A.J., Parker, D.J., Garcia-Carreras, L. and Webster, S., 2016: Simulation of vegetation feedbacks on local and regional scale precipitation in West Africa, Agricultural and Forest Meteorology, 222, pp.59-70. doi:10.1016/j.agrformet.2016.03.001.

Hohenegger, C.P., Brochaus, C.S., and Schar, C., 2009: The Soil Moisture-Precipitation feedbacks in simulations with explicit and parameterized convection, J. Climate **22**, 19,5003-5020.

Hong Song-You and Kalnay, E., 2000: Role of sea surface temperature and soil-moisture feedback in the 1998 Oklahoma–Texas drought. Nature,**408**, 842-844, doi:10.1038/35048548.

Hunt, KM.R. and Parker, D.J. , 2016: The movement of Indian monsoon depressions by interaction with image vortices near the Himalayan wall, Quarterly Journal of the Royal Meteorological Society, 142, pp.2224-2229. doi: 10.1002/qj.2812.

Joshi, P. K., and Tyagi, N. K., 1991: Sustainability of existing farming systems in Punjab and Haryana: Some issues in ground water used, Indian J. Agric. Econ., 46, 412– 421.

Kang, S.L., Davis, K.J., LeMoneM., 2007: Observations of the ABL structures over a heterogeneous land surface during IHOP 2002. J. Hydromet. 8, 221–244, DOI: 10.1175/JHM567.1.

Kang Song-Lak and Bryan, G. H., 2011: A Large-Eddy Simulation Study of Moist Convection Initiation over Heterogeneous Surface Fluxes. Mon. Wea. Rev., 139, 2901–2917. doi: http://dx.doi.org/10.1175/MWR-D-10-05037.1

Kishtawal, C.M., Niyogi, D., Tewari, M., Pielke Sr., R.A. and Shepherd, M., 2010: Urbanization signature in the observed heavy rainfall climatology over India, Int. J. Climat., 30 (13), 1908-1916.

Koster, R.D., and Coauthors, 2004: Regions of strong coupling between soil moisture and precipitation. Science, 305, 1138–1140.

Koster, R.D. and Coauthors, 2006: GLACE: The global land–atmosphere coupling experiment. Part I: Overview. J. Hydrometeor., 7, 590–610.

Krishnamurti, T. N., 1985: Summer monsoon experiment—a review. Mon. Weather Rev. 113,1590–1626.

Lal, M., 2001: Climatic change–implications for India's water resources. J. Indian Water Resour. Soc., 21, 101–119.

Lee, E., Chase, T.N., Rajagopalan, B., Barry, R.G., Biggs, T.W. and Lawrence, P.J., 2008: Effects of irrigation and vegetation activity on early Indian summer monsoon variability, Int. J. Climatol., 29, 573–581.

Liu, Y., and Avissar, R., 1996: Sensitivity of shallow convective clouds and precipitation induced by land surface forcings to dynamical and cloud microphysical parameters, J. Geophys. Res., 101, 7477-7497.

Liu, Y. and Avissar, R., 1999: A study of persistence in the land–atmosphere system using a general circulation model and observations. J. Climate 12: 2139–2153.

Lohar, D., and Pal, B.,1995: Effect of irrigation on premonsoon season precipitation over West Bengal,India., J. of Climate,8,10,2567-2570.

Marsham, J.H., Dixon, N., Garcia-Carreras, L., Lister, G.M.S. , Parker, D.J., Knippertz, P., and Birch C., 2013: The role of moist convection in the West African monsoon system—Insights from continental-scale convection-permitting simulations, Geophys. Res. Lett., 40, 1843–1849,_doi:10.1002/grl.50347.

McGregor, G. R. and Nieuwolt, S., 1998: Tropical Climatology, John Wiley & Sons Ltd, Second edition.

Meehl, G. A., 1994: Influence of the land surface in the Asian summer monsoon: External conditions versus internal feedbacks. Journal of Climate, 7, 1033–1049.

Mooley, D. A., Parthasarathy, B., 1984: Fluctuations in all India summer monsoon rainfall during 1871–1978. Climate Change, 6, 287–301.

Murakami, T., 1976: Cloudiness fluctuations during the summer monsoon. J. Meteorol. Soc. Jpn. 54:175–81.

Niyogi, D., Kishtawal, C., Tripathi, S. and Govindaraju, R.S., 2010: Observational evidence that agricultural intensification and land use change may be reducing the Indian summer monsoon rainfall, Water Resour. Res., 46, W03533, doi:10.1029/2008WR007082.

Oke, T. R., 1987: Boundary layer climates, Methuen & Co. Ltd,London, Second edition.

Ookouchi,Y., Segal, M., Kesseler, R.C., Pielke, R.A.,1984: Evaluation of soil moisture effects on the generation and modification of mesoscale circulations. Mon.Wea. Rev.,112,2281-2292.

Parker, D.J., 2002: The response of CAPE and CIN to tropospheric thermal variations. Quarterly Journal of the Royal Meteorological Society, 128, pp.119-130. doi:10.1256/00359000260498815

Parker, D.J., and Diop-Kane, M., 2017: Meteorology of tropical West Africa: The forecasters' handbook. Wiley, Oxford.

Pielke, R.A., and Avissar, R., 1990: Influenceo f landscapes tructure on local and regional climate, Landscape Ecol., 4, 133-155.

Pielke, R.A., 2001: Influence of the spatial distribution of vegetation and soils on the prediction of cumulus convective rainfall. Reviews of Geophysics, 39, 151–177.

Raman, S., Mohanty, U.C., and Reddy, N.C.,1998: Numerical simulation of the sensitivity of summer monsoon circulation and rainfall over India to land surface processes., Pure and Applied Geophysics.,Vol 152,4,781-809.

Romatschke, U., Medina, S. and Houze Jr., R.A., 2010: Regional, Seasonal, and Diurnal Variations of Extreme Convection in the South Asian Region. J. of Climate, **23**, 1, 419-439.

Roy, S.B., and Avissar, R., 2002: Impact of land use/land cover change on regional hydrometeorology in Amazonia. J. Geophys. Res., 107, 8037, doi:10.1029/2000JD000266.

Roy, S.B., 2009: Mesoscale vegetation–atmosphere feedbacks in Amazonia. J. Geophys. Res., 114, D20111, doi:10.1029/2009JD012001.

Sahai, A.K., Grimm, A.M., Satyam, V., Pant, G.B., 2003: Long-lead prediction of Indian summer monsoon rainfall from global SST evolution. Clim Dyn, **20**, 855-863.

Schär, C., Lüthi, D., Beyerle, U. and Heise, E., 1999: The soil-precipitation feedback: A process study with a regional climate model. J. Climate, **12**, 722–741.

Segal, M. and Arritt, R.W. ,1992: Nonclassical Mesoscale Circulations Caused by Surface Sensible Heat-Flux Gradients. Bulletin of the American Meteorological Society, 73, 1593–1604.

Shukla, J. and Mintz, Y., 1982: Influence of land-surface evapotranspiration on the earth's climate. Science 215, 1498–1501.

Shukla, J., Nobre, C., and Sellers, P., 1990: Amazon deforestation and climate change. Science, 215, 1498–1501.

Shukla, S.P., Puma, M.J. and Cook, B.I. , 2014: The response of the South Asian Summer Monsoon circulation to intensified irrigation in global climate model simulations. *Clim. Dyn.*, 42, no. 1-2, 21-36, doi:10.1007/s00382-013-1786-9.

Sinha Ray K.C., De U.S., 2003: Climate change in India as evidenced from instrumental records. WMO Bull., 52, 53–59.

Sikka D.R., Gadgil S. 1978: Large-scale rainfall over India during the summer monsoon and its relation of the lower and upper tropospheric vorticity. Indian J. Meteorol. Hydrol. Geophys. 29:219–31.

Stephens, G.L., L'Ecuyer, T., Forbes, R., Gettlemen, A., Golaz, J.-C. , Bodas-Salcedo, A., Suzuki, K., Gabriel, P. and Haynes, J., 2010: Dreary state of precipitation in global models, J. Geophys. Res., **115**, D24211, doi:10.1029/2010JD014532.

Stull, R., 1998: An Introduction to Boundary Layer Meteorology. Atmospheric sciences library, Kluwer Academic Publishers, London.

Stull, R., 2000:. Meteorology for Scientists and Engineers. Brooks/Cole, California, USA, 2nd edn.

Taylor, C.M., Clark, D.B., 2001: The diurnal cycle and African easterly waves: A land surface perspective. Q. J. R. Meteorol. Soc. 127: 845–867.

Taylor, C.M., and Ellis, R.J., 2006: Satellite detection of soil moisture impacts on convection at the mesoscale, Geophys. Res. Lett., 33, L03404.

Taylor, C.M., Parker, D.J. and Harris, P.P., 2007: An observational case study of mesoscale atmospheric circulations induced by soil moisture. Geophysical Research Letters, 34, 6.

Taylor, C.M., Harris, P.P. & Parker, D.J., 2010: Impact of soil moisture on the development of a Sahelian mesoscale convective system: A case-study from the AMMA Special Observing Period. Quarterly Journal of the Royal Meteorological Society, 136, 456–470.

Taylor, C.M., Gounou, A., Guichard, F., Harris, P.P., Ellis, R.J.,Couvreux, F. and Kauwe, M. D., 2011:Frequency of Sahelian storm initiation enhanced over mesoscale soil moisture patterns. Nature geoscience,4,430-433.

Taylor, C.M., De Jeu, R.A.M., Guichard, F., Harris, P.P., and Dorigo, W.A., 2012: Afternoon rain more likely over drier soils.Nature geosience,489,423-426.

Taylor, C.M., Birch, C.E., Parker, D.J., Dixon, N., Guichard, F., Nikulin, G., Lister, G.M.S., 2013: Modeling soil moisture-precipitation feedback in the Sahel: Importance of spatial scale versus convective parameterization,Geophysical Research Letters, 40, pp.6213-6218. doi: 10.1002/2013GL058511

Tennekes, H., 1973: A model for the dynamics of the inversion above a convective boundary layer. J. Atmos. Sci., 30, 558–567.

Tuinenburg, O.A., Hutjes, R.W.A., Jacobs, C.M.J., and Kabat, P., 2011: Diagnosis of Local Land–Atmosphere Feedbacks in India. J. of Climate,24,1,251-266.

Walker, J.M. and Rowntree, P.R., 1977: The effect of soil moisture on circulation and rainfall in a tropical model. Quart. J. Roy. Meteor. Soc., 103, 29–46.

Zampieri, M., D'Andrea, F., Vautard, R., Ciais, P., Nathalie de Noblet-Ducoudré, and Yiou, P., 2009: Hot European Summers and the Role of Soil Moisture in the Propagation of Mediterranean Drought. J. Climate, **22**, 4747–4758.

Zipser, E.J., Cecil, D.J., Liu, C., Nesbitt, S.W. and Yorty, D.P., 2006: Where are the most intense thunderstorms on earth? Bull. Amer. Meteor. Soc., 87, 1057–1071.

-